AD-A063 327 PURDUE UNIV LAFAYETTE IND SCHOOL OF ELECTRICAL ENGI--ETC F/G 17/5
IRCCD INTRUSION DETECTION.(U)
OCT 78 G R COOPER, C D MCGILLEM F30602-75-C-0082
UNCLASSIFIED RADC-TR-77-435 NL

1 OF 2
AD
A063327

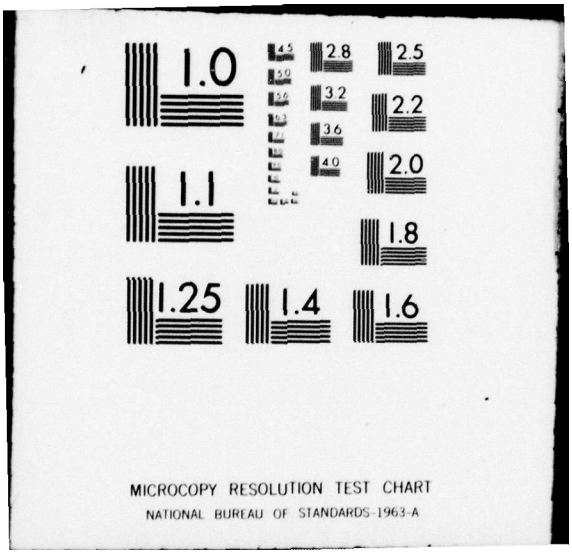
1.0
1.1
1.25
1.4
1.6
1.8
2.0
2.2
2.5
2.8
3.2
3.6
4.0
MICROCOPY RESOLUTION TEST CHART
NATIONAL BUREAU OF STANDARDS-1963-A

LEVEL II

12

RADC-TR-77-435
Phase Report
October 1978

IRCCD INTRUSION DETECTION

George R. Cooper
Clare D. McGillem

Purdue University

ROME AIR DEVELOPMENT CENTER
Air Force Systems Command
Griffiss Air Force Base, New York 13441

This report has been reviewed by the RADC Information Office (OI) and is releasable to the National Technical Information Service (NTIS). At NTIS it will be releasable to the general public, including foreign nations.

RADC-TR-77-435 has been reviewed and is approved for publication.

APPROVED: Jacob Scherer

JACOB SCHERER
Project Engineer

APPROVED: Joseph J. Naresky

JOSEPH J. NARESKY
Chief, Reliability & Compatibility Division

FOR THE COMMANDER: John P. Huss

JOHN P. HUSS
Acting Chief, Plans Office

If your address has changed or if you wish to be removed from the RADC mailing list, or if the addressee is no longer employed by your organization, please notify RADC (RBC) Griffiss AFB NY 13441. This will assist us in maintaining an current mailing list.

Do not return this copy. Retain or destroy.

63203F

UNCLASSIFIED

SECURITY CLASSIFICATION OF THIS PAGE (When Data Entered)

REPORT DOCUMENTATION PAGE	READ INSTRUCTIONS BEFORE COMPLETING FORM
1. REPORT NUMBER: RADC-TR-77-435	2. GOVT ACCESSION NO. / 3. RECIPIENT'S CATALOG NUMBER
4. TITLE (and Subtitle): IRCCD INTRUSION DETECTION,	5. TYPE OF REPORT & PERIOD COVERED: Phase Report, 1 Feb 77 - 30 Sep 77
	6. PERFORMING ORG. REPORT NUMBER: N/A
7. AUTHOR(s): George R. Cooper, Clare D. McGillem	8. CONTRACT OR GRANT NUMBER(s): F30602-75-C-0082
9. PERFORMING ORGANIZATION NAME AND ADDRESS: Purdue University, School of Electrical Engineering, West Lafayette IN 47907	10. PROGRAM ELEMENT, PROJECT, TASK AREA & WORK UNIT NUMBERS: 95670015 / 00
11. CONTROLLING OFFICE NAME AND ADDRESS: Rome Air Development Center (RBC), Griffiss AFB NY 13441	12. REPORT DATE: October 1978
	13. NUMBER OF PAGES: 112
14. MONITORING AGENCY NAME & ADDRESS (if different from Controlling Office): Same / 117 p.	15. SECURITY CLASS. (of this report): UNCLASSIFIED
	15a. DECLASSIFICATION/DOWNGRADING SCHEDULE: N/A

16. DISTRIBUTION STATEMENT (of this Report)

Approved for public release; distribution unlimited.

17. DISTRIBUTION STATEMENT (of the abstract entered in Block 20, if different from Report)

Same

18. SUPPLEMENTARY NOTES

RADC Project Engineer: Jacob Scherer (RBC)

19. KEY WORDS (Continue on reverse side if necessary and identify by block number)

IR Detectors
IR Arrays
Signal Processing
Electromagnetic Compatibility

20. ABSTRACT (Continue on reverse side if necessary and identify by block number)

This study investigates the performance of an IRCCD detector array in determining the presence of an intruder in the field of view of the array. Both analytical and computational results are presented.
Mathematical models for the detectors, for the background, and for specified classes of intruders have been developed. A signal processing technique is proposed and evaluated with respect to probabilities of detection and false

DD FORM 1 JAN 73 1473 EDITION OF 1 NOV 65 IS OBSOLETE

UNCLASSIFIED

SECURITY CLASSIFICATION OF THIS PAGE (When Data Entered)

292000

79 01 16 135

alarm. A comparison with theoretical optimum detectors is also made. A preliminary design for a microprocessor system to accomplish the signal processing is presented and a tentative cost estimate given.

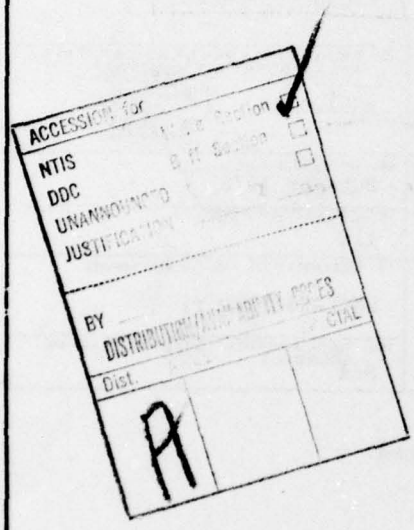

Preface

This effort was conducted by Purdue University under the sponsorship of the Rome Air Development Center Post-Doctoral Program for Rome Air Development Center. A. Robb Frederickson was the task project engineer and provided overall technical direction and guidance.

The RADC Post-Doctoral Program is a cooperative venture between RADC and some sixty-five universities eligible to participate in the program. Syracuse University (Department of Electrical Engineering), Purdue University (School of Electrical Engineering), Georgia Institute of Technology (School of Electrical Engineering), State University of New York at Buffalo (Department of Electrical Engineering) act as prime contractor schools with other schools participating via sub-contracts with the prime schools. The U.S. Air Force Academy (Department of Electrical Engineering), Air Force Institute of Technology (Department of Electrical Engineering), and the Naval Post Graduate School (Department of Electrical Engineering) also participate in the program.

The Post-Doctoral Program provides an opportunity for faculty at participating universities to spend up to one year full time on exploratory development and problem-solving efforts with the post-doctorals splitting their time between the customer location and their educational institutions. The program is totally customer-funded with current projects being undertaken for Rome Air Development Center (RADC), Space and Missile Systems Organization (SAMSO), Aeronautical System Division (ASD), Electronics Systems Division (ESD), Air Force Avionics Laboratory (AFAL), Foreign Technology Division (FTD), Air Force Weapons Laboratory (AFWL), Armament

Development and Test Center (ADTC), Air Force Communications Service (AFCS), Aerospace Defense Command (ADC), HQ USAF, Defense Communications Agency (DCA), Navy, Army, Aerospace Medical Division (AMD), and Federal Aviation Administration (FAA).

Further information about the RADC Post-Doctoral Program can be obtained from Mr. Jacob Scherer, RADC/RBC, Griffiss AFB, NY, 13441, telephone Autovon 587-2543, Commercial (315) 330-2543.

TABLE OF CONTENTS

1.1 OVERVIEW OF PROGRAM

1.1.1 Problem Definition

The problem addressed in this program is that of processing information produced at the output of an infrared detector array to determine the presence or absence of intruders in the field of view of each element of that array. The change produced by each detector in the array is stored in a charge-coupled device (CCD) and read out serially at periodic intervals. The physical and electrical characteristics of the detector array and CCD are assumed to be known.

It is convenient to divide the problem into three major area. These are:

a) What is the response of the detectors to intruders having specified size, speed and thermal properties?

b) What signal processing techniques are most suitable for distinguishing between responses created by intruders of interest and response created by irrelevant objects?

c) What performance can be achieved with the candidate system that appears to most nearly meet the requirements?

These three aspects of the problem are discussed in detail in the following sections.

1.1.2 Objectives of the Investigation

The objectives of this investigation follow immediately from the problem definition stated above. However, a more precise statement of these objectives is desirable as a means of both summarizing the scope of the investigation and indicating the sequence in which the problems were addressed. Thus, the objectives may be described as follows:

1) Develop reasonable models for the specified classes of intruders and backgrounds.

2) Determine the detector response to each of the intruder and background models.

3) Carry out a theoretical analysis of the basic detection problem.

4) Conceive various practical implementations of the detection scheme and evaluate their relative merits.

5) Select a detection scheme and identify the optimum parameters for that scheme.

6) Evaluate the performance of the selected detection method with respect to the specified intruder models.

7) Prepare a preliminary design and rough cost estimate for a breadboard realization of the proposed detection method.

1.1.3 Brief Summary of Results

Although the main body of this report is a detailed presentation of the results of this investigation, a brief summary of the major achievements

provides a useful introduction to this material. All of the objectives outlined above have been achieved.

1) Intruder models have been developed for all of the specified classes. These models are simple enough to permit computer evaluation, but also represent accurately the size, speed, temperature and thermal emissivity of each class of intruder. Models of the background have also been developed for a wide range of circumstances. In addition, the effects of solar illumination and atmospheric precipitation have been modeled on a simplified basis.

2) A computer program has been developed that computes the detector output, as a function of time, as any intruder model enters the field of view at any angle and with any speed.

3) The theoretical optimum detector has been analyzed and evaluated for cases that permit comparison with the practical implementation.

4) A proposed practical implementation has been selected and the optimum parameters determined by "worst case" analysis.

5) The proposed detection method has been evaluated with respect to the background and intruder models by calculating the probabilities of false alarm and the probabilities of detection for each of the models. Two important conclusions from this study are:

   (a) The probabilities of false alarm due to system and background noise are negligibly small when the decision thresholds are adjusted to reject non-threat classes of intruders.

(b) The probabilities of detection for other classes of intruders are essentially unity under the same threshold conditions.

The major deficiency of the proposed system appears to be the possibility of false alrms due to scattered clouds or sun glint.

6) The preliminary design of a microprocessor that can accomplish the necessary data processing for the detection algorithm has been prepared. The estimated cost of the electronics components only for a breadboard model on a "make-one" basis is about $1200 and the dc power requirements are about 15 amperes at 5 volts.

7) It is recommended that the development of a working model be initiated and some steps to be taken in this direction are outlined.

2.1 SIGNAL CHARACTERISTICS

2.1.1 Detector Response

The intent of this section and the two following sections is to state the principal equations that have been used to calculate the signals that are generated by the detector array. These equations have been obtained from the literature and from information supplied by ETSD personnel and no attempt has been made to attribute them to specific sources.

The detector elements are Schottky interval emission photodiodes having an electron yield of

$$\eta(\nu) = \frac{C_1(h\nu-\psi_{ms})^2}{h\nu} \qquad (\frac{\text{electrons}}{\text{photon}}) \qquad (1\text{-}1)$$

where

$h = 6.6256 \times 10^{-34}$ (Ws^2) (Planck's constant)

ν = photon frequency (s^{-1})

ψ_{ms} = barrier height (Ws)

and C_1 is a factor determined by the geometrical, optical and transport properties of the photodiode. It is convenient to express the electron yield in terms of wave number, $\tilde{\nu}$, since the eventual integration is carried out in this variable. Thus, if

$$\tilde{\nu} = \frac{\nu}{c} \tag{1-2}$$

then

$$\eta(\tilde{\nu}) = \frac{hc(C_1(\tilde{\nu}-\tilde{\nu}_0))}{\tilde{\nu}} \tag{1-3}$$

where

$\tilde{\nu}_0 = \psi_{ms}/hc$

$c = 3 \times 10^{10}$ cm/s

For a black body, at absolute temperature T, the spectral radiant photon emittance as function of wave number is

$$\phi(\tilde{\nu},T) = \frac{2c\tilde{\nu}^2}{\exp(\tilde{\nu}hc/kT)-1} \tag{1-4}$$

where

$$k = 1.38 \times 10^{-23} \quad Ws/^{o}K \quad \text{(Boltzmann's constant)}$$

in photons per second, per steradian, per cm^2, per cm^{-1} wavenumber. If the black body is at a distance R from the detector, and if it is imaged onto a detector cell by lense having a diameter D, then the solid angle subtended by the detector is

$$\Omega = \frac{\pi}{4} \left(\frac{D}{R}\right)^2 \quad \text{(steradian)} \tag{1-5}$$

Furthermore, if the target has an area of $A_0(cm^2)$ and its image completely covers a detector cell having an area of $A_e(cm^2)$, then the number of photons arriving at the detector cell is

$$\frac{\pi A_e \mathfrak{I}}{2F^2} \phi(\tilde{\nu},T)$$

in photons per second per cm^{-1} wavenumber where $\mathfrak{I}$ is the transmittance of the optics (≤ 1) and F is the f-number of the optics.

The number of electrons produced in a stare time t_s when the detector element is filled by a black body at temperature T can now be expressed as

$$N_{BB} = \frac{\pi A_e \mathfrak{I} t_s}{2F^2} \int_{\tilde{\nu}_1}^{\tilde{\nu}_2} \phi(\tilde{\nu},T)\eta(\tilde{\nu})d\tilde{\nu} \quad \text{(electrons)} \tag{1-6}$$

where $\tilde{\nu}_1$ and $\tilde{\nu}_2$ are determined by the detector cutoff and the optical system cutoff.

The electrons produced by the detector are converted to voltage, stored in the CCD, and subsequently read out as voltages. However, under the assumption that relationship between electrons and voltage is a linear one, it does not really matter what the constant of proportionality is since all of

the subsequent computations are performed in terms of ratios.

The number of electrons given by (1-6) is in reality the mean value of the number of electrons collected in one stare time. The actual number of electrons in each stare time is a random variable having a Poisson distribution. One of the characteristics of the Poisson distribution is that the mean and variance are identical [1, p. 145]. However, the Poisson distribution, being discrete, is difficult to handle analytically in making studies of probability of detection and probability of false alarm. Fortunately, the number of electrons is so large (greater than 10^5) that the Gaussian approximation to the Poisson distribution is extremely good. Thus, the electrons produced in each stare time will be assumed to be a Gaussian random variable with a mean and variance given by (1-6), or by modifications of (1-6) to be discussed subsequently.

2.1.2 Background Signal

In the absence of an intruder each cell of the array is viewing only background. In order to calculate the signal produced by this background it is necessary to make two modifications to (1-6). In the first place, the background is not a black body. For all of the calculations made here, it will be treated as a gray body with an emissivity of ε_B ($0 \leq \varepsilon_B \leq 1.0$) that is not a function of wavelength. Thus, it is only necessary to multiply (1-6) by ε_B to account for this.

Secondly, it is necessary to account for attenuation of the background emitted signal by the atmosphere. This attenuation is described by the atmospheric transmittance defined as

$$\tau(R) = e^{-\alpha_1 R} \qquad (1\text{-}7)$$

where α_1 is the attenuation coefficient in nepers/meter and R is the distance to the background in meters. It is customary to express attenuation coefficients in dB/km but, because of the short distances involved here, a value in dB/m is used. Thus, let

$$\alpha = \frac{10\alpha_1}{\ln 10} = 4.343\alpha_1 \quad \text{(dB/m)}$$

so that

$$\tau(R) = e^{-.2302\alpha R} \tag{1-8}$$

The original computations were performed with tabulated data for $\tau(R)$ that were wavelength dependent. However, because of the limited number of conditions for which data was available, and because the effect of atmospheric attentuation was minimal, it was decided to employ (1-8) instead. Values of α ranging from 0 to .07 dB/m appear to cover all conceivable atmospheric conditions.

It is further assumed that the atmosphere is emitting radiation as a black body at the same temperature as the background. Thus, the number of electrons resulting from background emission at temperature T_B is

$$N_{BE} = \frac{\pi A_e \mathfrak{J} t_s}{2F^2} \int_{\tilde{\nu}_1}^{\tilde{\nu}_2} \{\epsilon_B \phi(\tilde{\nu}, T_B)\tau(R) + \phi(\tilde{\nu}, T_B)[1-\tau(R)]\}\eta(\tilde{\nu})d\tilde{\nu} \tag{1-9}$$

The result given by (1-9) is applicable for both day and night operation but during the daytime there is an additional signal resulting from the reflected signal from background. There are many possibilities for this but the only one considered here assumes that the reflection is due entirely to direct sunlight. In this case the electrons resulting from the reflected

signal only becomes

$$N_{BR} = \frac{\pi A_e \Omega t_s}{2F^2} \int_{\tilde{\nu}_1}^{\tilde{\nu}_2} (1-\epsilon_B)\left(\frac{A_{sun}}{R_{sun}^2}\right)\cos\theta_{sun}\, \phi(\tilde{\nu}, T_{sun})\, (R)\eta(\tilde{\nu})\, d\tilde{\nu} \qquad (1\text{-}10)$$

where

A_{sun} = area of the sun

R_{sun} = distance to the sun

θ_{sun} = angle of incidence on the background surface

T_{sun} = 6000°K, temperature of the sun.

Because of the dependence on sun angle, all calculations were made with a compromise value of $\theta_{sun} = 30°$.

On the basis of the above discussion, the background signal may be expressed as:

Night: $N_B = N_{BE}$ (1-11)

Day: $N_B = N_{BE} + N_{BR}$ (1-12)

Some of the parameters that enter into the computation of these values, and were held fixed throught the computations, are:

$A_e = 5.16 \times 10^{-9}$ cm^2 (1 mil x 8 mil)

$\mathfrak{I} = .75$

$F = 1.0$

$C_1 = 0.1 \quad (ev)^{-1}$

Unless otherwise noted, the wave number limits were taken to be

$\tilde{\nu}_1 = \tilde{\nu}_0 = 2380 \qquad (\lambda = 4.2\ \mu m)$

$\tilde{\nu}_2 = 2945 \qquad (\lambda = 3.4\ \mu m)$

2.1.3 Target Signal

When an intruder (target) enters the field of view of any cell there will be a change in the photon arrival rate. This change will depend upon the emissivity of the target relative to the background, the temperature of the target relative to the background, and the fraction of the field of view of that cell that is occupied by the target.

The number of electrons that would be produced by emission from a target that fills the entire field of view would be, by analogy to (1-9),

$$N_{TE} = \frac{\pi A_e \mathfrak{I} t_s}{2F^2} \int_{\tilde{\nu}_1}^{\tilde{\nu}_2} \{\varepsilon_T \phi(\tilde{\nu}, T_T)\tau(R) + \phi(\tilde{\nu}, T_T)[1-\tau(R)]\}\eta(\tilde{\nu})d\tilde{\nu} \qquad (1\text{-}13)$$

Similarly, in the daytime there will be an additional number of electron due to the reflected signal from the sun. This is, by analogy to (1-10),

$$N_{TR} = \frac{\pi A_e \Omega t_s}{2F^2} \int_{\tilde{\nu}_1}^{\tilde{\nu}_2} (1-\varepsilon_T)\left(\frac{A_{sun}}{R_{sun}^2}\right) \cos\theta_{sun}\, \phi(\tilde{\nu}, T_{sun})\tau(R)\eta(\tilde{\nu})d\tilde{\nu} \qquad (1\text{-}14)$$

In both of the above expressions ε_T is the emissivity of the target and T_T is the temperature of the target.

When the target does not fill the field of view of the cell in question, the above numbers must be modified. Specifically, if the target occupies a fraction δ ($0 \leq \delta \leq 1$) of the field of view, the target signal may be expressed as

$$\text{Night:} \quad N_T = \delta N_{TE} + (1-\delta)N_{BE} \qquad (1\text{-}15)$$

$$\text{Day:} \quad N_T = \delta(N_{TE} + N_{TR}) + (1-\delta)(N_{BE} + N_{BR}) \qquad (1\text{-}16)$$

2.1.4 Signal-to-Noise Ratio

The most important parameter in determining the detectability of any target is the signal-to-noise ratio. This is defined as the ratio of the square of the change in mean value due to the target to the variance of the signal when there is background only. Since the mean value and variance are identical, this signal-to-noise ratio may be expressed as

$$SNR = \frac{(N_T - N_B)^2}{N_B} \qquad (1\text{-}17)$$

Under conditions of both night and day, this becomes

$$\text{Night:} \quad SNR = \frac{\delta^2 (N_{TE} - N_{BE})^2}{N_{BE}} \tag{1-18}$$

$$\text{Day:} \quad SNR = \frac{\delta^2 [(N_{TE}+N_{TR}) - (N_{BE}+N_{BR})]^2}{N_{BE} + N_{BR}} \tag{1-19}$$

2.2 SYSTEM DESIGN CONSIDERATIONS

2.2.1 Signal Processing Requirements

The basic objective of the signal processing is to determine when the mean value of the signal produced by each detector cell changes from its normal value by an amount sufficient to indicate the presence of a target in the field of view of that cell. Obviously, in order to accomplish this objective it is necessary to establish what the normal value is. Unfortunately, the normal value may be different for each cell and it will probably be a slowly changing function of time. Because of the large number of cells in each array, this operation alone represents a substantial computational load. However, there are other operations that must be performed regardless of what technique is selected to make a decision. Hence, the purpose of this section is to list some of these signal processing requirements as a preliminary to selecting a proposed system.

A/D Conversion: Because of the large number of operations that need to be performed it appears that the only feasible approach is to accomplish them digitally. Thus, the first step in any system is to convert the analog signals that come from the CCD into digital form. The major considerations in performing this conversion are the number of quantizing levels used and the amplitude separation represented by these levels. There is little point in

having each quantum smaller than the rms noise associated with the signal from each cell. It is anticipated that the rms noise will be on the order of 1 millivolt.

The typical mean value of the voltage from each cell will range from 100 to 400 millivolts, and can be limited to this range, or a smaller range, by controlling stare time. Hence, it appears that 256 amplitude levels, separated by 1 millivolt, should provide an adequate range. Furthermore, 256 levels requires only 8 bits out of the A/D converter and this is a convenient number for most microprocessors to handle.

Since the CCD is read out serially, a single A/D converter is all that is required for each array. Each conversion should be accomplished in about 4 microseconds.

Stare-Time Control: The photon count on each cell of the array may change by factors of 50 to 100 between day and night operation or because of changes in background conditions. It appears to be necessary, therefore, to be able to change the stare time in order to avoid CCD saturation at one extreme or signals at the noise level at the other extreme. Because the ambient illumination affects all cells in the array, a reasonable approach to developing an appropriate control signal is to determine an average signal over all cells, or at least over a subset of cells that spans the overall field of view. Hence, another operation that must be performed in any system is that of averaging signals across the array at any one stare time.

Reference Signal Construction: Any decision operation must be based on comparing the most recent output from the array with a reference signal of some sort. There are a variety of possibilities for the choice of a reference signal, including:

a) Previous array output

b) A time average of previous array outputs

c) Adjacent cell outputs at the same time

d) A combination of (a) and (c).

Regardless of which method is selected, however, some operations must be performed on the signals from the array in order to construct the desired reference signal.

Comparison Operation: Several different methods of making the comparison between the reference signal and the current array output are also possible. The most common operations are subtraction and correlation.

Decision Operation: After the comparison has been performed, it is necessary to make a decision as to the significance of the comparison result. Although the ultimate decision is binary, (i.e., either there is an intruder or not) that decision may be arrived at by making several preliminary decisions. Thus, the eventual decision may require a significant amount of data processing.

False Alarm Control: It is always possible to improve the probability of correctly deciding that an intruder is present at the expense of increasing the probability of false alarm. Since the average level of the signals out of the array may change over a wide range, the appropriate level at which a decision of intruder present should be made will also change. Thus, in order to maintain the probability of false alarm at a satisfactorily small value, it is nessary to adjust the decision levels as external conditions change. This implies that some computation must be performed in order to determine what the appropriate levels are at any instant of time.

Automatic Self-Checking: There is a finite probability that any given cell in the array may fail. Such a failure may result in a false alarm, if it occurs rapidly, but a slow deterioration might never be observed in this way. Therefore, it is essential that some provision be made for automatically checking the quality of each cell on a periodic basis. This check requires some additional processing capability in the system.

2.2.2 Data Storage Requirements

The data storage requirement of the processing system is addressed separately because it is a vital factor in determining what is feasible and what is not. It is not intended to discuss the requirements in detail here, but only to outline the scope of the problem.

First it may be noted that to store the data from one stare time requires $8 \times 256 = 2048$ bits of storage. Next, suppose the reference signal were constructed from an average over all of the data for the previous 60 seconds, and that the stare time is 0.1 seconds. The total storage requirement for this one function for this single array would be

$$B = \frac{60}{.1} \times 2048 = 1.2288 \times 10^6 \quad \text{bits}$$

It is clear that some compromise must be made between requirements that are desirable and those that are feasible.

Other parts of the system also require data storage. For example, most targets will be in the field of view for several stare times. If the target is one that is difficult to detect it may be desirable to utilize the data from several stare times in order to make the decision. Thus, it may be necessary to store data before making the comparison and again before making the decision.

2.2.3 Other Considerations

The intent of this section is to list other aspects of system performance that need to be considered in proposing a tentative system design. These aspects will not be discussed in detail; in fact, the requirements are self-evident in most cases.

a) The system must operate over a wide range of temperatures. In this regard, the use of digital processing is a considerable advantage.

b) No manual adjustments should be required after the initial installation.

c) The system must respond to both slowly moving and rapidly moving intruders. The slowest speed of interest is on the order of .025 m/s and greatest speed of interest is on the order of 40 m/s.

d) The system should function under adverse weather conditions such as fog, rain, and snow.

e) The system should be capable of distinguishing between small intruders, such as rabbits and squirrels, and larger intruders such as dogs and men.

f) The system should ignore natural phenomena such as clouds, sun glint, lighting, etc.

g) The system should ignore lights in the field of view that are turned on or off and reflections from headlights of vehicles passing outside the field of view.

h) System cost, reliability, and maintainability are also important characteristics, but they cannot be adequately addressed in this preliminary study.

2.2.4 Survey of Candidate Systems

One way of classifying different processing systems is to base the classification on the form of the reference and type of comparison that is made. On this basis the most promising candidates for consideration may be tabulated as shown in Table I. Any combination of one reference signal and one comparison method constitutes a candidate system; thus defining eight systems.

Table I. Classification of Candidate Systems

Reference Signal	Comparison Method
1. Previous output, same cell	A. Difference
2. Adjacent cell, same time	B. Correlation
3. Previous output and adjacent cell	
4. Average of previous outputs, same cell	

It is not the purpose of this section to present analyses of all candidate systems. Instead, some problems with specific techniques that are deemed to be sufficiently serious to discourage further consideration will be pointed out.

The difficulty with using the previous output from each cell as the reference (1) is that for a slowly moving target the change in cell output from one stare time to the next may be insufficient to provide detection. This difficulty can be alleviated to some extent by using the output that occurred n stare times earlier as the reference. A further difficulty with

either approach, however, is that the reference is just as noisy as the raw data and, hence, larger signals are required to achieve a good probability of detection along with a small probability of false alarm.

When the reference is derived from the adjacent cell (or cells) (2) there are two difficulties. One problem arises if one cell is constantly viewing a discrete object that is different from the rest of the background (e.g., a lamppost or signpost). If no past history is used, this cell will always declare a target present. The second difficulty is the noise in the reference as discussed above.

Using (1) and (2) in combination (3) represents a more viable approach than either one above. However, it appears to offer no advantage over (4) and, when employed to extent that appears to be necessary, is even more complex to implement.

The correlation method of comparison is considered next. A possible method of accomplishing this is shown in Fig. 2-1. Although the method shown here involes correlation with the preceding sample only, it can be extended to include more than one previous sample. The input, $x_k(\ell)$, is the output of the

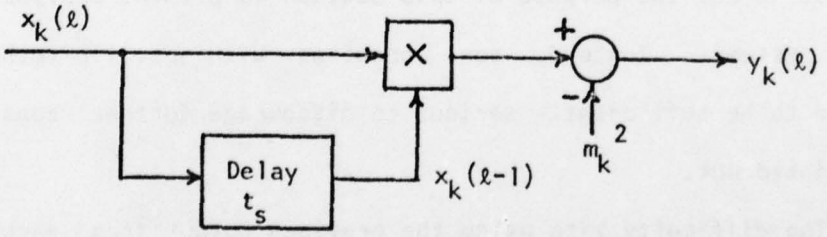

Fig. 2-1. Correlation method of comparison.

kth sensor cell at the ℓth stare time, and the reference, m_k, is the mean value of this output. If a change of Δx occurs in the signal at the ℓth

stare time and if there are independent noises at the two stare times, then the output $y_k(\ell)$ is

$$y_k(\ell) = [m_k+\Delta x+n_k(\ell)][m_k+n_k(\ell-1)] - m_k^2$$

$$= \Delta x[m_k+n_k(\ell-1)] + m_k[n_k(\ell)+n_k(\ell-1)] + n_k(\ell)n_k(\ell-1) \qquad (2\text{-}1)$$

The mean value of this output is

$$E[y_k(\ell)] = m_k\Delta x \qquad (2\text{-}2)$$

and its variance is

$$\text{Var}[y_k(\ell)] = \sigma_n^4 + (\Delta x+2m)^2\,\sigma_n^2 \qquad (2\text{-}3)$$

where σ_n^2 is the variance of the noise. Thus, the signal-to-noise ratio at the output is

$$(\text{SNR})_c = \frac{(m_k\Delta x)^2}{\sigma_n^4+(\Delta x+2m_k)^2\,\sigma_n^2} = \frac{(\Delta x)^2}{\frac{\sigma_n^4}{m_k^2} + (\frac{\Delta x}{m_k} + 2)^2\,\sigma_n^2} \qquad (2\text{-}4)$$

The difference method of comparison is shown in Fig. 2-2.

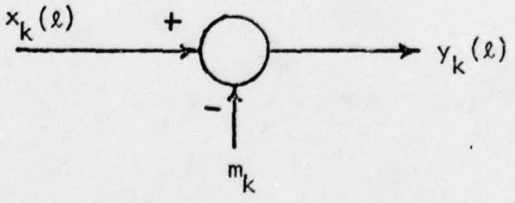

Fig. 2-2. Difference method of comparison.

Under the same circumstances as above, the output in this case is

$$y_k(\ell) = [m_k + \Delta x + n_k(\ell)] - m_k = \Delta x + n_k(\ell) \tag{2-5}$$

The mean value of this output is

$$E[y_k(\ell)] = \Delta x \tag{2-6}$$

and its variance is

$$\text{Var}[y_k(\ell)] = \sigma_n^2 \tag{2-7}$$

yielding a signal-to-noise ratio of

$$(\text{SNR})_d = \frac{(\Delta x)^2}{\sigma_n^2} \tag{2-8}$$

Comparison of (2-8) with (2-4) reveals that the difference method of comparison yields a higher signal-to-noise ratio under all circumstances. This aspect, combined with the fact that the correlation method is more difficult to implement, appears to dictate the use of the difference method. Thus, the candidate system that appears to have the greatest promise is 4A. It is this system that is analyzed in more detail.

2.3 PROPOSED SYSTEM DESIGN

2.3.1 General Description

The system that is proposed for analysis and evaluation is one in which the reference signal is constructed by averaging the output of each cell over a time interval that is long compared to the time that an intruder is likely to remain in the field of view, and the comparison is made by subtracting the reference signal from the most recent output of each cell. A block diagram of this system is shown in Fig. 3-1, and the operation performed by each block are discussed in the following paragraphs.

Sensor Array. This block contains the IR detector cells, the CCD, and the associated circuitry required to read out the signals from the CCD. The stare time adjustment is also accomplished here.

A/D Converter. Converts each output from the CCD into an 8-bit binary sequence. Since there are 4μ seconds for each converson, the bit rate out of the A/D converter is 2Mbps during read out. Data is available for 1.024 ms during each stare time. The output of the A/D converter is denoted as $\underline{x}(\ell)$, which is a vector having 256 elements (the number of cells in the array), each element of which is an 8-bit word.

Background Spatial Average. The outputs from a subset of cells that are more or less uniformly spaced in the array are averaged as a means of obtaining a signal that can be used to adjust the stare time. If D such cells are used, they can be defined by a vector

$$\underline{u}_D^T = (0,1,0\cdots 0,1,0)$$

in which D of the elements are unity and the rest are zero. The average at

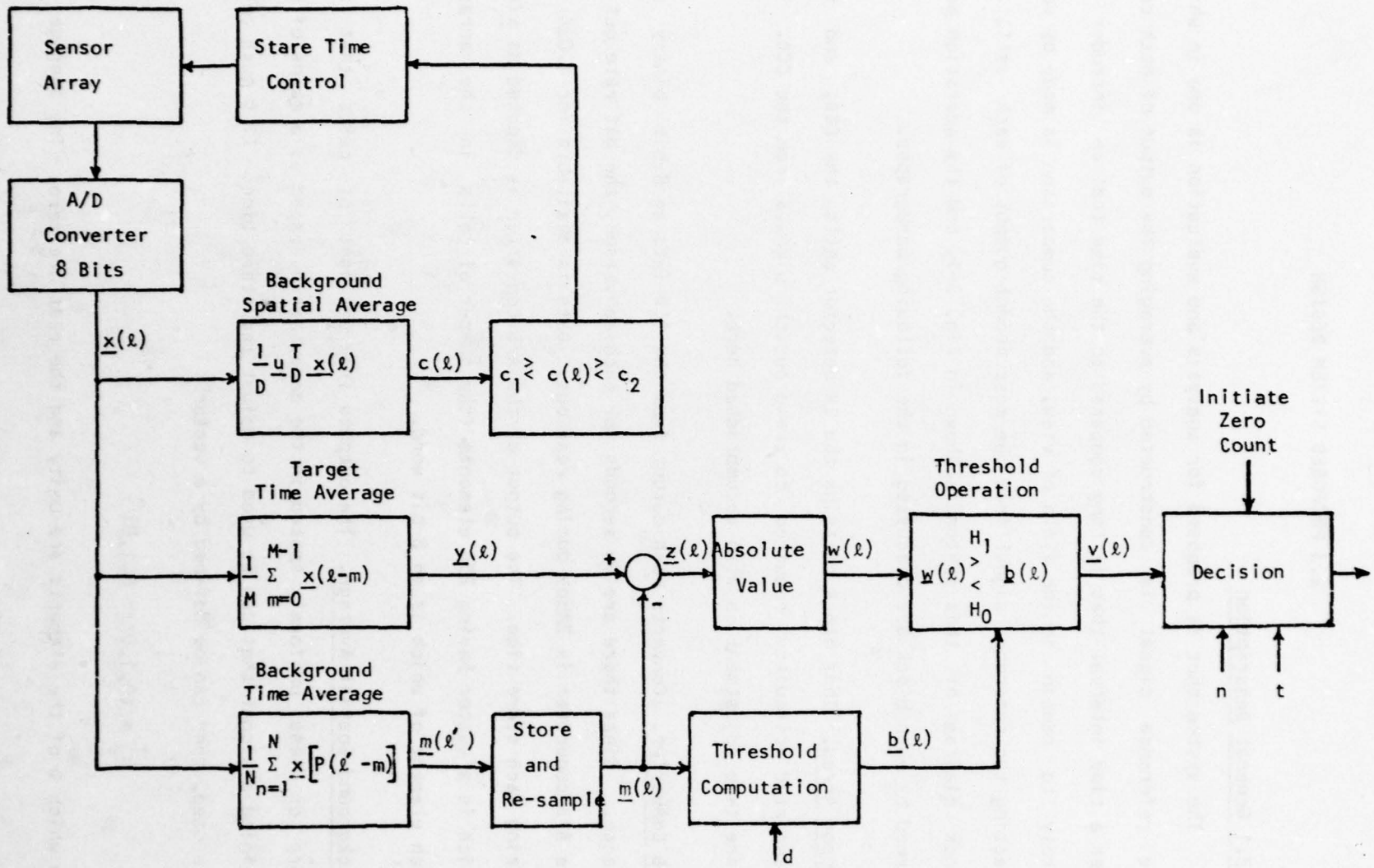

Figure 3-1. Block diagram of proposed system.

each stare time is given by

$$c(\ell) = \frac{1}{D} \underline{u}_D^T \underline{x}(\ell) \qquad (3\text{-}1)$$

Stare Time Control. The value of $c(\ell)$ is used to make adjustments in the stare time. A possible rule for doing this is as follows:

1) Set two thresholds, c_1 and c_2, where c_2 is somewhat lower than the level at which saturation occurs and c_1 is on the order of 250 mv less than c_2.

2) Adjustments to stare time are:

$c_1 \leq c(\ell) \leq c_2$: No change

$c(\ell) > c_2$: Reduce stare time by 2

$c(\ell) < c_1$: Increase stare time by 2

The value of D must be large enough that the presence of a target in one of the cells entering into the average of (3-1) will not significantly affect the average. It is believed that D = 16 is sufficient. In this case the elements of $\underline{u}_D$ would be

$$u_k = 1 \quad , \quad k = 8 + 16j \quad , \quad j = 0, 1, 2, \ldots, 15$$

$$= 0 \quad , \quad \text{otherwise} .$$

It may be noted that a decision to change or not change the stare time is made after each stare time and that there is no long- term time average. Such a time average is not necessary because the hysteresis in the decision rule prevents oscillation across the boundary.

Target Time Average. The possibility of averaging the target signal over

several stare times is included in order to take advantage of the fact that most targets remain in the field of view for several stare times. Subsequent evaluation of the system performance indicates that such averaging is probably not necessary under most circumstances, but the possibility is retained here in order to insure the greatest system flexibility.

The target time average for each cell is the average of the M most recent outputs for that cell. Thus, it may be defined as

$$\underline{y}(\ell) = \frac{1}{M} \sum_{m=0}^{M-1} \underline{x}(\ell-m) \tag{3-2}$$

If this operation is not used, then M=1 and $\underline{y}(\ell) = \underline{x}(\ell)$. If this operation is used, the value of M should be no larger than is necessary to span the number of stare time that the fastest moving small target is in the field of view.

Background Time Average. It is necessary to generate a reference signal for each cell. The method employed here is to perform a long-time average on the background signal generated by each cell. Since the important criterion is the length of time over which the average is taken rather than the number of samples actually averaged, the proposed method performs the average over a set of stare times separated in time by P stare time intervals in order to reduce data storage requirements. Thus, the background time average can be expressed as

$$\underline{m}(\ell') = \frac{1}{N} \sum_{n=1}^{N} \underline{x}[P(\ell'-n)] \tag{3-3}$$

in which the index $\ell' = \ell/P$ corresponds to every Pth stare time. The total time interval over which this average is taken is PNt_s and should be long

compared to the time that a target remains in the field of view. This is because any target that remains in the field of view this long becomes part of the background average and is no longer detectable.

Although the product PN is the important parameter for this operation, the parameter N does play a role in determining the variance of the average. In order to reduce this variance to a value significantly smaller than the variance of the target signal, it is necessary that N>>M.

Store and Re-sample. Since a new reference signal is created only once every P stare times, but a reference is needed every stare time, it is necessary to store the reference signal and re-sample it at the higher rate. Thus, there will be P successive vectors, $\underline{m}(\ell)$, that are identical.

Comparison Operation. The comparison operation in this sytem is simple vector subtraction. Thus,

$$\underline{z}(\ell) = \underline{y}(\ell) - \underline{m}(\ell) \qquad (3\text{-}4)$$

in which each element of $\underline{z}(\ell)$ is the difference between the output of that particular cell and the background average for that particular cell. In the absence of a target, each element of $\underline{z}(\ell)$ is an 8-bit word representing a zero-mean random variable.

Absolute Value Operation. The change in the mean value of $\underline{z}(\ell)$ that results from a target entering the field of view can be either positive or negative. In order to avoid the need for establishing two thresholds, it convenient to perform an absolute-value operation. Thus, $\underline{w}(\ell)$ is a vector, each element of which is the absolute value of the corresponding element of $\underline{z}(\ell)$. That is, the kth element is

$$w_k(\ell) = |z_k(\ell)| \tag{3-5}$$

Threshold Computation. The decision as to the presence or absence of a target is based on comparing each element of $\underline{w}(\ell)$ with a threshold $\underline{b}(\ell)$. The proper value for the threshold depends upon the variance of $\underline{w}(\ell)$. As is shown subsequently, this variance is uniquely related to the mean value of $\underline{m}(\ell)$. Thus, this vector provides the input necessary to calculate the correct threshold values. The threshold also depends upon the desired probability of false alarm. The method of calculation is described in a subsequent section.

Threshold Operation. This operation compares each element of $\underline{w}(\ell)$ with the corresponding element of the threshold vector, $\underline{b}(\ell)$. If the threshold is exceeded, a logical 1 is produced, if not a logical 0 is produced. These results are used to form a vector $\underline{v}(\ell)$, each element of which is a 3-bit word corresponding to the outcomes of the threshold comparisons for three adjacent cells. If the result of the ith comparison is $a_i(\ell)$= 0 or 1, then the vector $\underline{v}(\ell)$ is

$$\underline{v}(\ell) = \begin{bmatrix} a_1(\ell) & a_2(\ell) & a_3(\ell) \\ a_2(\ell) & a_3(\ell) & a_4(\ell) \\ a_3(\ell) & a_4(\ell) & a_5(\ell) \\ \cdot & \cdot & \cdot \\ \cdot & \cdot & \cdot \\ a_{253}(\ell) & a_{254}(\ell) & a_{255}(\ell) \\ a_{254}(\ell) & a_{255}(\ell) & a_{256}(\ell) \end{bmatrix} \tag{3-6}$$

This will be a (254x1) vector unless the extremal cells of adjacent arrays are incorporated in this operation, in which case it would be (256x1). This

latter mode of operation implies a central processor operating on the outputs of all arrays rather than a microprocessor associated with each array.

Decision. In the absence of a target, most of the elements of $\underline{v}(\ell)$ are zeros. When a detectable target enters the field of view, the elements of $\underline{v}(\ell)$ corresponding to the appropriate cells will change to ones and will remain ones for as many stare times as the target is in the field of view. In order to provide discrimination between desired and undesired targets, the eventual decision is based on the states of n/3 successive threshold comparisons in each of the three cells associated with any element of $\underline{v}(\ell)$. A decision of "target present" is made of t or more of the comparison in any block of n are one.

As an illustration suppose that n=12 and t=8. The block of digits corresponding to cells i, (i+1) and (i+2) after the ℓth stare time would be

$$v_i(\ell) = \begin{bmatrix} a_i(\ell) & a_{i+1}(\ell) & a_{i+2}(\ell) \\ a_i(\ell-1) & a_{i+1}(\ell-1) & a_{i+2}(\ell-1) \\ a_i(\ell-2) & a_{i+1}(\ell-2) & a_{i+2}(\ell-2) \\ a_i(\ell-3) & a_{i+1}(\ell-3) & a_{i+2}(\ell-3) \end{bmatrix} \tag{3-7}$$

If 8 or more of these digits are ones, a decision of "target present" is made. If not, a decision of "no target" is made. This decision operation is performed once every stare time.

Self-Checking Feature. An essential part of the proposed system is the ability to periodically check its own operation and give an indication that all cells are functioning and that all of the computation is being performed correctly. This feature is indicated on the block diagram of Fig. 3-1 by the input to the decision block labeled "Initiate Zero Count", and function

is performed as follows:

1) At appropriate time intervals (e.g., once every five minutes) a heater near the sensor array is activated. This heater should have a short time constant (<0.1 second) and be positioned so that all cells of the sensor are illuminated equally. The temperature differential established by the heater should be slightly greater than that necessary to result in a decision of target present.

2) At the time the heater is activated, the decision logic should be altered to count the number of zeros in every set of n observation rather than the number of ones, and t is set equal to n/3.

3) If the system is operating properly, every threshold should be exceeded and there should be no zeros. If any cell is not functioning, it will produce zeros and an alarm will be sounded for that cell. Likewise if the thresholds or the computations are incorrect, and if this error has not previously caused an alarm, it will do so when the decision is complemented.

2.3.2 Analysis of System Operation

Although the system operation described above appears to be complex, because of the large amount of data that needs to be handled in each step, the analysis of this operation is really quite straightforward. Because the operations performed on the output of each cell of the sensor are the same, the analysis is carried out for a single cell. To further simplify the analysis, the output of each cell is considered to be a continuous random variable rather than a quantized one. Hence, the analysis is for an analog system rather than a digital one. Because the quantizing error is much

smaller than the expected signal levels, either with or without a target, this approximation should be a good one. Furthermore, it should be emphasized that the computer evaluation of the system did perform the appropriate quantization so that even this approximation did not exist in that study.

When there is no target present, the output of any one cell in any one stare time is a random variable, χ_0. Because of the Poisson distribution of the number of electrons contributing to this output, the random variable χ_0 has a mean value of

$$m_0 = \beta N_B \tag{3-8}$$

where N_B is the average number of electrons as defined by (1-11) or (1-12), and

$$\beta = \frac{e}{C_0} \tag{3-9}$$

where $e = 1.6 \times 10^{-19}$ coulombs is the electronic charge and C_0 is the equivalent capacitance of the CCD transfer circuit that determines the output voltage. For example, if $c_0 = 0.5$ pF, as assumed in our calculations, then $\beta = 3.2 \times 10^{-7}$. Because the variance of a Poisson distribution is the same as its mean, the random variable χ_0 has a variance of

$$\sigma_0^2 = \beta^2 N_B$$

Because N_B is so large, it is reasonable to assume that χ_0 is a continuously distributed random variable with a Gaussian probability density function. It is further assumed that the variations in χ_0 are independent from one stare time to the next because the variations in the number of electrons are independent. Thus, it is possible to express the means and

variances of the target time average and the backgrond time average, when no target is present, in terms of m_0 and σ_0^2. The target time average is

$$y = \frac{1}{M} \sum_{m=0}^{M-1} x_m \tag{3-10}$$

where x_m is the cell output at the mth stare time preceding the current one. It follows that the mean value of y is

$$\bar{y}_0 = E[y] = \frac{1}{M} \sum_{m=0}^{M-1} E\left[x_m\right] = \frac{1}{M} \sum_{m=0}^{M-1} m_0 = m_0 \tag{3-11}$$

Similarly, because of independence, the variance of y is

$$\sigma_{yo}^2 = E\left[(y-\bar{y})^2\right] = \frac{1}{M^2} \sum_{m=0}^{M-1} \sum_{m'=0}^{M-1} E[(x_m-x_0)(x_{m'}-x_0)]$$

$$= \frac{1}{M^2} \sum_{m=0}^{M-1} E[(x_m-x_0)^2] = \frac{1}{M^2} \sum_{m=0}^{M-1} \sigma_0^2 = \frac{\sigma_0^2}{M} \tag{3-12}$$

The background time average is

$$m = \frac{1}{N} \sum_{n=1}^{N} x_n \tag{3-13}$$

where x_n is the cell output at nPth stare time preceding the current one. By analogy to (3-11) and (3-12), the mean and variance of this average is

$$\bar{m}_0 = m_0 \tag{3-14}$$

$$\sigma_{mo}^2 = \frac{\sigma_o^2}{N} \tag{3-15}$$

The output of the comparison operation is

$$z = y-m \tag{3-16}$$

If it is assumed that P>M, a condition that will almost certainly be true, then Y and M contain no outputs from the same stare times and, hence, will be independent. Thus, the mean and variance of z, when there is no target, are

$$\overline{z}_o = \overline{y}_o - \overline{m}_o = m_o - m_o = 0 \tag{3-17}$$

and

$$\sigma_{zo}^2 = \sigma_{yo}^2 + \sigma_{mo}^2 = \sigma_o^2\left[\frac{1}{M} + \frac{1}{N}\right] \tag{3-18}$$

Since z is also a Gaussian random variable, the probability that its magnitude

$$w = |z| \tag{3-19}$$

exceeds a threshold value, b, is simply

$$p_o = Pr[z>b] + Pr[z<-b] = 2\,Q\left[\frac{b}{\sigma_{zo}}\right] \tag{3-20}$$

where

$$Q(\alpha) = \frac{1}{\sqrt{2\pi}} \int_{\alpha}^{\infty} e^{-u^2/2} du$$

is the complementary Gaussian distribution function. The relation

$$Q(\alpha) = 1-Q(-\alpha) \tag{3-21}$$

is also used in evaluating that portion of (3-20) that pertains to z<-b. the probability p_o is related to the probability of false alarm and this relationship is derived subsequently.

When a target enters the field of view of any cell, both the mean and variance of the cell output change. Specifically, the new mean value is

$$m_1 = \beta N_T \tag{3-22}$$

where N_T is the average number of electrons as defined by (1-15) or (1-16). Similarly, the new variance becomes

$$\sigma_1^2 = \beta^2 N_T \tag{3-23}$$

However, these values will change from stare time to stare time as the target moves into and out of the field of view; that is, the fractional area δ is a function of time. It is necessary, therefore, to expand the above notation to let m_ℓ be the mean value of the cell output at the ℓth stare time, when a target is present, and σ_ℓ^2 is the variance at the same time.

The target time average at the ℓth stare time, by analogy to (3-11), is

$$\overline{y}_\ell = \frac{1}{M} \sum_{m=0}^{M-1} E\left[\chi_m\right] = \frac{1}{M} \sum_{m=0}^{M-1} m_{\ell-m} \tag{3-24}$$

and the variance, by analogy to (3-12), is

$$\sigma_{y\ell}^2 = \frac{1}{M^2} \sum_{m=0}^{M-1} E\left[(\chi_m-\chi_o)^2\right] = \frac{1}{M^2} \sum_{m=0}^{M-1} \sigma_{\ell-m}^2 \tag{3-25}$$

The background time average can be handled in a similar fashion to yield a mean and variance of

$$\bar{m}_{\ell} = \frac{1}{N} \sum_{n=1}^{N} m_{\ell-nP} \tag{3-26}$$

and

$$\sigma^2_{y\ell} = \frac{1}{N^2} \sum_{n=1}^{N} \sigma^2_{\ell-nP} \tag{3-27}$$

Again under the assumption that $P > M$, the mean and variance of z_{ℓ}, the output of the comparison circuit, are

$$m_{z\ell} = \frac{1}{M} \sum_{m=0}^{M-1} m_{\ell-m} - \frac{1}{N} \sum_{n=1}^{N} m_{\ell-nP} \tag{3-28}$$

and

$$\sigma^2_{z\ell} = \frac{1}{M^2} \sum_{m=0}^{M-1} \sigma^2_{\ell-m} + \frac{1}{N^2} \sum_{n=1}^{N} \sigma^2_{\ell-nP} \tag{3-29}$$

It may be noted that the mean value is no longer zero. Hence, the probability that $w_{\ell} = |z_{\ell}|$ will exceed the threshold b is not the same as it was when there was no target present. The situation is represented graphically in Fig. 3-2. It is clear that the probability that w_{ℓ} exceeds

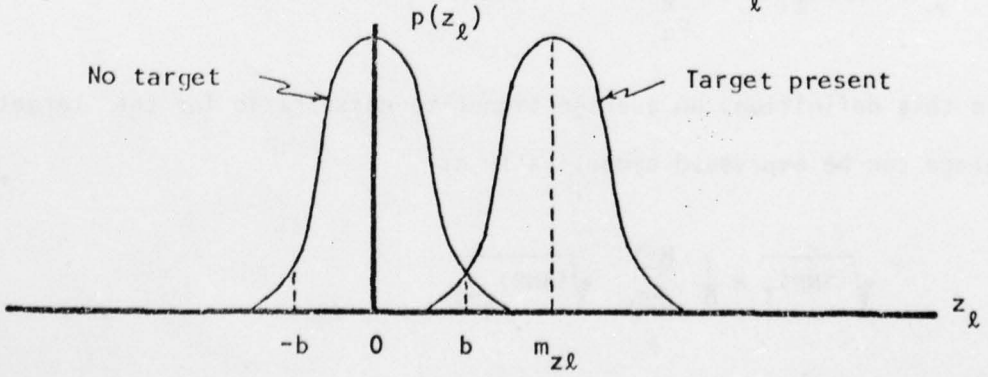

Fig. 3-2. Illustrating the probability of exceeding the threshold.

the threshold is

$$p_\ell = Pr\left[z_\ell > b\right] + Pr\left[z_\ell < -b\right]$$

$$= Q\left[\frac{b-m_{z\ell}}{\sigma_{z\ell}}\right] + Q\left[\frac{m_{z\ell}+b}{\sigma_{z\ell}}\right]$$

$$= 1-Q\left[\frac{m_{z\ell}-b}{\sigma_{z\ell}}\right] + Q\left[\frac{m_{z\ell}+b}{\sigma_{z\ell}}\right] \qquad (3\text{-}30)$$

The probability p_ℓ is related to the probability of detection and this relationship is presented subsequently.

It may also be noted that (3-30) includes the case of no target simply by setting $m_{z\ell}=0$ and $\chi_{z\ell} = \chi_{zo}$.

For computational purposes it is convenient to calculate the signal-to-noise ratio for each stare time since this parameter is the one that is most significant in determining the performance. The signal-to-noise ratio for the ℓth stare time is

$$(SNR)_\ell = \frac{(m_\ell - m_o)^2}{\sigma_o^2} \qquad (3\text{-}31)$$

From this definition, an average signal-to-noise ratio for the target time average can be expressed symbolically as

$$\sqrt{(SNR)_T} = \frac{1}{M}\sum_{m=0}^{M-1}\sqrt{(SNR)_{\ell-m}} \qquad (3\text{-}32)$$

Similarly, an average signal-to-noise ratio for the background time average can be expressed symbolically as

$$\sqrt{(SNR)_B} = \frac{1}{N} \sum_{n=1}^{N} \sqrt{(SNR)_{\ell-nP}} \tag{3-33}$$

Also let

$$S_\ell = \frac{m_\ell - m_o}{m_o} \tag{3-34}$$

and define

$$S_T = \frac{1}{M^2} \sum_{m=0}^{M-1} S_{\ell-m} \tag{3-35}$$

and

$$S_B = \frac{1}{N^2} \sum_{n=1}^{N} S_{\ell-nP} \tag{3-36}$$

Finally, define

$$G = \frac{MN}{M+N}$$

and

$$d = Q^{-1}(p_o/2) \tag{3-37}$$

where p_o is the desired value of p_o as determined by the desired probability of false alarm and $Q^{-1}(\cdot)$ is the inverse Q-function. Thus, from (3-20) threshold value, b, is

$$b = d\sigma_{zo} = d\sigma_o\sqrt{\frac{1}{M} + \frac{1}{N}} \tag{3-38}$$

If all of the above definitions are substituted into (3-30), the result is

$$p_\ell = 1-Q\left\{\frac{\sqrt{G}\left[\sqrt{(SNR)_T}-\sqrt{(SNR)_B}\right]-d}{\sqrt{G(S_T+S_B)+1}}\right\}+Q\left\{\frac{\sqrt{G}\left[\sqrt{(SNR)_T}-\sqrt{(SNR)_B}\right]+d}{\sqrt{G(S_T+S_B)+1}}\right\} \quad (3\text{-}39)$$

The advantage to this formulation can be seen by writing the signal-to-noise ratio at the ℓth stare time, (3-31), as

$$(SNR)_\ell = \frac{m_\ell - m_o^{\,2}}{\sigma_o^2} \simeq \frac{\beta N_{T\ell} - \beta N_B^{\,2}}{\beta^2 N_B} = \frac{N_{T\ell} - N_B^{\,2}}{N_B} \quad (3\text{-}40)$$

and the parameter S_ℓ, (3-34), as

$$S_\ell = \frac{m_\ell - m_o}{m_o} = \frac{\beta N_{T\ell} - \beta N_B}{\beta N_B} = \frac{N_{T\ell} - N_B}{N_B} \quad (3\text{-}41)$$

It is noted that these parameters can be expressed entirely in terms of the number of electrons and do not require a knowledge of the parameter β which converts electrons to volts. Thus, (3-39) is general and would be applicable to <u>any</u> array of sensors having any transfer efficieny for the CCD.

It is true that a knowledge of β is necessary to actually evaluate the threshold b as defined by (3-38). However, the value of b is only required in the operating system and is not required in calculating p_ℓ. In the operating system, σ_o (which is a factor of b) is proportional to $\sqrt{m_o}$ and an estimate of m_o is continuously available at the output of the background time average. Thus, b is proportional to $\sqrt{m_o}$ and the constant of proportionality is obtained from actual adjustment in the operating system to achieve the desired performance.

The final step in the analysis of system operation is to relate p_o and p_ℓ to the probability of false alarm and the probability of detection. As discussed in Sec. 2.3.1, the final decision is based on observing the number of times the threshold has been exceeded in the n/3 most recent stare times in 3 adjacent channels. If t or more of these observations exceed the threshold, a decision of "target present" is made.

For the case in which a target is not actually present, the probability of false alarm is related to p_o by the binomial distribution since p_o is the probability that noise alone will exceed the threshold. Thus, the probability of false alarm is given by

$$P_F = \sum_{j=0}^{n-t} \binom{n}{j} (1-p_0)^j \, p_0^{n-j} \tag{3-42}$$

The importance of this relation lies in the fact that extremely small values of P_F can be obtained with only moderately small values of p_o.

By way of illustrating the above point, suppose that a 5 km perimeter is viewed by 130 arrays each containing 256 sensors and each sensor views 0.15 m of the perimeter. Thus, there are a total of 33280 sensors. If only one false alarm per day, due to system noise, is desired, and if the stare time is 0.1 second, then the probability of false alarm for each sensor would have to be

$$P_F = \frac{0.1}{33,280(24)(3600)} = 3.48 \times 10^{-11}$$

which is an extremely small value. However, by selecting n=12 and t=8, the p_o required to achieve this is 0.0229.

When a target enters the field of view, not all of the p_ℓ will have the same value since they correspond to different observation times and dif-

ferent cells. Thus, there will be a set of n values of p_ℓ. Designate these n values as p_i and let $q_i = 1-p_i$. The probability of detection is then given by

$$P_D = 1 - \sum_{j=0}^{t-1} \sum^{j} (p_i \cdots p_k \, q_f \cdots q_g) \qquad (3\text{-}43)$$

where the second sum is over all combinations of p_i, q_i containing j value of p_i and n-j values q_f. To illustrate this more clearly, let n=3. Then

$$\sum^{j=o} (p_i \cdots, q_f \cdots) = q_1 \, q_2 \, q_3$$

$$\sum^{j=1} (\quad) = p_1 \, q_2 \, q_3 + p_2 \, q_1 \, q_3 + p_3 \, q_1 \, q_2$$

$$\sum^{j=2} (\quad) = p_1 \, p_2 \, q_3 + p_1 \, p_3 \, q_2 + p_2 \, p_3 \, q_1$$

$$\sum^{j=3} (\quad) = p_1 \, p_2 \, p_3$$

In addition, if t=2 in this example, then j=0 and j=1 appear in (3-43) and the probability of detection becomes

$$P_D = 1 - q_1 \, q_2 \, q_3 - p_1 \, q_2 \, q_3 - p_2 \, q_1 \, q_3 - p_3 \, q_1 \, q_2$$

Clearly, this becomes a very involved computation for large values of n and t.

Again, the importance of this result is that values of P_D very close to 1 can be obtained with much smaller values of p_ℓ. To illustrate this point further, suppose it is desired to achieve a probability of detection of

0.999 and all of the p_ℓ values are the same (e.g. a target has completely covered the field of view of 3 cells for at least n/3 stare times). Then for n=12 and t=8 again, the required value of p_ℓ is only 0.784.

2.3.3. Comparison with An Optimum System

It is of interest to compare the performance of the proposed system with that of an optimum system. It is to be expected that the optimum system will perform somewhat better for at least three reasons:

1) The optimum detector requires nonlinear processing of the observed data, while the proposed system is linear except for the absolute value operation on z.

2) The optimum detector requires that data from all cells and for all observation times be processed to make a single decision. The proposed system uses data from only 3 cells and M observation times for each decision.

3) The thresholds of the optimum are assumed to be known exactly from a complete knowledge of the background and target characteristics. In the proposed system the threshold is computed from an estimate of the variance of the observed processes.

The analysis of the optimum detector is presented in Appendix A in its general form. Because of computational difficulties in integrating multidimensional Gaussian density functions, the only situation for which it is feasible to make a numerical comparison is the single observation case. The special result for the optimum system for this condition is also given in Appendix A. For the proposed system, this condition corresponds to setting M=n=t=1. The resulting comparison is shown in Fig. 3-3 by displaying the

probability of detection as a function of $(SNR)_T$ for a false alarm probability of 6.94×10^{-10}. It is evident that the proposed system is suboptimum, but only by a small amount x - less than 1 dB.

It is not known whether the proposed system is better or worse relative to the optimum system when more than one observation is considered, because the optimum system cannot be computed for this case without utilizing an excessive amount of computing time. Furthermore, since the numerical evaluation of the proposed system performance produced results that exceeded expectations, the expenditure of such computing effort for the sake of making further comparisons does not seem justified.

2.3.4. Selection of System Parameters

In order to evaluate the performance of the proposed system it is first necessary to select the operating parameters. This was accomplished by varying the parameters, one at a time, and computing the resulting probability of false alarm and probability of detection for two "worst case" targets. These worst case targets are designated as

I. The most detectable target for which a decision of "no target" is desired. This turned out to be the target model for a squirrel against the most contrasting background.

II. The least detectable target for which a decision of "target" is desired. This is the target model for a crawling man against the least contrasting background.

The parameter variations for each of these targets are described in the following paragraphs.

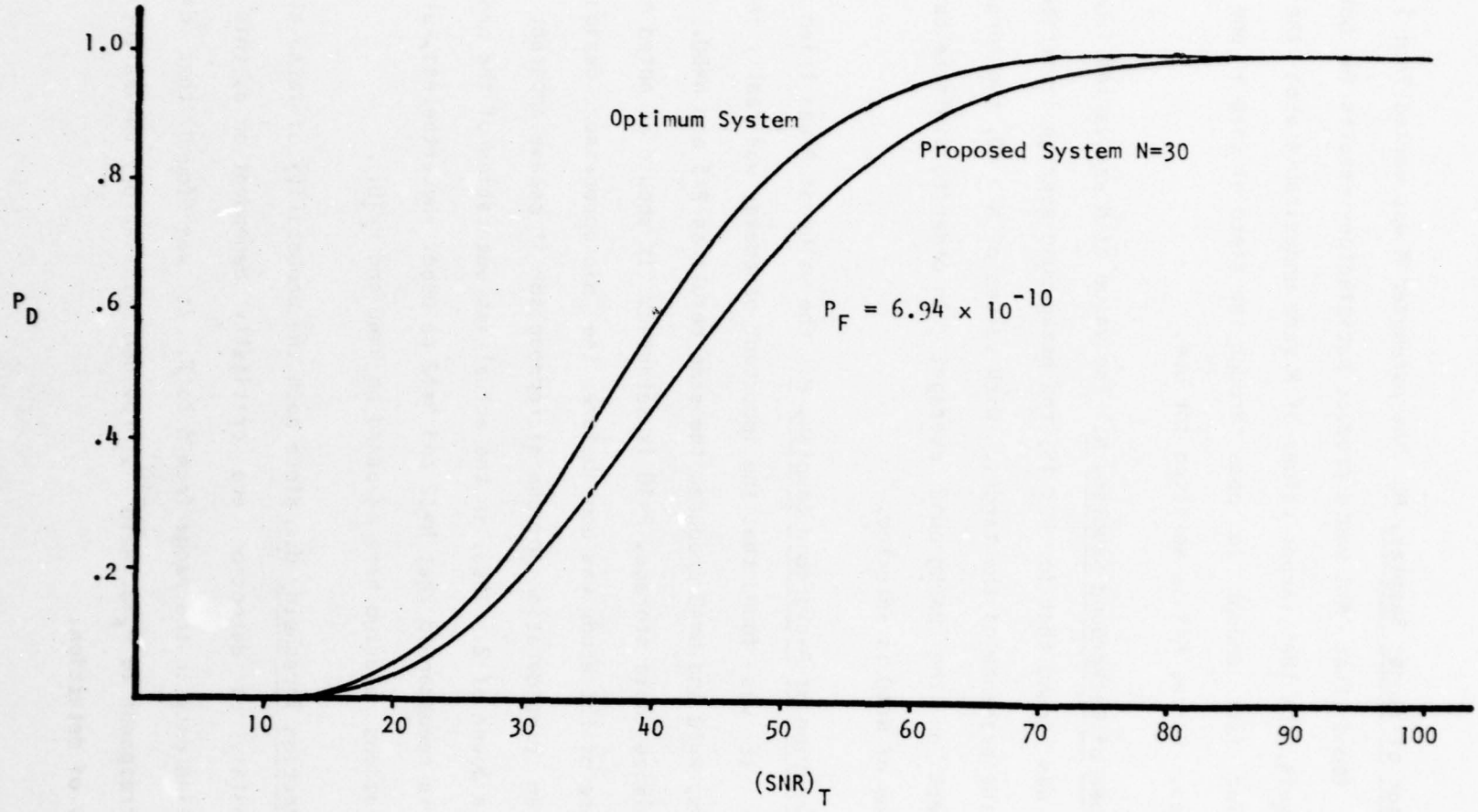

Figure 3-3. Single Observation Probability of Detection

Number of Target Samples, M. The parameter M was varied from 1 to 10. It was found that M=1 would produce satisfactory results for both worst case targets, and that larger values of M were undesirable when the target was moving fast enough to pass through the field of view in one or two stare times. Hence, M=1 is selected for use.

Number of Background Samples, N. The value of N was varied from 1 to 80. It was found that for $N \leq 15$, the background average is seriously affected by the presence of the target. With values of $N \geq 40$, the target had little effect on the background average. In order to minimize data storage, a value of N=40 is selected.

Separation of Background Samples, P. the value of P was tried at both 5 and 10. It was found that the important parameter was really the product NP. Thus, P=10 and N=40 produced the same result as P=5 and N=80. In order to minimize data storage, P=10 is selected. It should be noted here that this phase of the study was done before the microprocessor design was begun. After consideration of the microprocessor it became apparent that N should be a power of 2. Thus, in the actual implementation of the proposed system it is recommended that N=32 and P=12 be used. Nevertheless, all of the computations reported here as based on N=40 and P=10.

Detection Threshold, d. Since both the probability of false alarm and probability of detection are critically dependent on d, this parameter was varied only in the range from 6 to 7. It was found that d=6.168, which corresponds to $P_F=6.94\times10^{-10}$, provided satisfactory values for the probability of detection.

Decision Threshold, t. The number of observations used to provide a final decision is arbitrarily set at n=12, because this is a multiple of 3 and is not too large to prohibit efficient computation. The threshold, t, was then varied from 6 to 9. It was found that in order to detect target II, t must be less than 9; and in order to reject target I, t must be greater than 7. Thus, t=8 is selected.

A number of parameters were not varied in these tests. These are described below.

Stare Time, t_s. A value of t_s=0.1 second was found to be satisfactory to avoid saturation and still provide adequate signal levels for both target cases.

Depression Angle, θ_D. The detector array was aimed at an angle $\theta_D = 5.65^o$ below the horizon in order to provide a range on the order of 100 meters.

Quantization Levels. Since 8 bits yields 256 quantization levels, and this number yields a quantizing error on the same order of magnitude as the system noise, this value was selected. Furthermore, 8 bits is a convenient number for most microprocessors.

Optical Parameter. The detector bandwidth used for these tests was $3.4 < \lambda < 4.2$ um. The lense system was assumed to have a focal length of 1.7 cm and an f-number of 1. Atmospheric attenuation was assumed to be 0.01 dB/m.

2.4. EVALUATION OF PROPOSED SYSTEM

2.4.1. Differential Sensitivity

One way of evaluating the performance of the proposed system is to determine the amount that a target's temperature and/or emissivity must differ from the background in order for the target to be detectable. For small changes in temperature or emissivity, the change in probability of detection is expected to be a linear one. However, the fraction of the field of view covered by target, δ, also is important.

A convenient graphical presentation of this differential sensitivity is to plot lines of constant probability of detection on a plane whose coordinates are $\delta\Delta\varepsilon$ and $\delta\Delta T$, where

$$\Delta\varepsilon = \varepsilon_T - \varepsilon_B$$

and

$$\Delta T = T_T - T_B$$

The slopes and positions of these lines of constant P_D depend upon the background temperature and emissivity, as well as the parameters of the system. Hence, the data from which the plots are constructed must be obtained by direct calculation of P_D for a series of small values of $\Delta\varepsilon$ and ΔT. The results of this computation are displayed in Fig. 4-1 through 4-18 for three different background temperatures, three different background emissivities, and for both night and day.

Several points are worth noting in connection with these results:

1) The lines of constant P_D have a negative slope for night operation and a positive slope for day operation. This is because the solar

reflected signal is predominate in the day and this signal is proportional to $1-\varepsilon$. This also suggests that at some solar illumination level the sensitivity will be independent of the temperature change.

2) In every case there is a curve for which $P_D=0$. This is a condition in which the change in temperature and change in emissivity exactly compensate one another.

3) For night operation, the sensitivity increases as the background emissivity and the background temperature increase.

4) For day operation, the sensitivity increases as the background emissivity increases and the background temperature decreases.

2.4.2. Dependence on Signal-to-Noise Ratio

A second method of evaluating the performance of the proposed system is to determine the overall probability of detection, P_D, as a function of the signal-to-noise ratio at each observation. This relationship has been computed for the parameters selected in Sec. 2.3.4 and is displayed in Fig. 4-19. For purposes of comparison, the single-observation detection curve of Fig. 3-2 is also shown. It is apparent that the use of multiple observations significantly increases the steepness of the detection curve. This is desirable because it increases the probability of detection for those targets that should be detected and reduces the probability of false alarm for those targets that should not be detected.

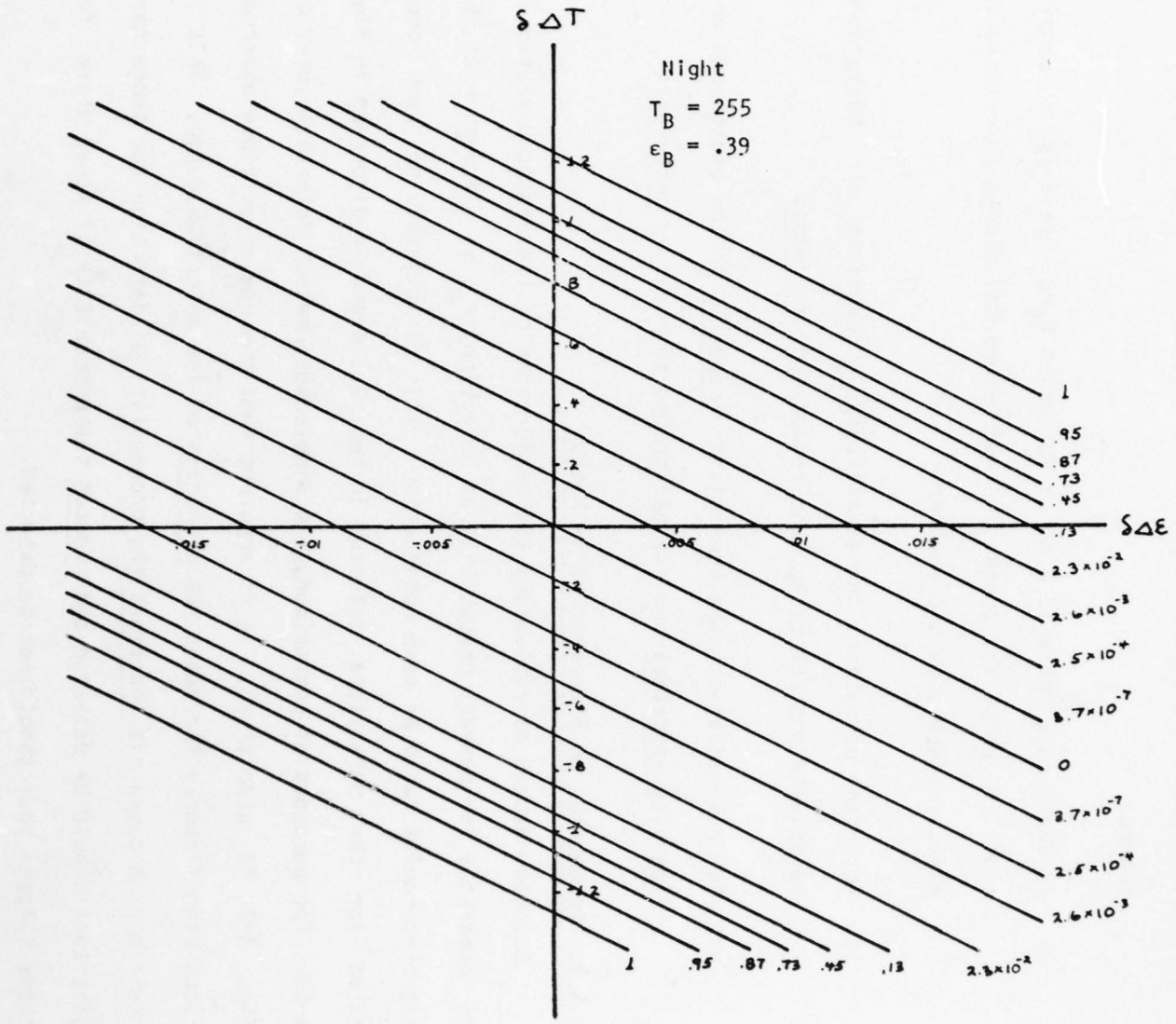

Figure 4-1. Differential sensitivity plot. Parameter is probability of detection.

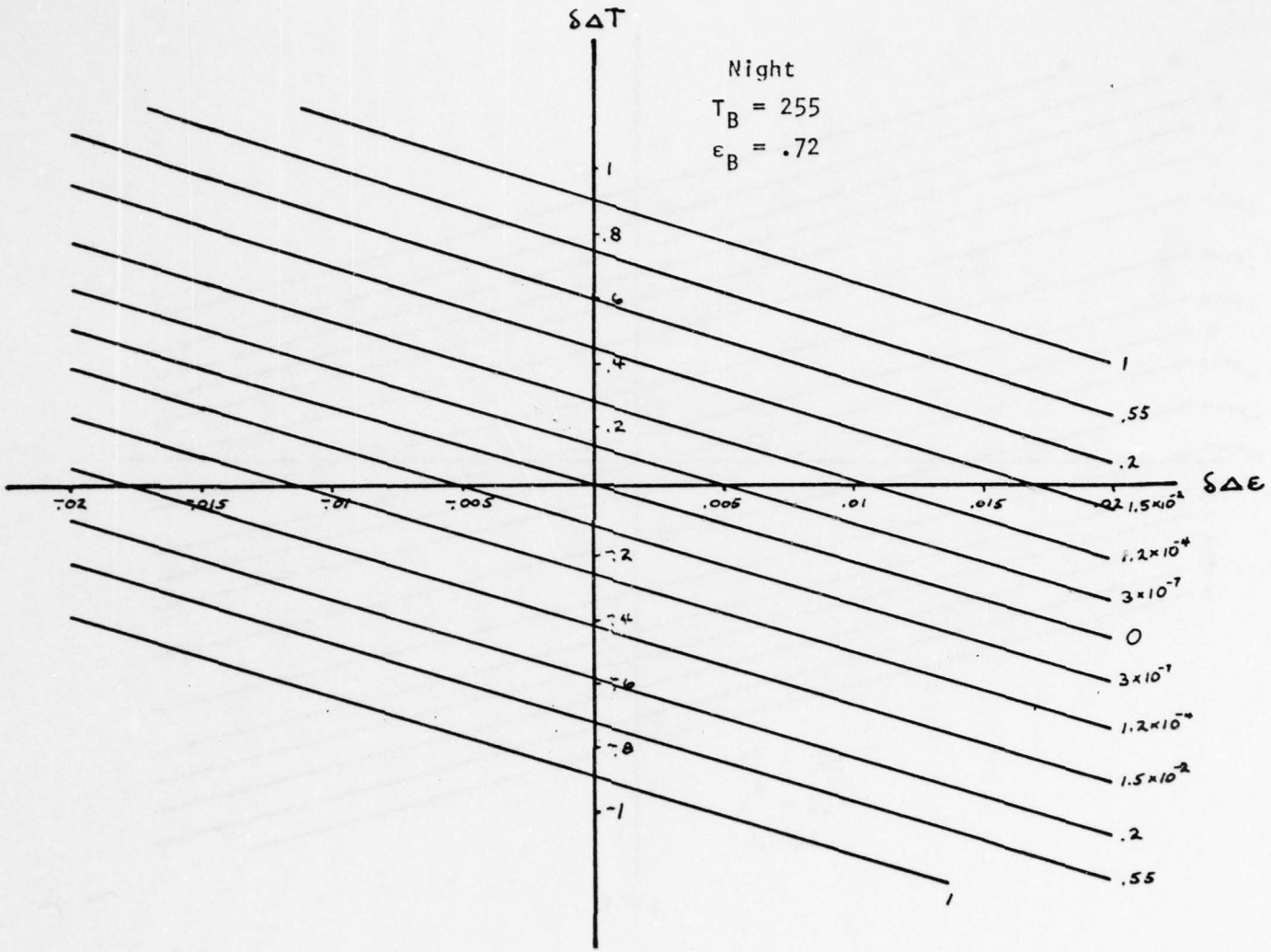

Figure 4-2. Differential sensitivity plot. Parameter is probability of detection.

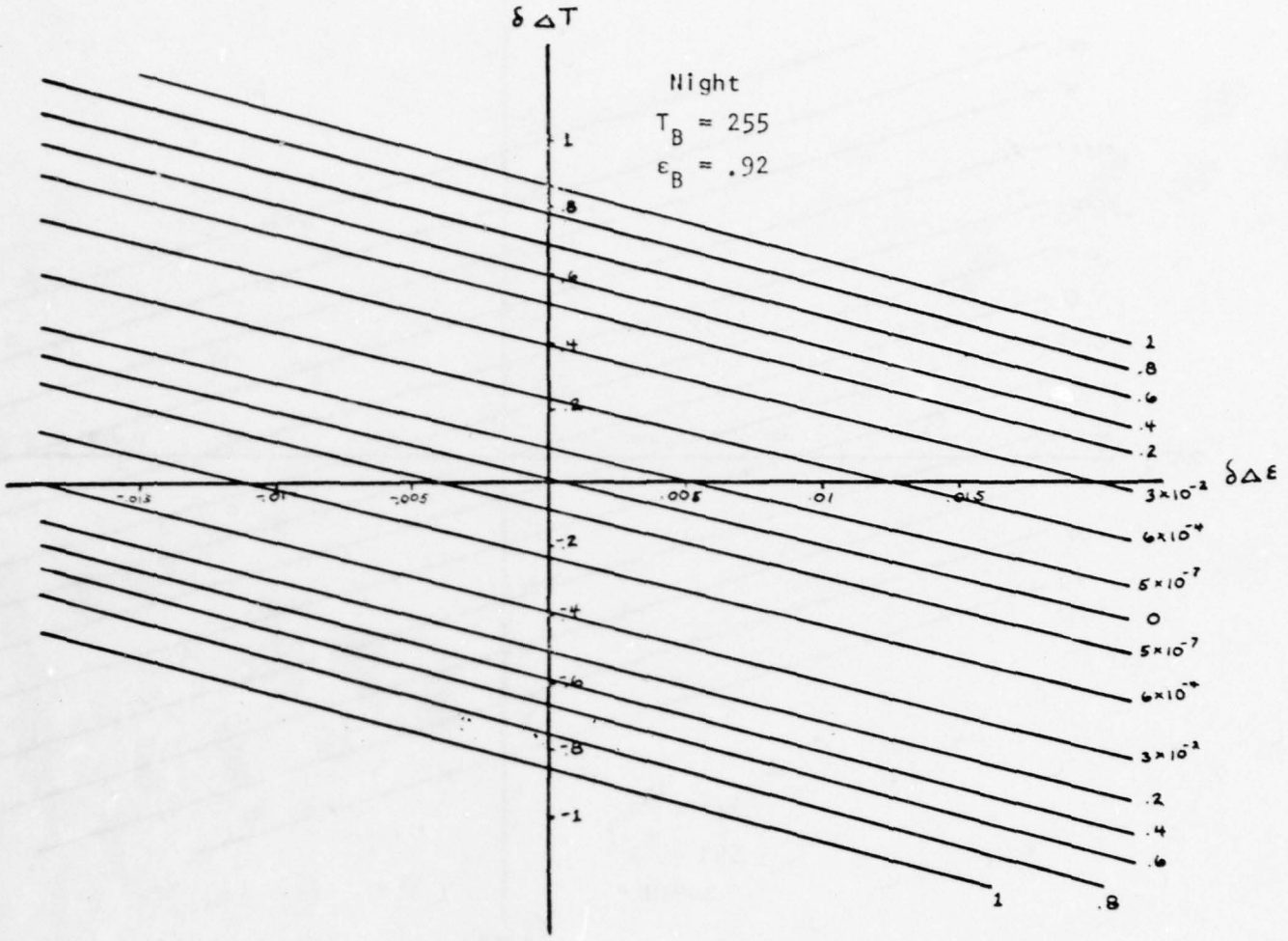

Figure 4-3. Differential sensitivity plot. Parameter is probability of detection.

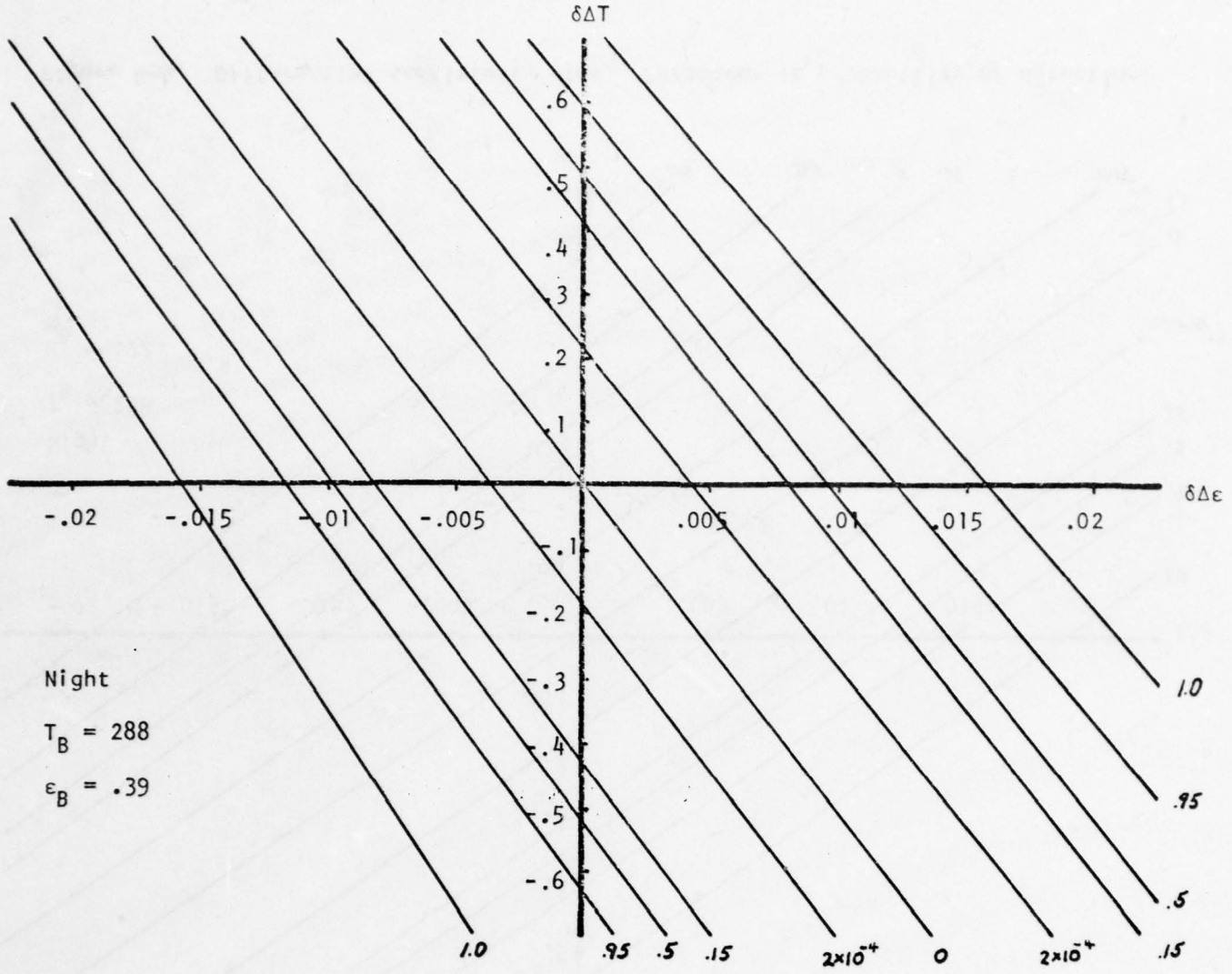

Figure 4-4. Differential sensitivity plot. Parameter is probability of detection.

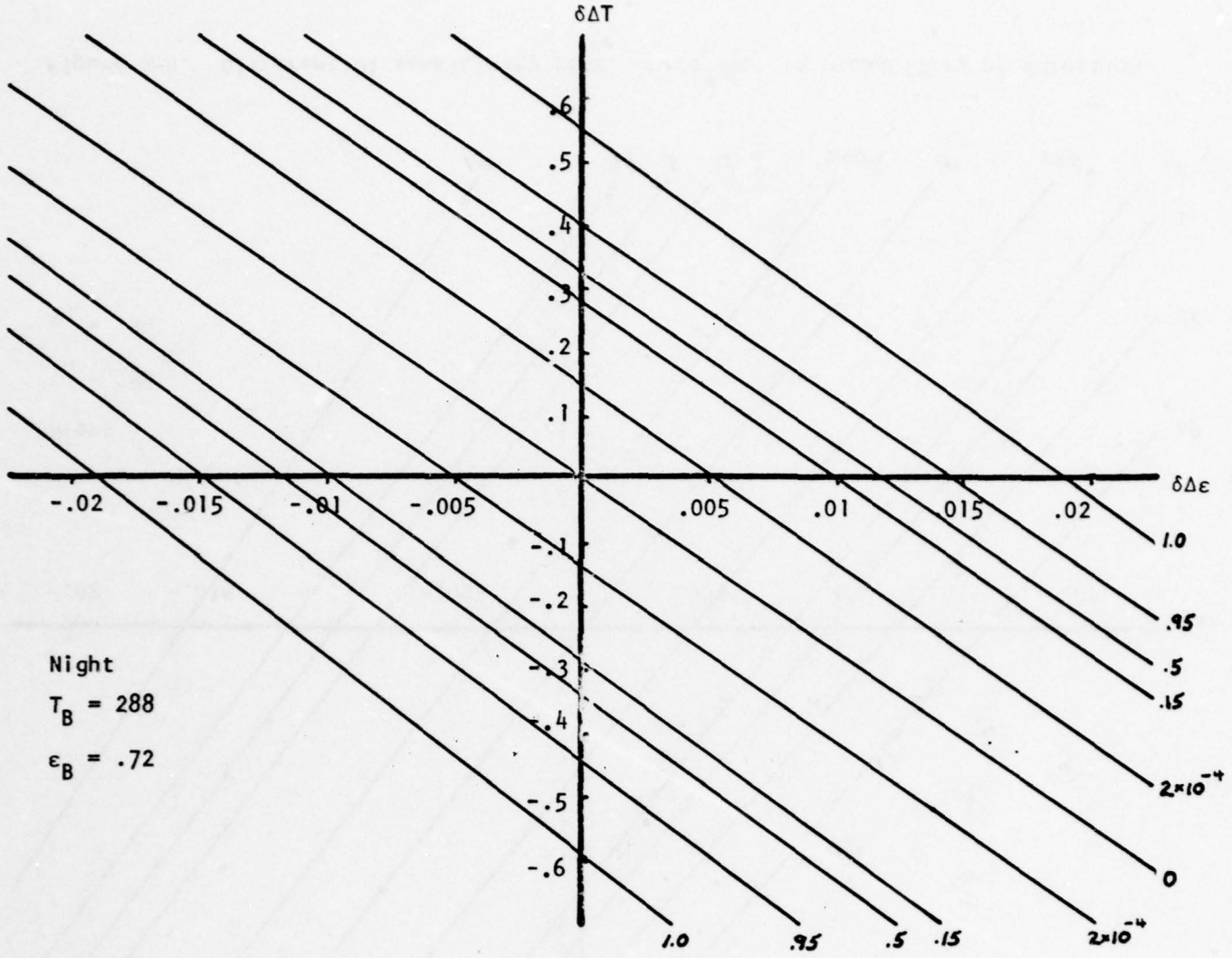

Figure 4-5. Differential sensitivity plot. Parameter is probability of detection.

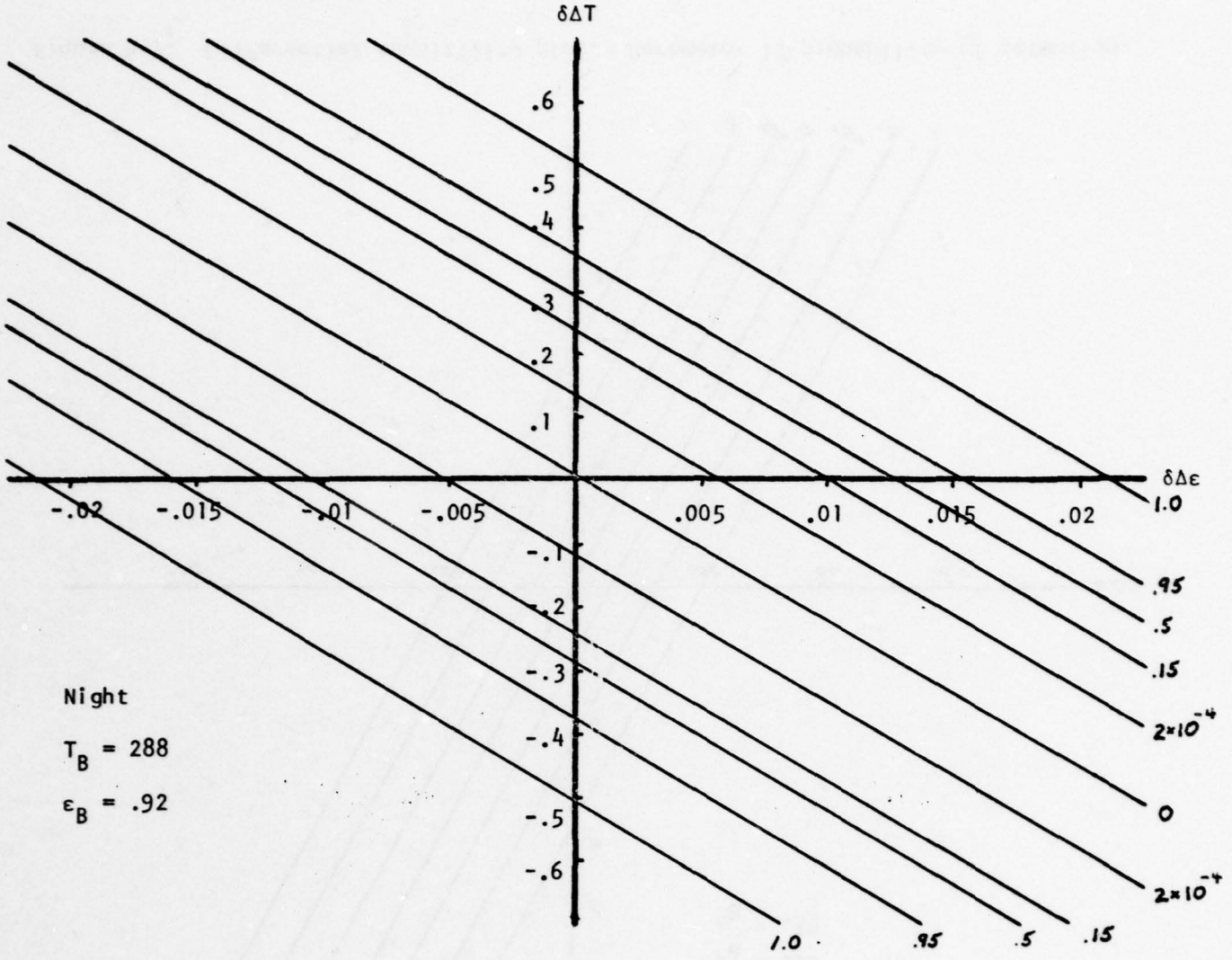

Figure 4-6. Differential sensitivity plot. Parameter is probability of detection.

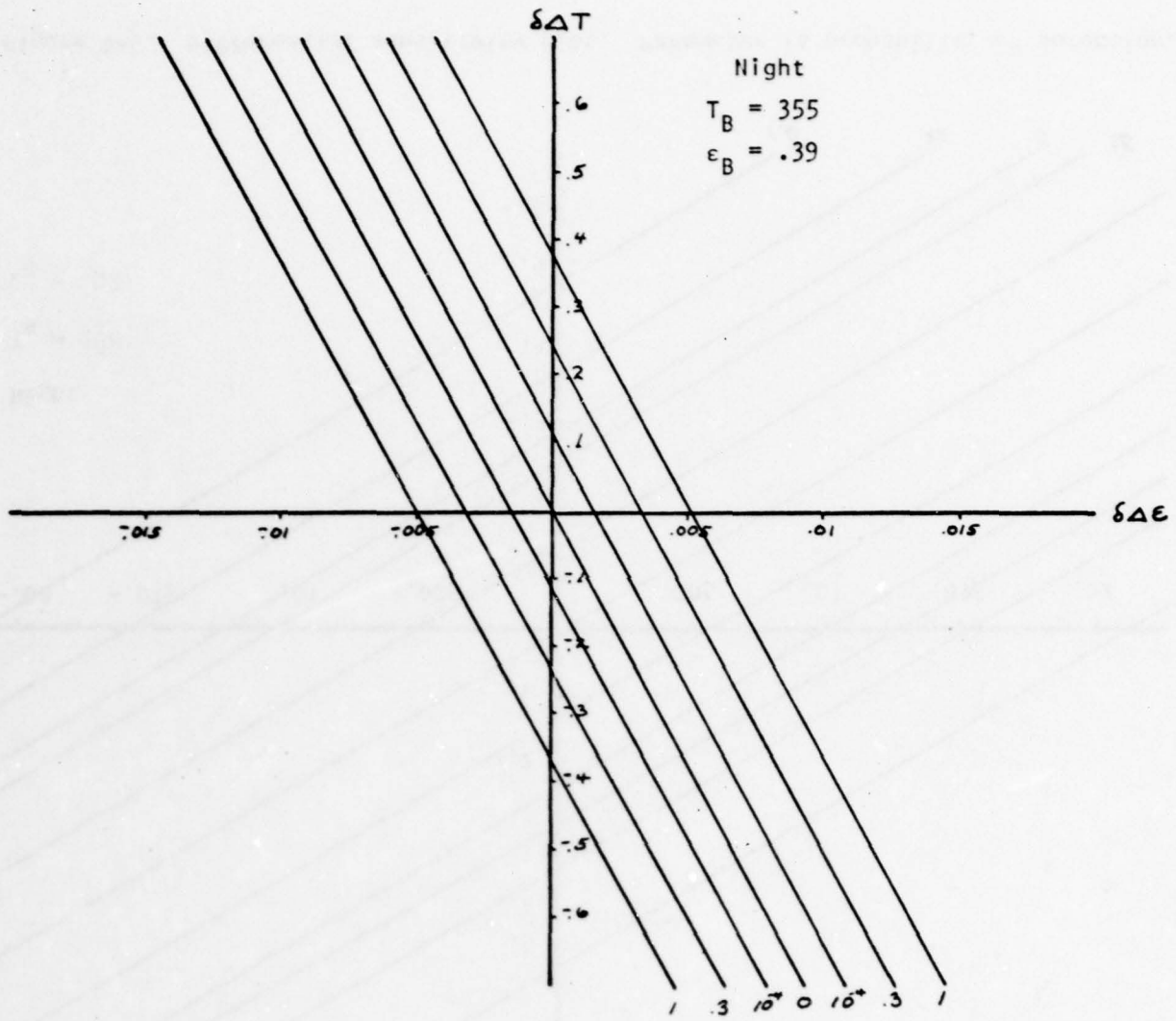

Figure 4-7. Differential sensitivity plot. Parameter is probability of detection.

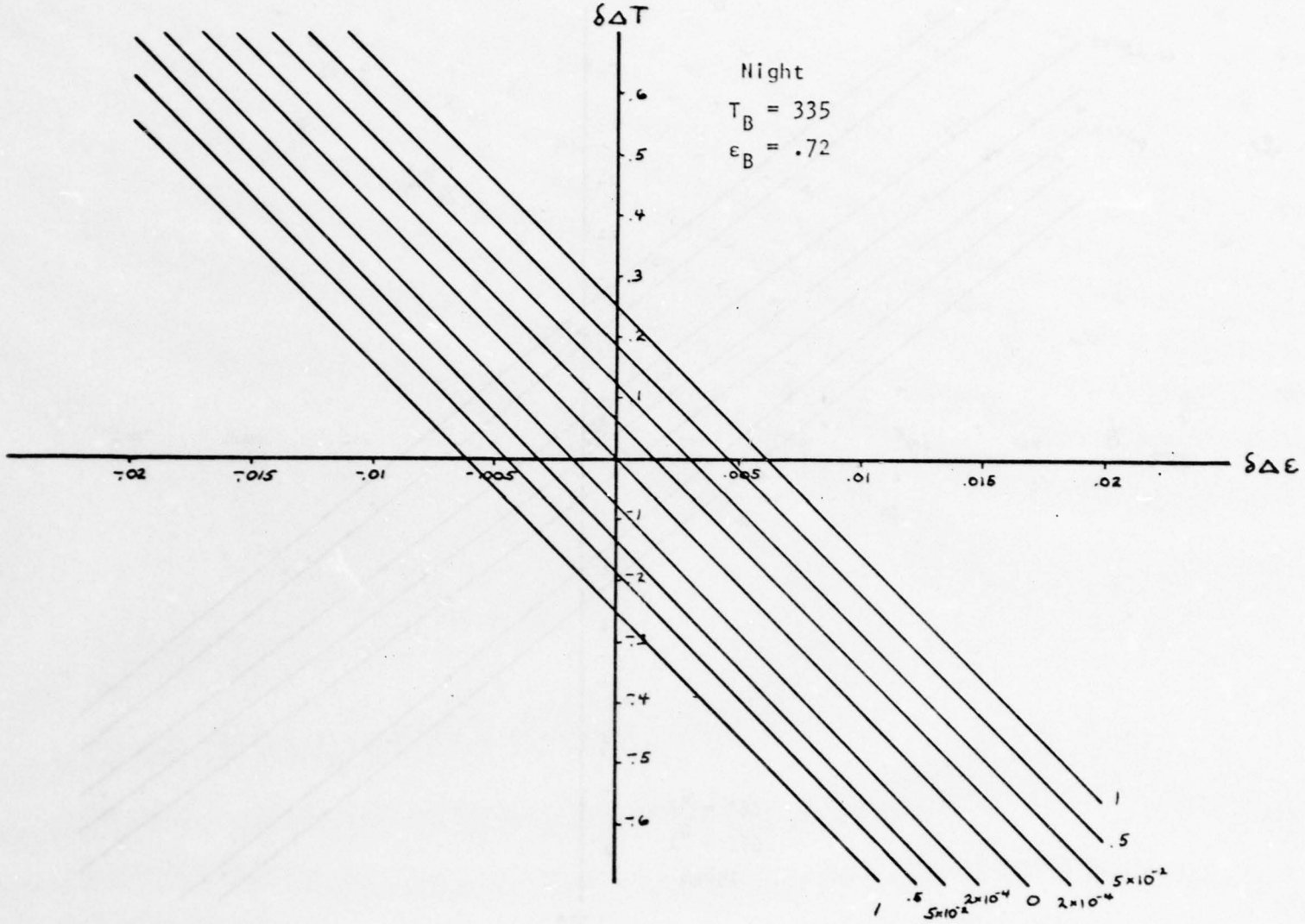

Figure 4-8. Differential sensitivity plot. Parameter is probability of detection.

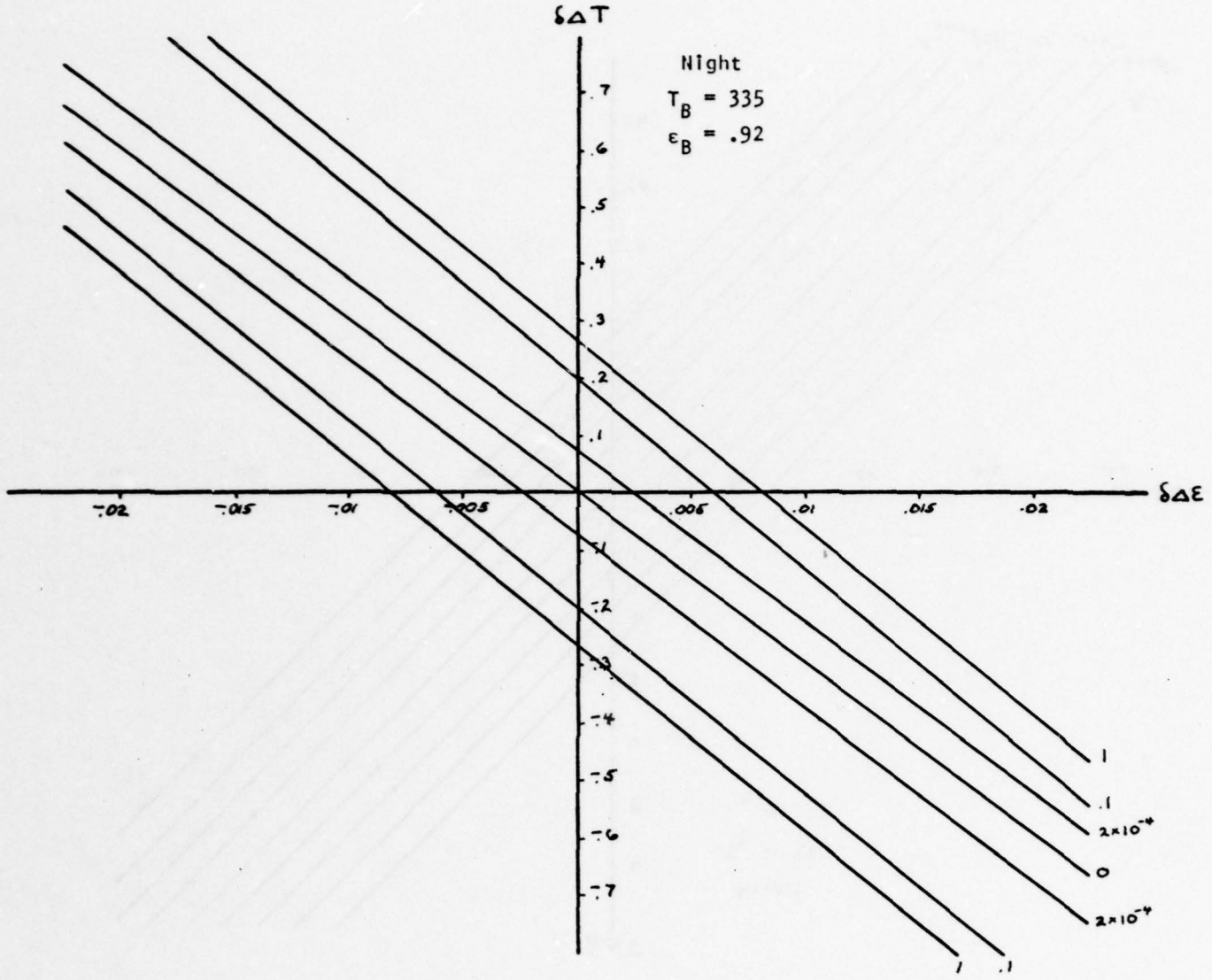

Figure 4-9. Differential sensitivity plot. Parameter is probability of detection.

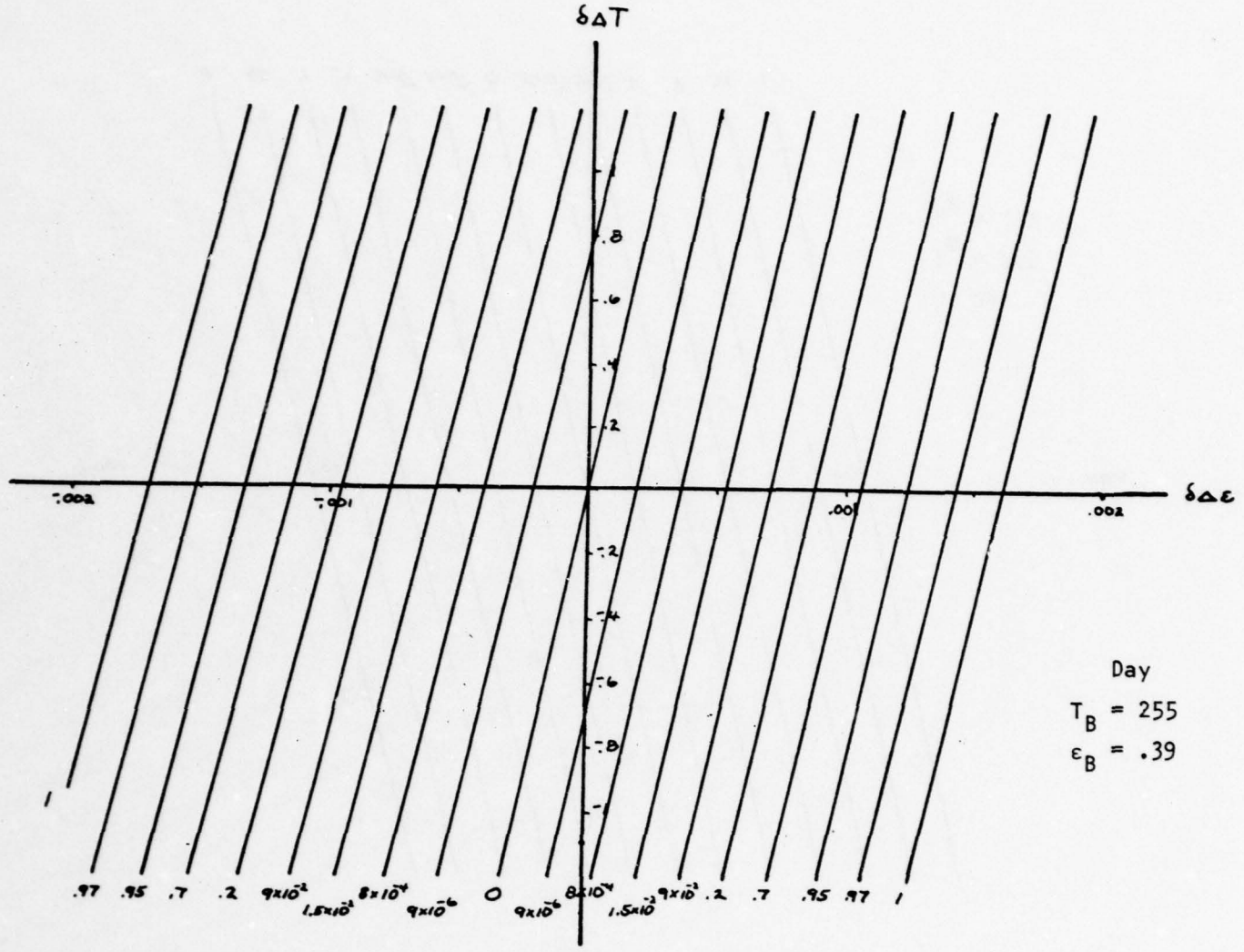

Figure 4-10. Differential sensitivity plot. Parameter is probability of detection.

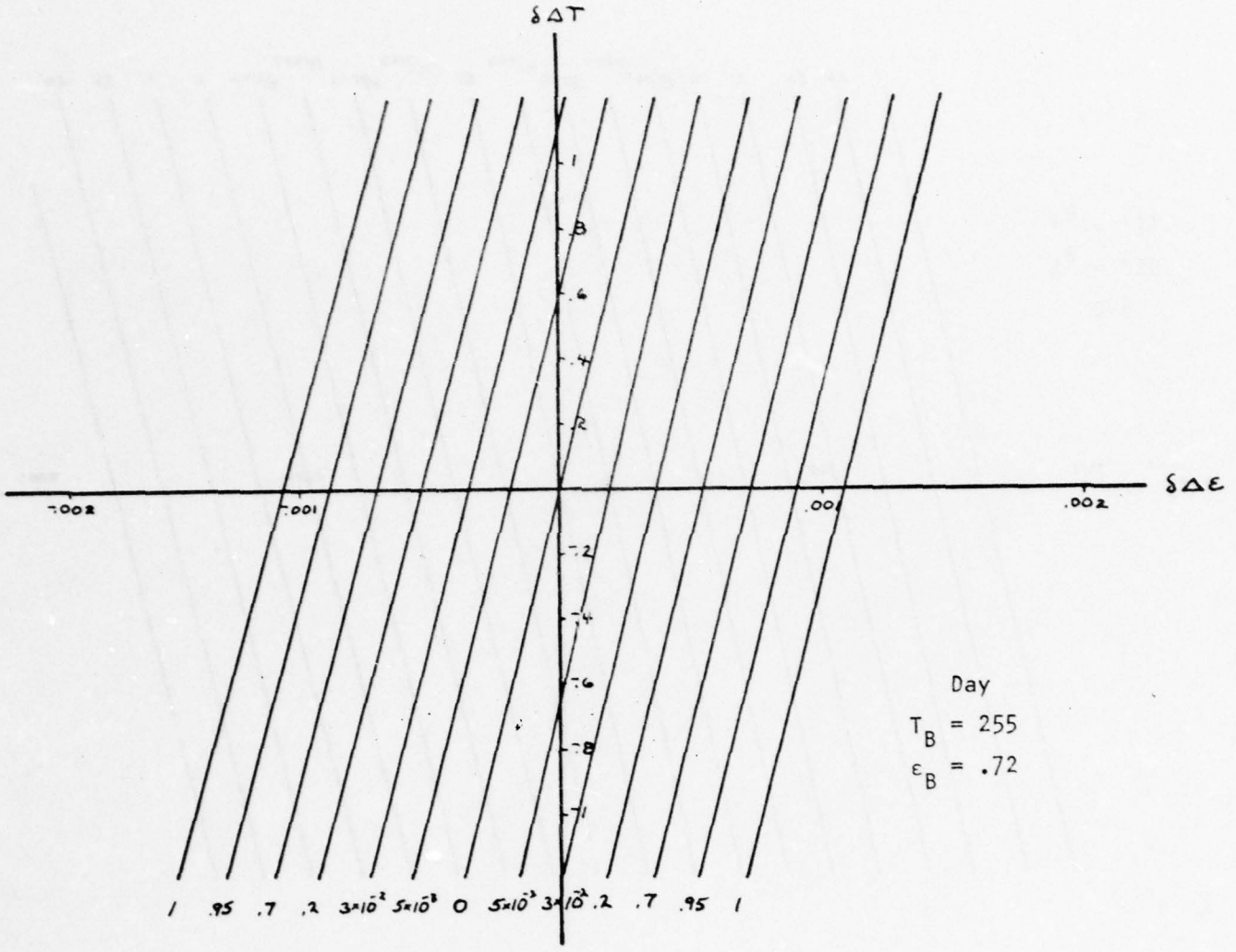

Figure 4-11. Differential sensitivity plot. Parameter is probability of detection.

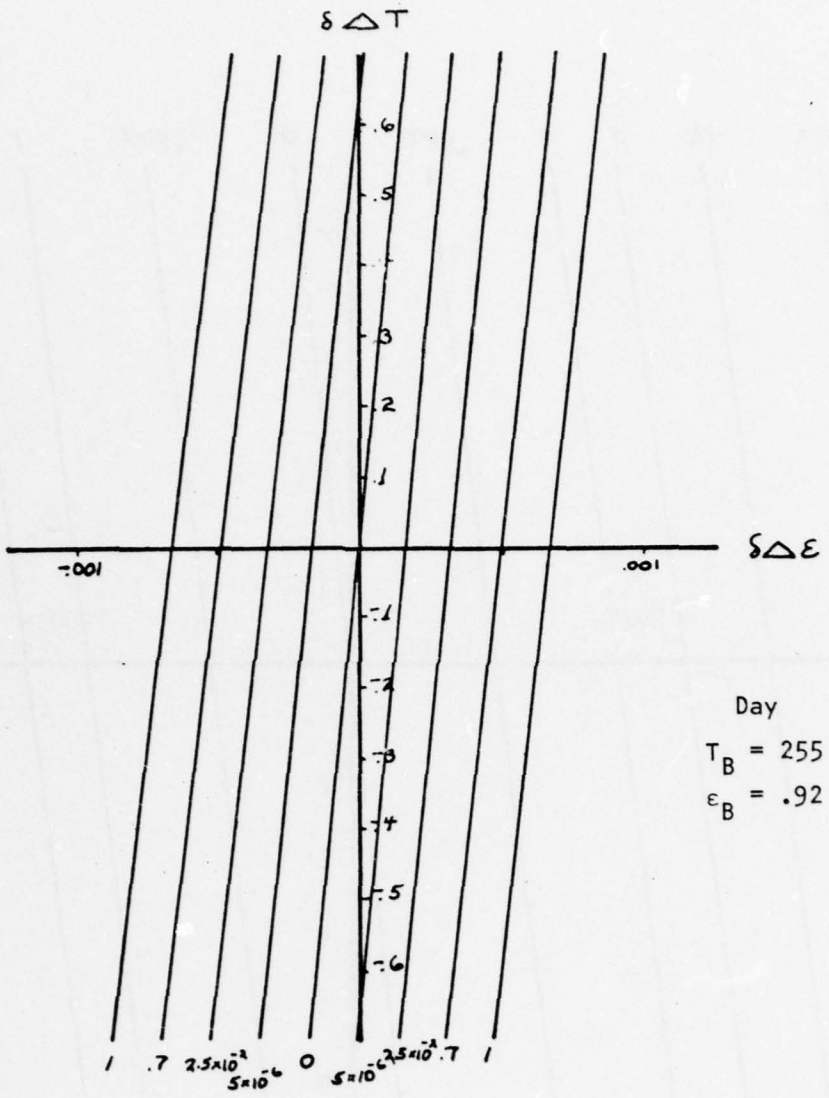

Figure 4-12. Differential sensitivity plot. Parameter is probability of detection.

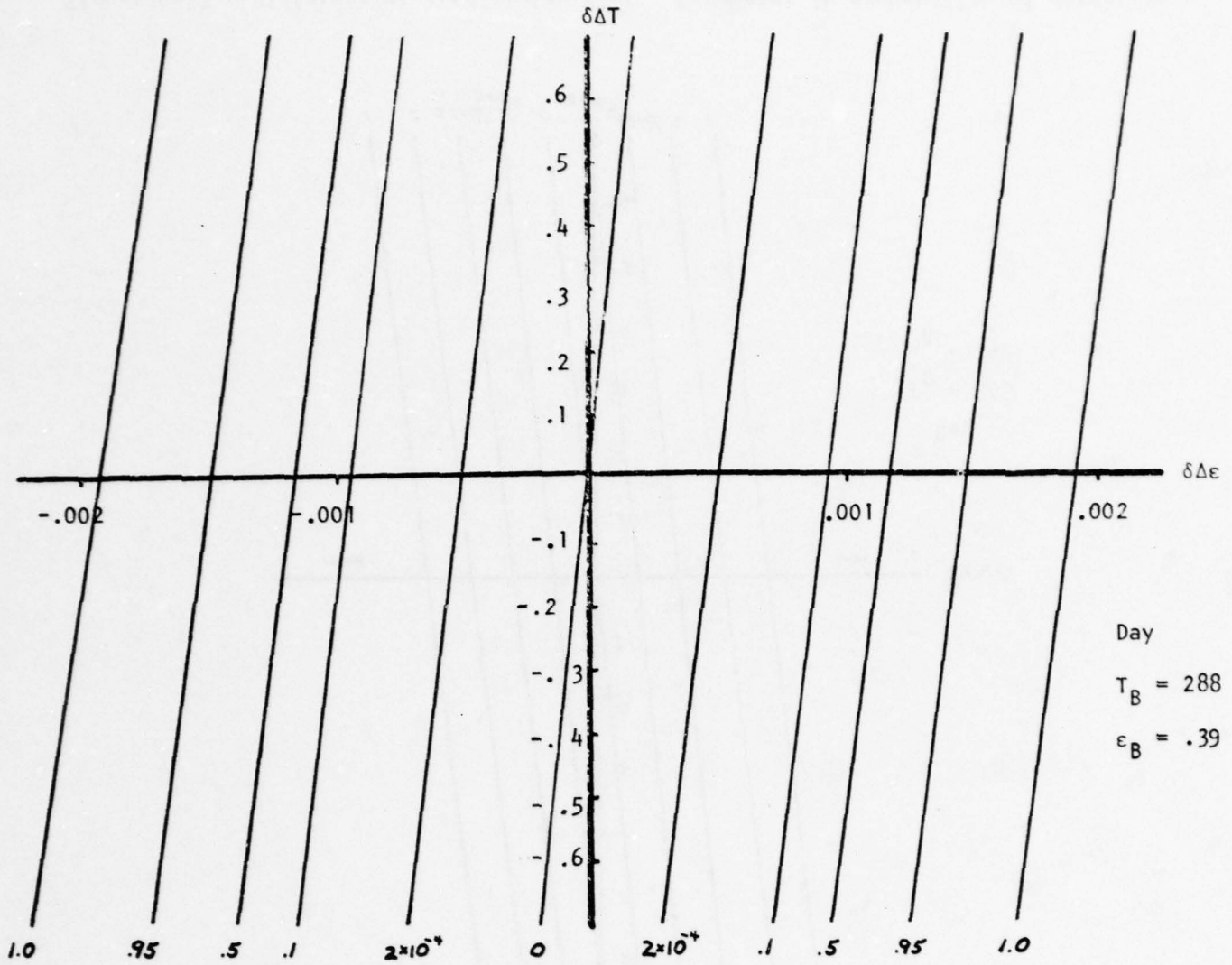

Figure 4-13. Differential sensitivity plot. Parameter is probability of detection.

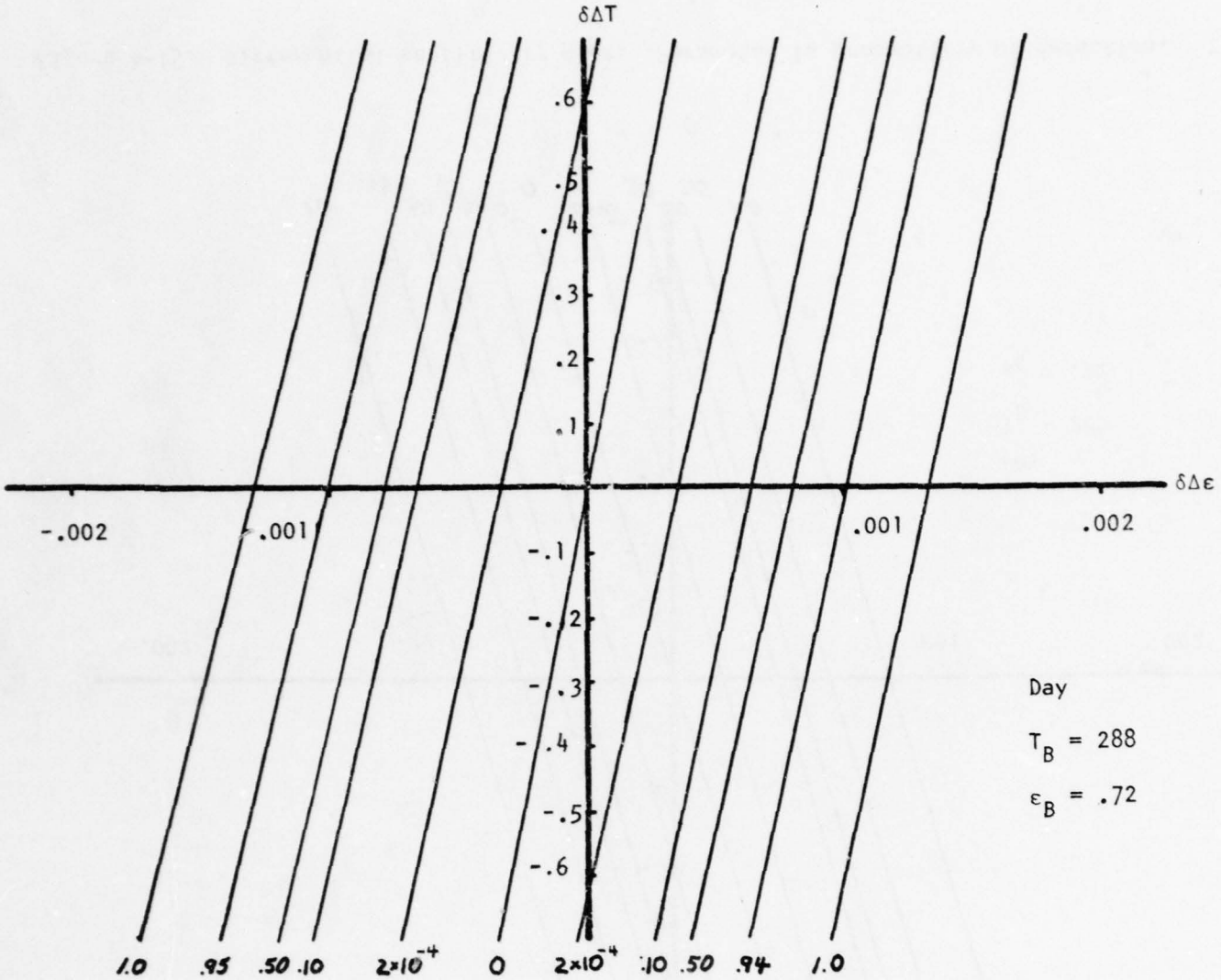

Figure 4-14. Differential sensitivity plot. Parameter is probability of detection.

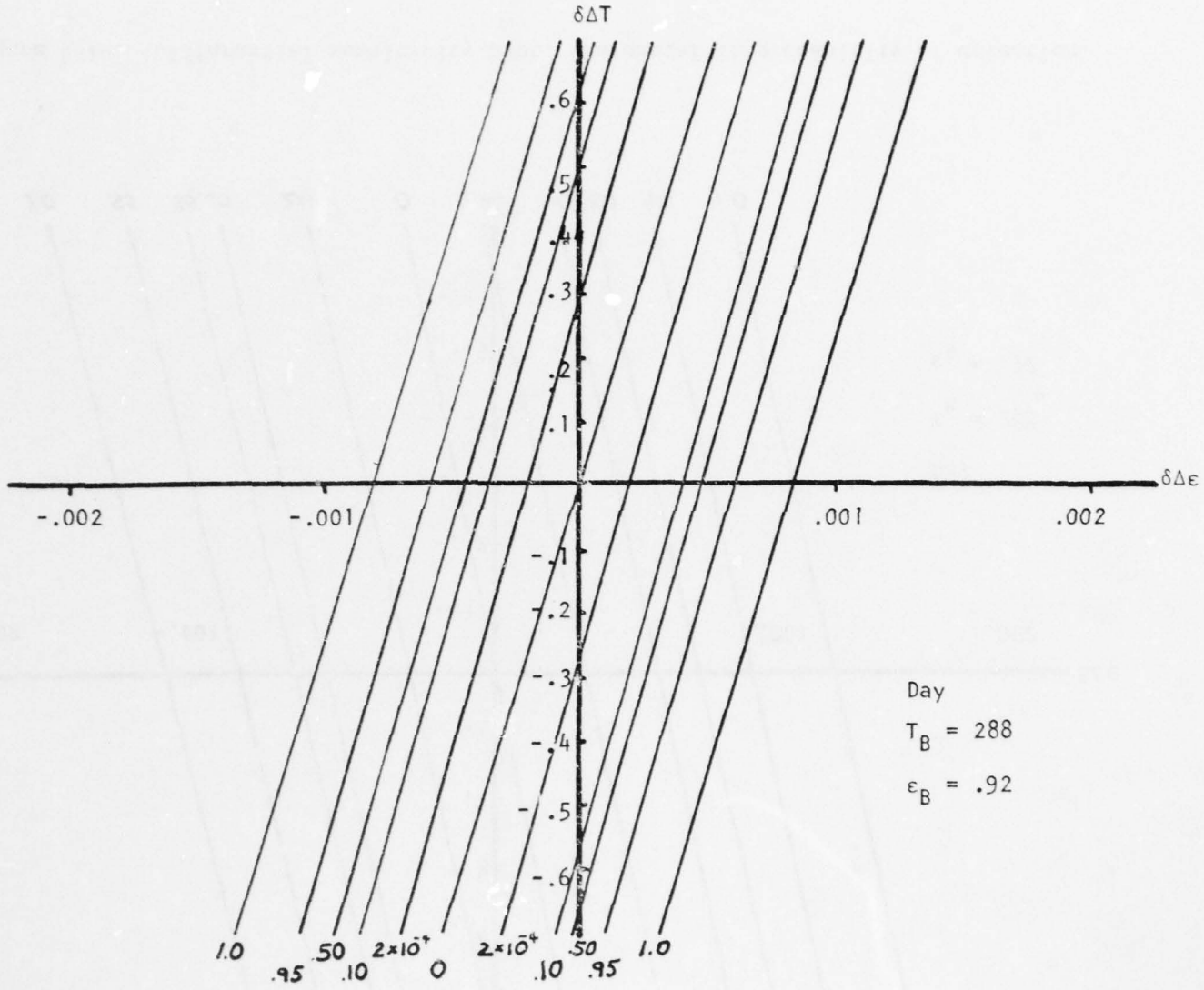

Figure 4-15. Differential sensitivity plot. Parameter is probability of detection.

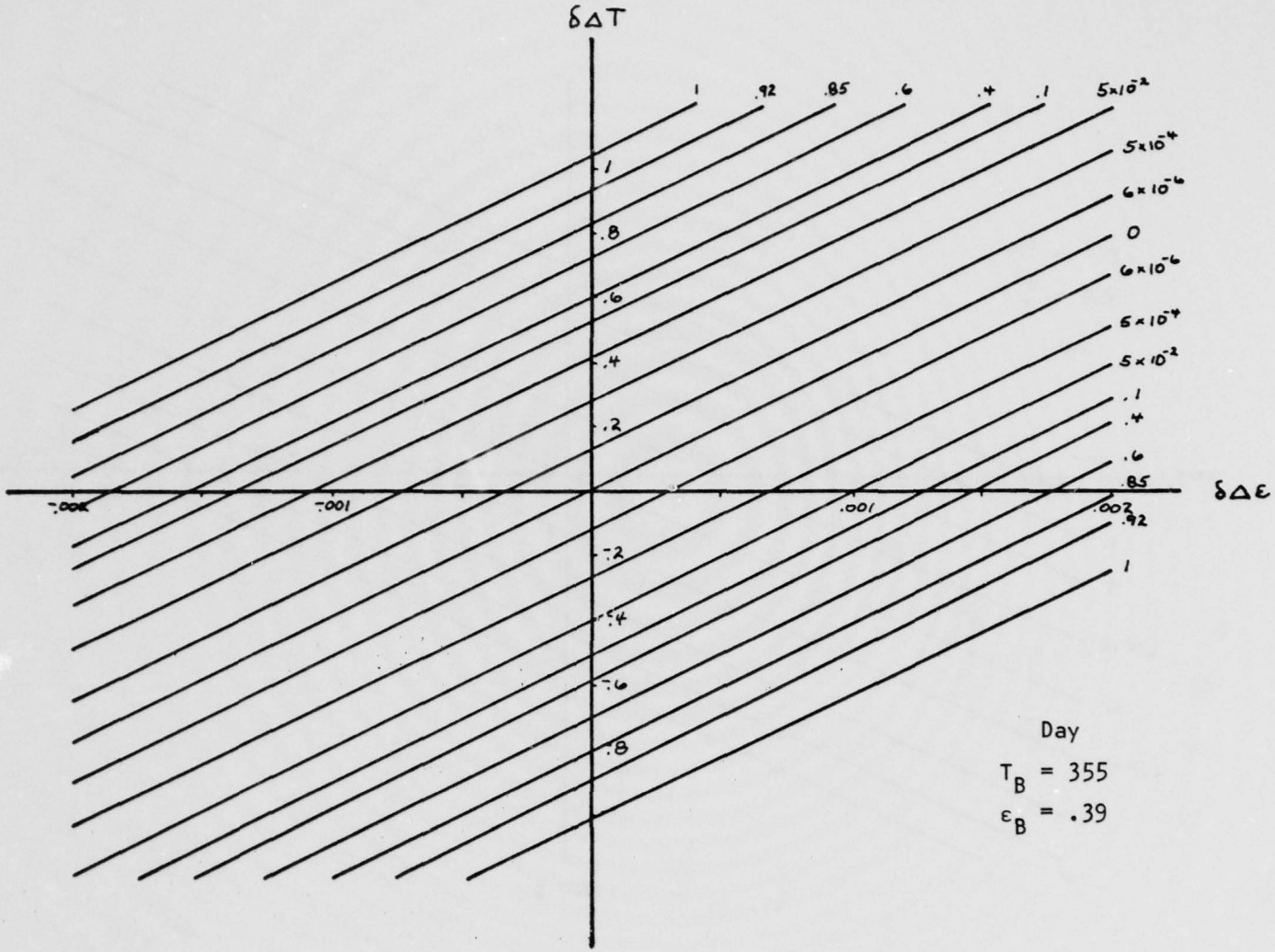

Figure 4-16. Differential sensitivity plot. Parameter is probability of detection.

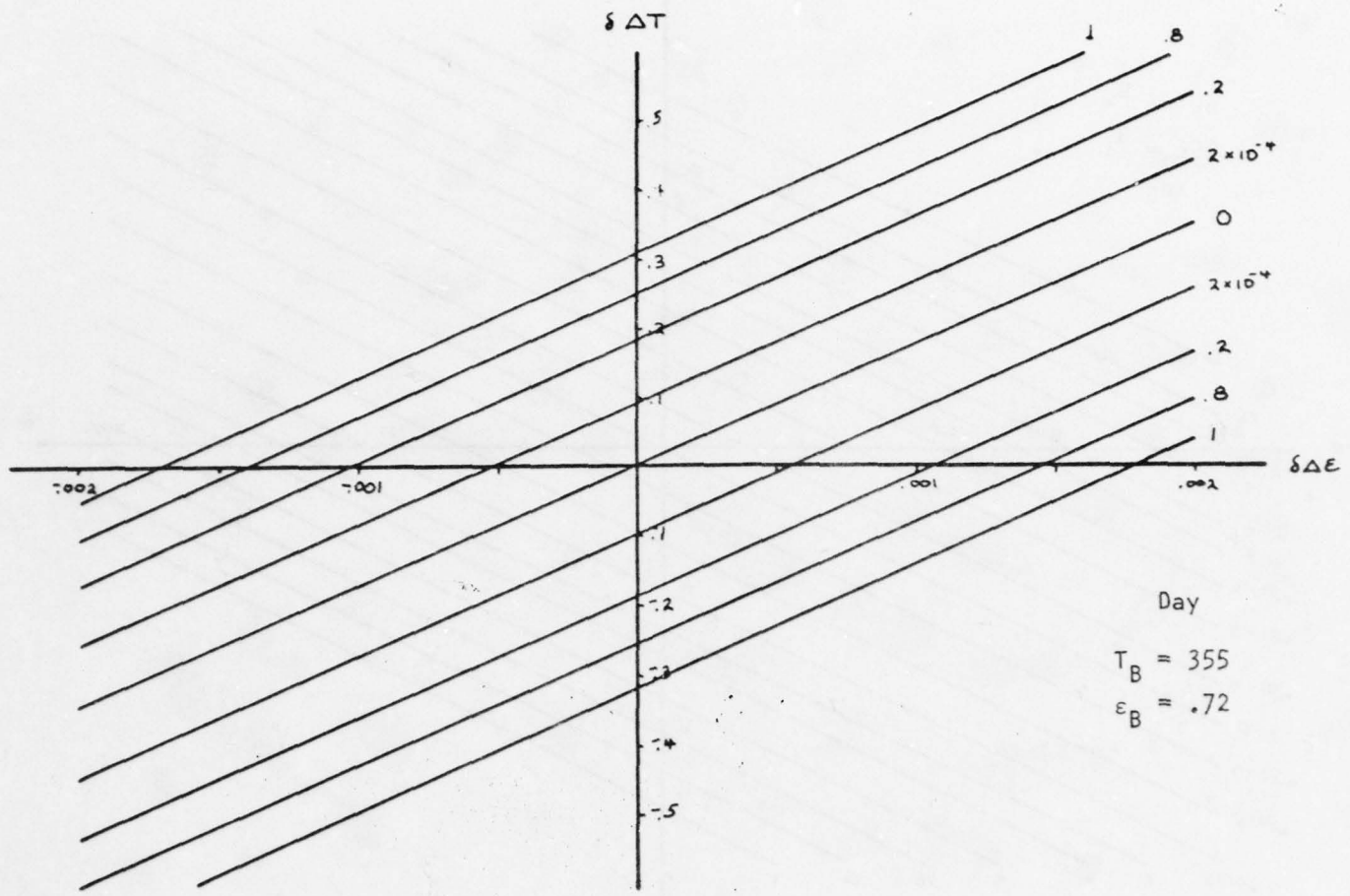

Figure 4-17. Differential sensitivity plot. Parameter is probability of detection.

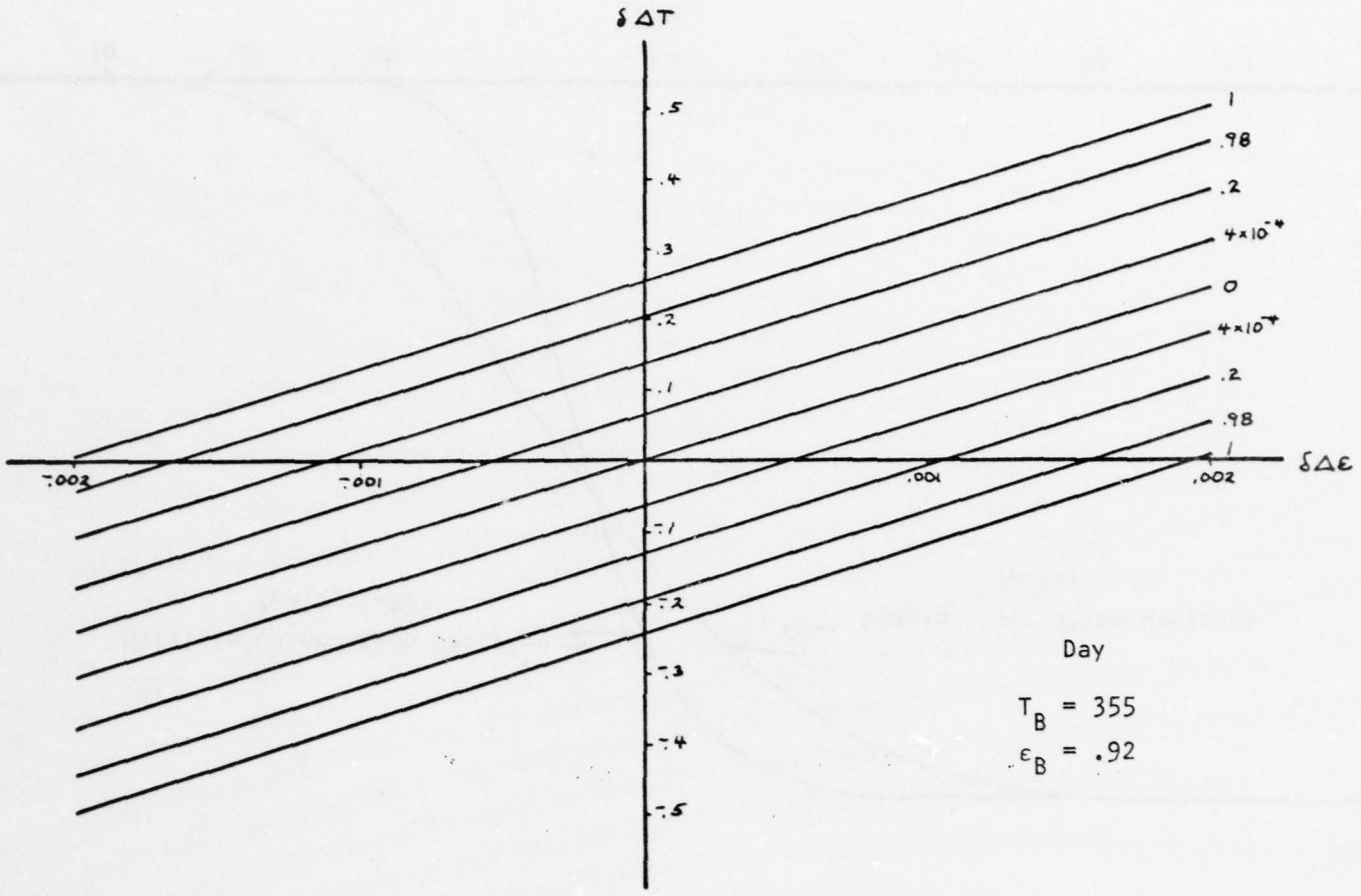

Figure 4-18. Differential sensitivity plot. Parameter is probability of detection.

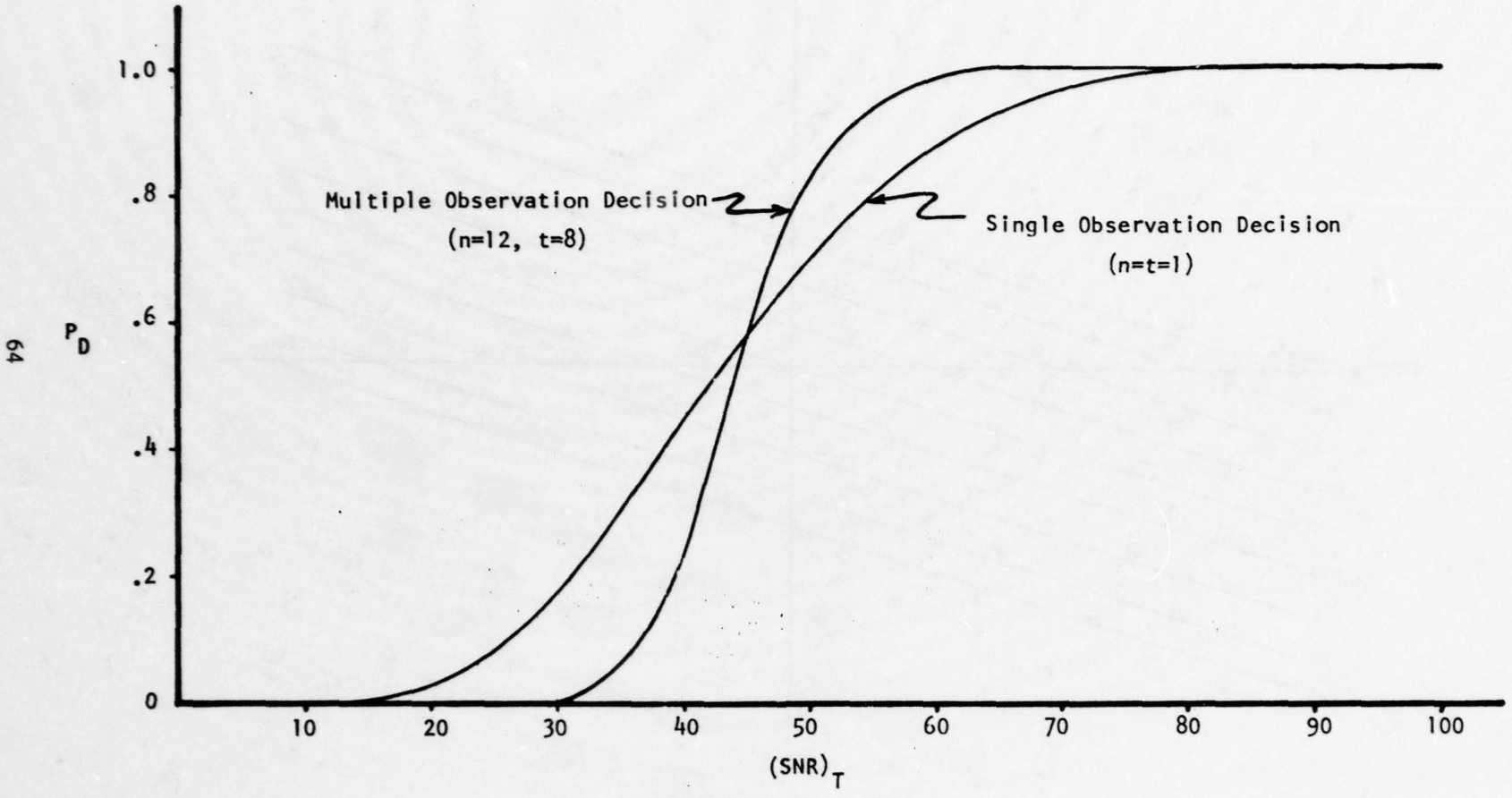

Figure 4-19. Probability of detection as a function of signal-to-noise ratio in each observation.

2.4.3. Target and Background Models.

The purpose of this section is to tabulate the models for the targets and backgrounds that were used to evaluate the performance of the proposed system.

The targets are modeled by rectangular parallelepipeds whose dimensions are seclected to approximate the target's size. They are assumed to enter the detector's field of view with a specified velocity and a specified angle as shown in Fig. 4-20. Their emissivity and temperature are selected to correspond to the physical characteristics of the surface. The data were obtained from a variety of the references listed at the end of this report.

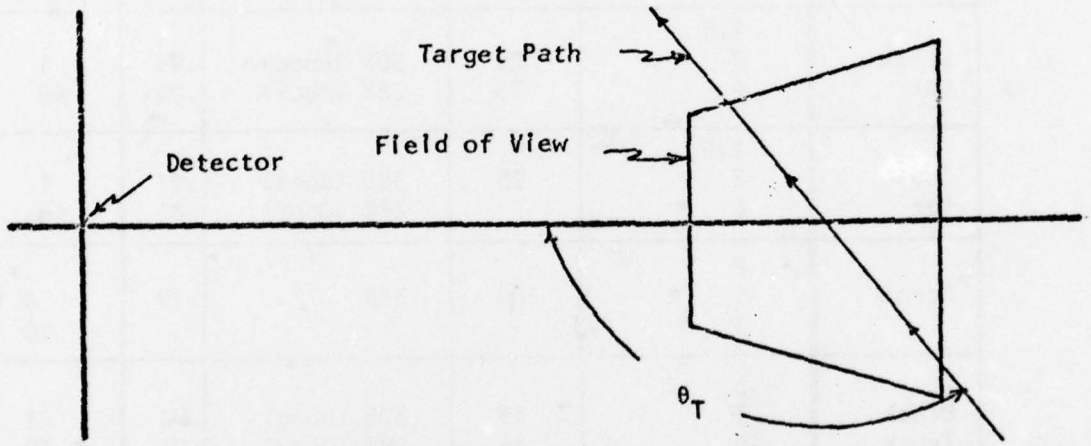

Fig. 4-20. Motion of target through the field of view of a single cell.

For some target models it was found to be appropriate to consider different parts of the surface to be at different temperatures or emissivities. These characteristics, as well as the dimensions and emissivities and speeds are tabulated in Table 4-1 for all of the targets considered.

The field of view that was used for most calculations is shown in Fig. 4-21 as a ground projection. This is

Table 4-1. Tabulation of Target Models.

Target	Dimensions (m) Height Width Length	Temperature, Emissivity and Percent Area			Speed Range m/s
		%	T_T (°K)	ε_T	
Squirrel	0.1 0.1 0.3	60 40	305 (Body) 288 (Tail)	.79 .79	0.1 1.0
Dog	0.6 0.2 1	100	305	.79	0.1 5.0
Man Crawling	0.8 0.6 2	20 80	305 (Skin) 288 (Clothing)	.98 .80	0.025 1.0
Man Walking	2 0.6 0.3	20 80	305 (Skin) 288 (Clothing)	.98 .80	0.1 10
Black Car	1.5 2 6	25 75	305 (Hood) 288 (Body)	.94 .94	1 40
Red Car	1.5 2 6	25	305 (Hood) 288 (Body)	.81 .81	1 40
Horse	2 1 3	100	305	.79	0.1 10
Black Truck	3 3 10	15 85	305 (Hood) 288 (Body)	.94 .94	1 30

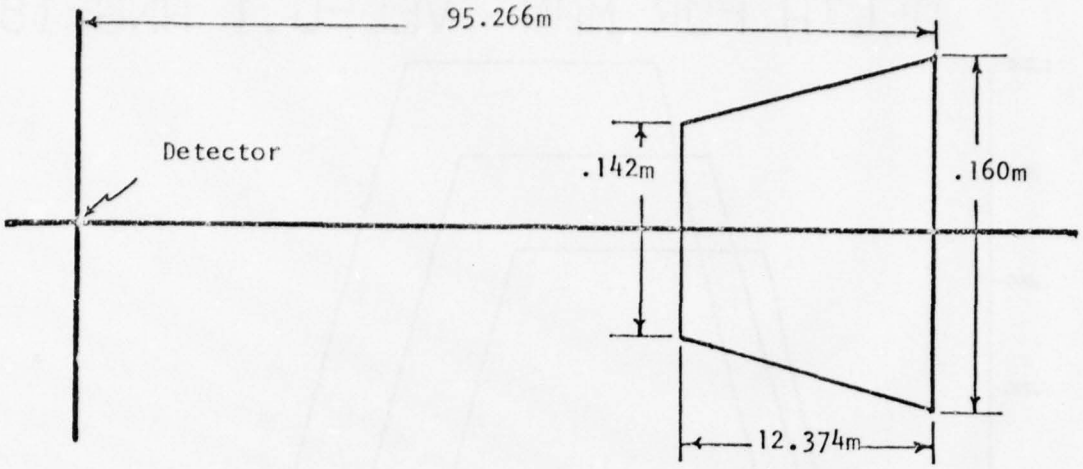

Fig. 4-21. Ground projection of field of view.

based on the cell size and optics as shown in Fig. 4-22.

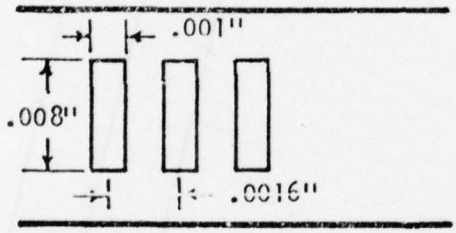

Lense System

f.ℓ. = 1.7 cm

f/1

Fig. 4-22. Detector cell size and optical system.

As a means of obtaining some feeling for the length of time that a target is in the field of view of a given cell, and the fraction of the total area that it covers, a computer program was developed to plot this information. Figures 4-23 through 4-28 display the fractional area, δ, as a function of time, for three adjacent cells. Thus, not only is the length of time the target is in any one cell apparent, but the time displacement from one cell to the next is evident. This information is relevant when it is recalled that the final decision operation is based on the responses of three adjacent cells.

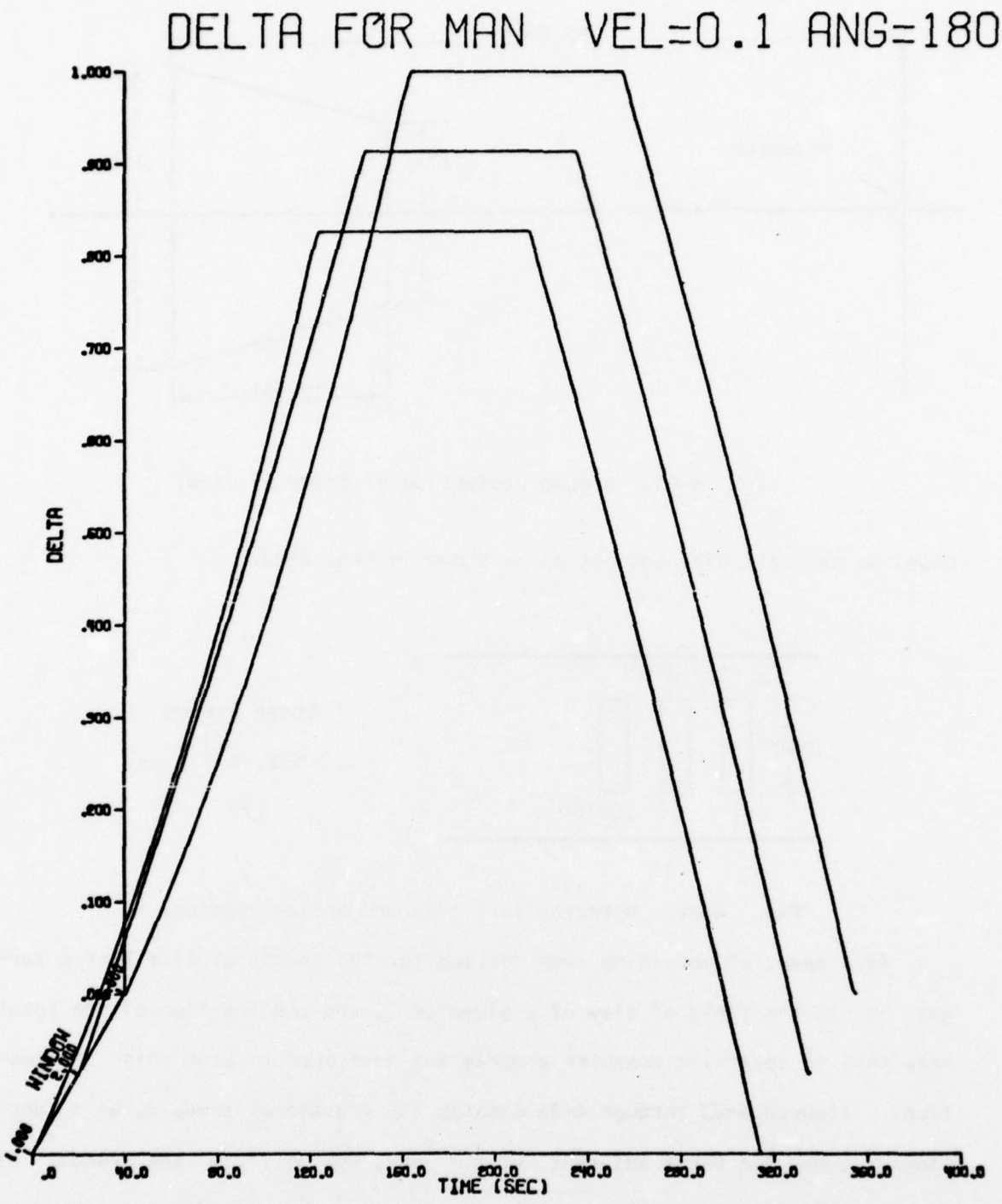

Figure 4-23. Fractional area of target in three adjacent cells.

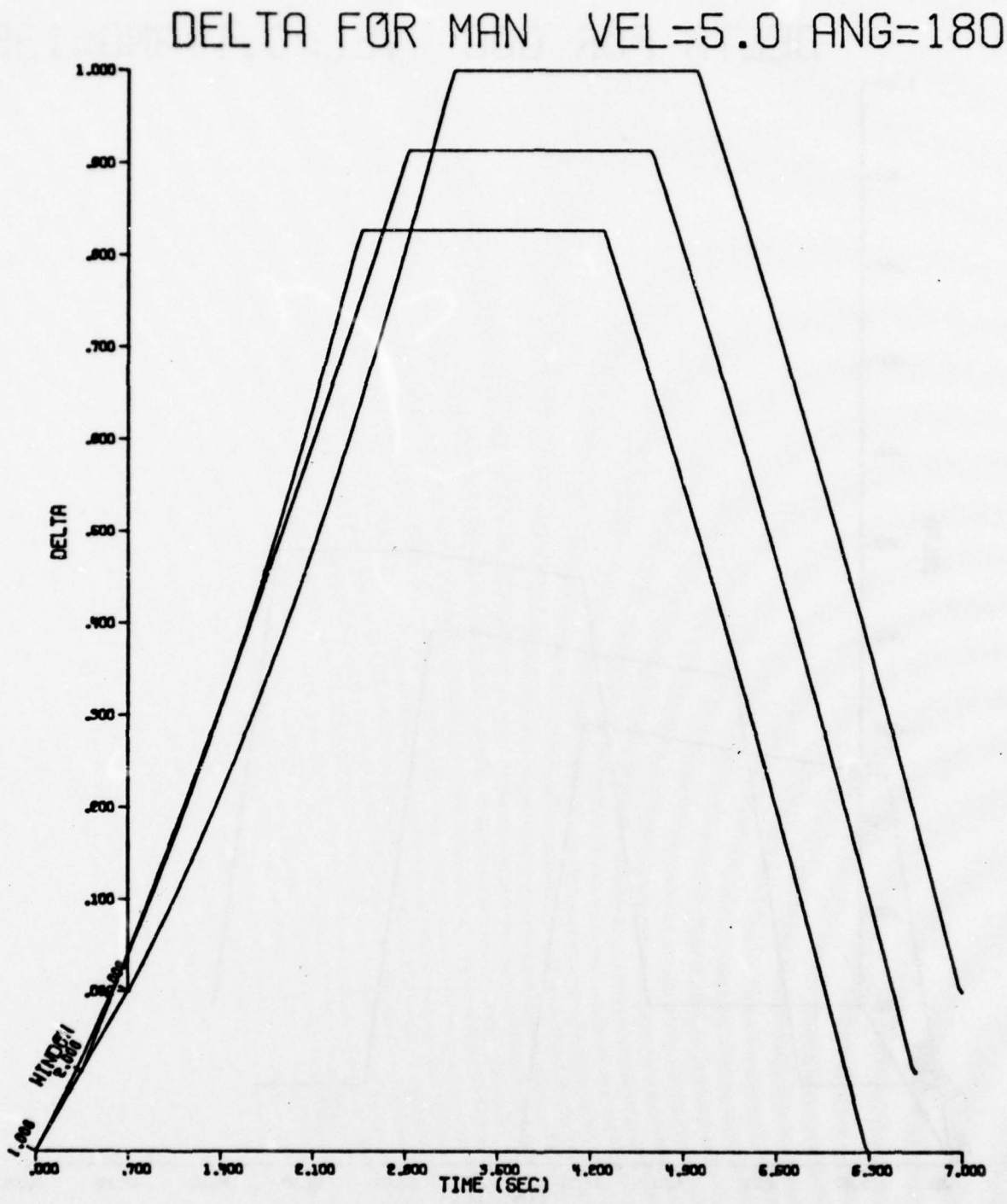

Figure 4-24. Fractional area of target in three adjacent cells.

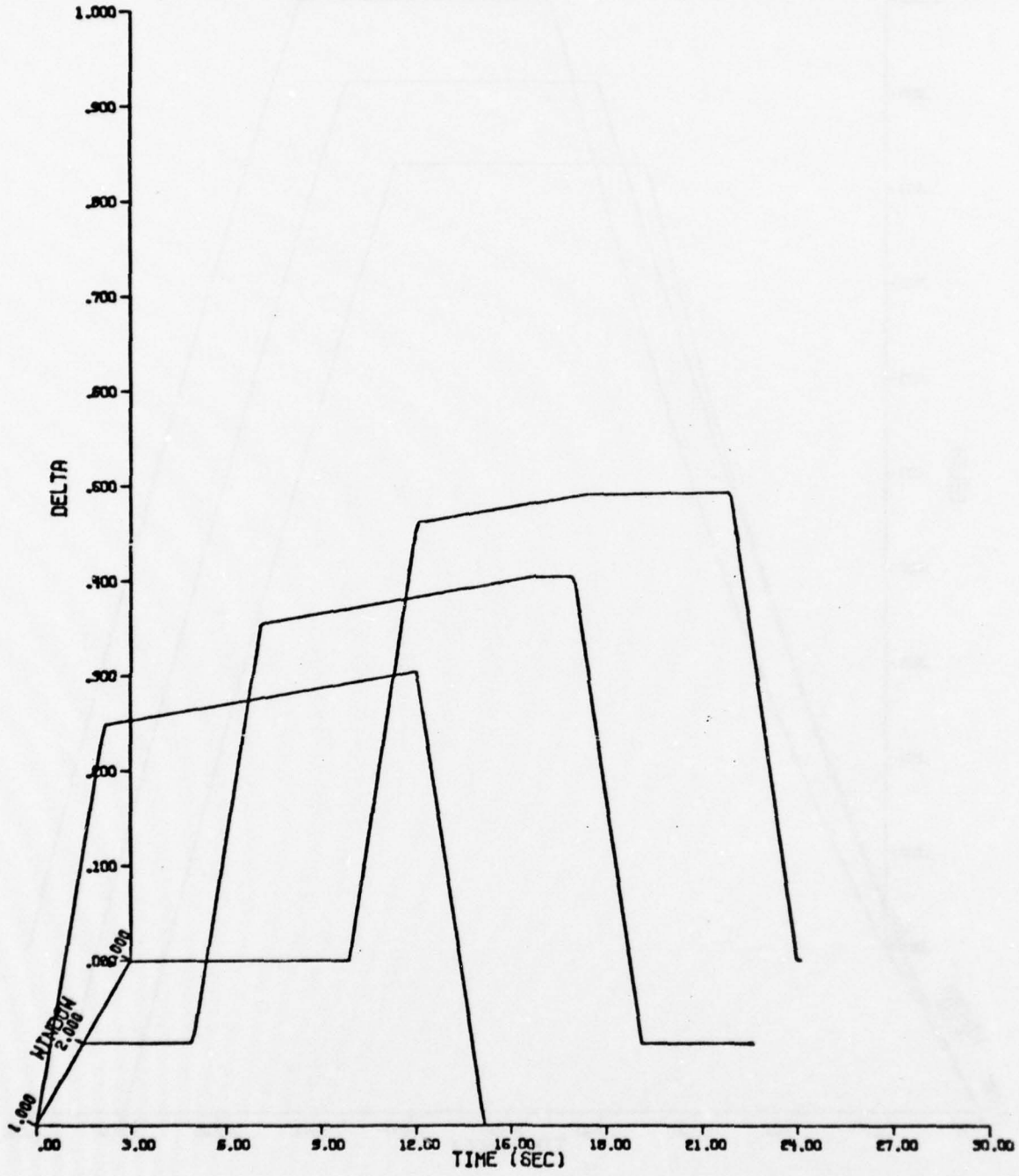

Figure 4-25. Fractional area of target in three adjacent cells.

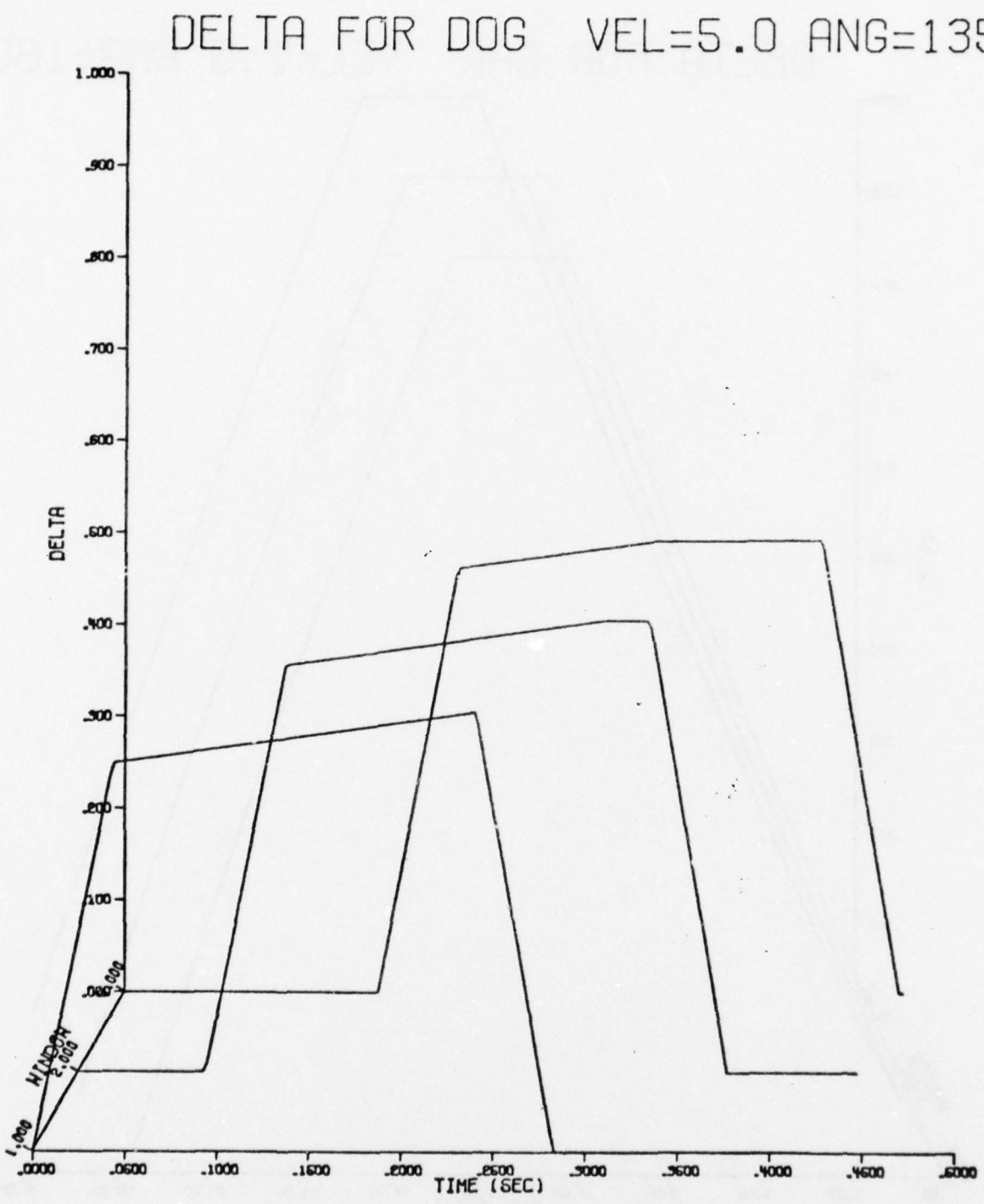

Figure 4-26. Fractional area of target in three adjacent cells.

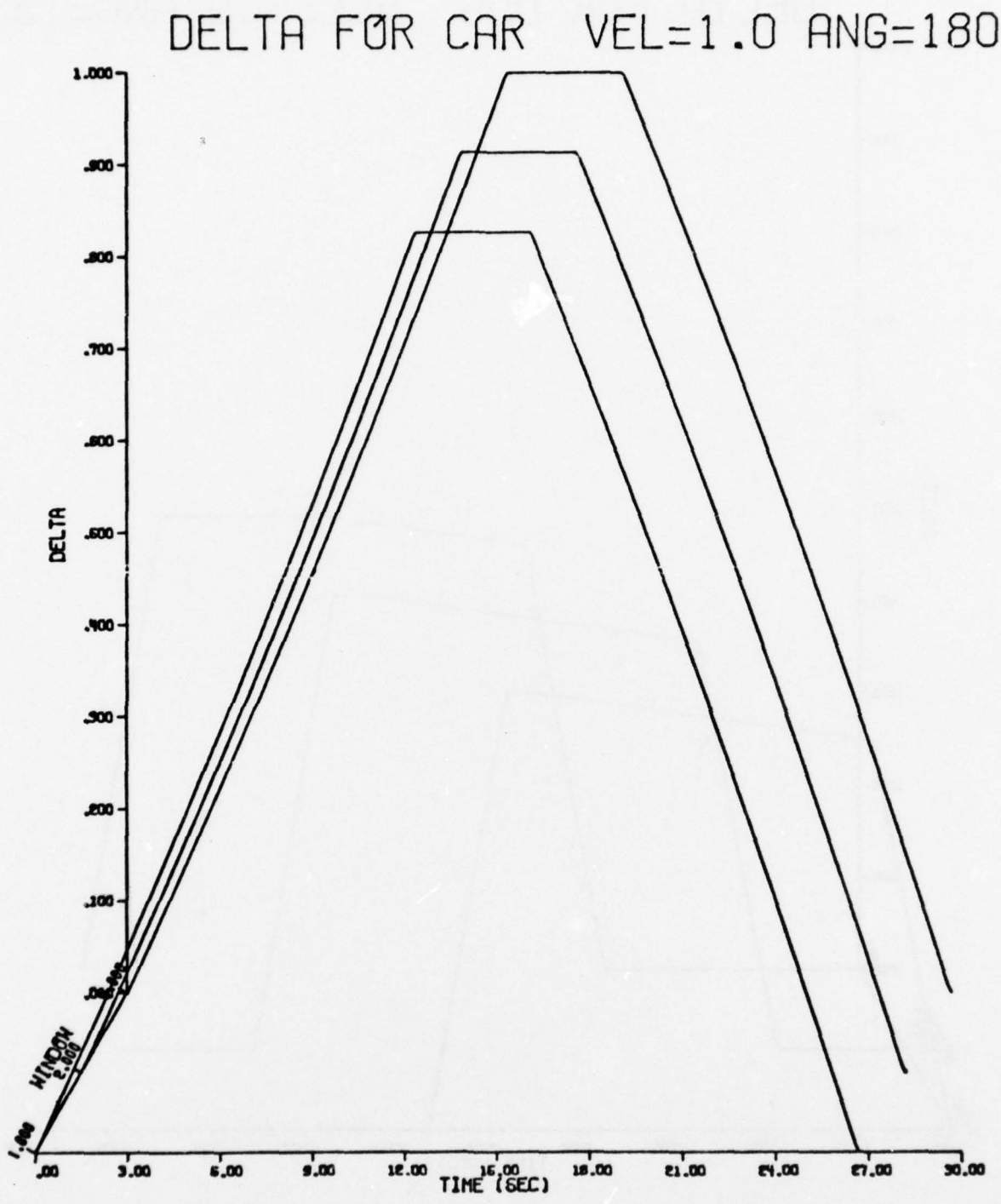

Figure 4-27. Fractional area of target in three adjacent cells.

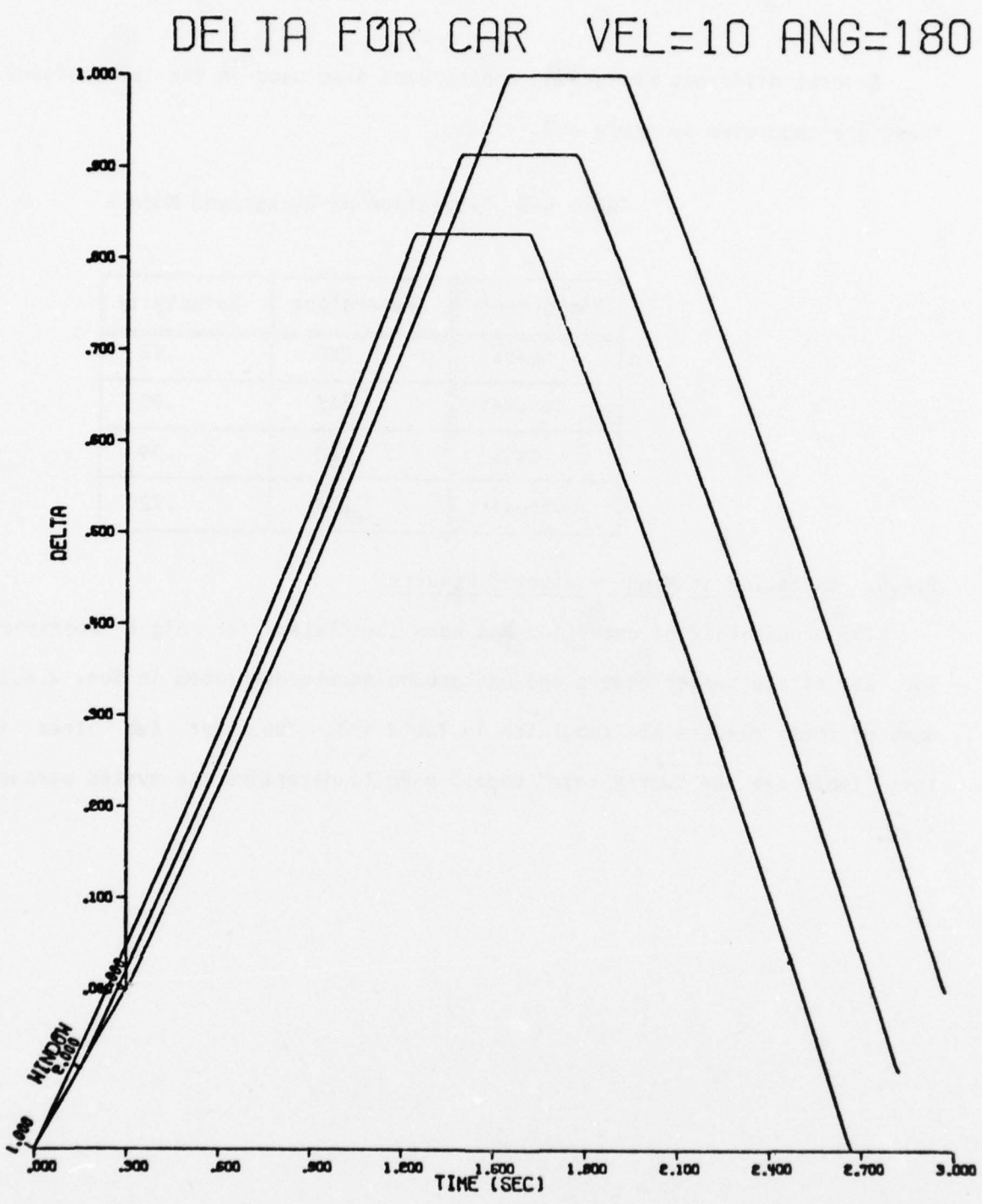

Figure 4-28. Fractional area of target in three adjacent cells.

Several different background models were also used in the calculations. These are tabulated in Table 4-2.

Table 4-2 Tabulation of Background Models

Background	Temperature	Emissivity
Grass	288	.92
Concrete	316	.95
Soil	288	.39
Composite	294	.72

2.4.4. Operation at Night--Selected Results

The probability of detection has been calculated for night operation for all of the target models and background models described in Sec. 2.4.3. Some of these results are tabulated in Table 4-3. The first two items in this table are the "worst case" models used to determine the system parameters.

Table 4-3. Selected Results for Night Operation

Target	Background	Angle of Entry	Speed m/s	P_D
Squirrel	Soil	90^o	1	5.6×10^{-8}
		180^o	1	6.9×10^{-10}
Man Crawling	Grass	90^o, 157.5^o, 180^o	1	1.0
		157.5^o, 180^o	.025	1.0
Black Car	Any	90^o, 180^o	30	1.0
Red Car	Any	90^o, 180^o	30	1.0
Dog	Grass	90^o	1	1.0
		180^o	.025	1.0

2.4.5 Operation in Daylight--Selected Results

The probability of detection has been calculated for daylight operation (assuming bright sunlight) for all of the target models and background models. Some of these results are tabulated in Table 4-4.

Table 4-4. Selected Results for Day Operation

Target	Background	Angle of Entry	Speed m/s	P_D
Squirrel	Soil	90^o	1	2.54×10^{-2}
		180^o	1	4.97×10^{-14}
Man Crawling	Grass	90^o, 157.5^o, 180^o	1	1.0
		157.5^o, 180^o	.025	1.0
Black Car	Any	90^o, 180^o	30	1.0
Red Car	Any	90^o, 180^o	30	1.0
Dog	Grass	90^o	1	1.0
		180^o	.025	1.0

2.4.6. Consideration of Atmospheric Conditions

The atmospheric attenuation is modeled by an exponential function

$$\tau\ (R,\lambda) = e^{-\alpha(\lambda)R} \qquad (4\text{-}1)$$

where λ = wavelength

$\alpha(\lambda)$ = absorption coefficient

R = range of observation

It has been observed from experimental data that when the wavelength range considered is in the 3.4 μm to 4.2 μm region then the atmospheric attenuation is nearly constant over this range of wavelength. In this case, (4-1) becomes

$$\tau = e^{-\alpha_1 R} \qquad (4\text{-}2)$$

$$= e^{-.2302\alpha R}$$

where α_1 = absorption coefficient in (nepers/m)

α = absorption coefficient in (d B/m)

R = range of observation in(m).

Equation (4-2) was used in the calculations.

The values of the absorption coefficient cover a variety of atmospheric conditions ranging from α = .01 for a clear day, to α = .06 for heavy snow fall. Calculations have been made for absorption coefficient values of

α = .01, .02, .03, .04, .05, .06, .07, (dB/m)

The effect of the atmospheric attenuation is to reduce the signal-to-noise ratio of the target models. This results in decreasing the probability of detection.

The probability of detection for the target models considered has been calculated for all atmospheric conditions. However, the results are not

significantly different from those shown in Tables 4-3 and 4-4.

2.4.7 Consideration of Sun Glint

All of the target models considered thus far have been assumed to be diffuse reflectors. There is a possibility, however, that motionless objects having specular reflecting points may be in the field of view of one or more cells. Such specular reflecting points might occur on parked vehicles, aircraft, or other objects located in the field of view for temporary storage. Presumably, objects permanently located in the field of view can be painted appropriately to eliminate specular reflecting points.

As a result of the sun's motion, it's image from any specular surface may appear and disappear in the field of view of any cell. If the appearance or disappearance is rapid enough the resultant change in illumination will result in a decision of target present. Of course, once the image has been in the field of view for a period of time longer than the background averaging time, it becomes part of the background and a decision of no target is once again made.

In order to determine the seriousness of the sun glint problem, calculations were made of the probability of detection as the sun's image appeared in a given field of view. For the purpose of these calculations the specularly reflecting surface was considered to be a set of plane facets such that the sun's image can enter the fields of view of three adjacent cells almost simultaneously. This is believed to be a "worst case" assumption since the image from a curved surface would be more diffuse and, hence, would not change in intensity as rapidly. The time required for the sun's image to cross the edge of the surface and increase to maximum intensity is simply the time required for the sun to move its own diameter. Since the sun subtends an angle of 0.533^{o} at the earth's surface, and has an angular

velocity of .025° per minute, the time in question is about 128 seconds. The background averaging time for the proposed system is 40 seconds so it can be expected that significant changes in image intensity can take place rapidly enough to result in a decision of target present.

Calculations of the probability of detection have been made assuming the rate of change implied by the above numbers. In all cases the probability of detection reached unity. It appears, therefore, that sun glint may be a potential problem in the proposed system.

One way of alleviating the sun glint problem is to reduce the background averaging time so it becomes part of the background before the target time average becomes large enough to result in a detection. The difficulty with this solution is that it would also reduce the probability of detection for slowly moving targets such as the man crawling at .025 meters per second.

2.4.8. Consideration of Cloud Motion

Experimental data indicates that a cumulus type cloud will attenuate the sun's radiation by about 225 dB/km of cloud thickness. Thus, a cloud drifting between the sun and the field of view of any cell will drastically reduce the reflected signal from the background, and this change may result in a decision of target present.

In calculating the probability of detection due to cloud motion, a number of assumptions were made. Specifically,

1) The cloud velocity is assumed to be 0.2 meters per second. This corresponds to a slowly moving cloud in a breeze of about .5 mph. Clouds moving faster than this are more likely to be detected.

2) The reflected signal from the background is assumed to be attenuated linearly with time until it reaches zero when the field of view is entirely covered. The maximum length of time for this to take place occurs when the cloud is moving at an angle of $\theta_T = 0^o$ or 180^o and is about 62 seconds. The change would be more rapid for other angles of approach and, hence, detection would be more probable.

Calculations of the probability of detection based on the above assumptions yielded a value of unity even when the emissivity of the background is 0.92, corresponding to the minimum reflected signal. Thus, it appears that cloud motion may also be a problem with the proposed system.

Decreasing the background averaging time is not likely to be effective in dealing with cloud motion because under conditions of higher wind velocities the clouds will be moving at about the same speed as many of the targets that are to be detected.

A possible, but not desirable, solution to the problem of cloud motion is to simply delay declaring any decision until more cells have been affected. From this information, some estimate of the size of the affected area can be made. If the area affected is larger than that of any target of interest, the disturbance is assumed to be a cloud and a decision of no target is made. However, if the number of cells affected is small enough to indicate a target of normal size, a decision of target present is made. The obvious problem with this solution is the large amount of delay (on the order of 50 seconds) required to announce the presence of any target.

2.4.9. Consideration of Incandescent Lamps

The presence of lighting fixtures in the field view of any cell raises the possibility of a false alarm resulting from the light being turned on or off. In the wavelength region of interest the incandescent lamp is the one

that is most likely to be a problem since its spectral radiation is greater in this region than that of other common types of light sources.

For purpose of calculation, a 500 W lamp operating at a temperature of 2960^{o} was assumed. It was further assumed that 80% (i.e., 400W) of the total input power is radiated with a spectral characteristic corresponding to black body emission at the specified temperature. The probability of detection was then calculated for this lamp when it is turned on or off. This probability of detection in each cell was found to be unity in all cases. However, if there is a lamp in only one cell, a target will not be declared because the adjacent cells are not affected. If there are lamps in two or more adjacent cells, being turned on or off at the same time, then a target will be declared.

There are two obvious ways to deal with this problem:

1) Introduce a shield between the lamp and the detector that is opaque in the wavelength range of the detector. It may or may not be opaque in the visible range, depending upon the illumination requirements. With sufficient mass, or sufficient separation from the lamp, the change in temperature of this shield will be slow enough to avoid detection.

2) Derive signals from the lamp switching system to instruct the detection system to ignore the observed changes until they have been absorbed into the background average. This action need be taken only for the cells whose field of view contain the lamp so that all other cells are in full operation.

2.4.10. Use of Optical Filters

All of the system performance reported in the preceding sections assumed a wavelength range in the optical system of 3.4 to 4.2 micrometers.

Some sample calculations were also made in two different wavelength ranges; one range being from 3.2 to 3.54 micrometers and the other from 3.75 to 4.2 micrometers. In both cases it is assumed that cold filters are used so that their emission in the stop bands can be ignored.

In both wavelength regions the probability of detection is essentially the same as it is for the original band for the same class of targets and background. The major difference is that saturation occurs in the 3.2 to 3.54 mm range for stare times of 0.1 second because of the increased detector response in this wavelength interval. With the use of stare-time control this is not a problem, but there does not appear to be any advantage to using the smaller wavelength interval since system noise is not a limiting factor.

2.5. SYSTEM IMPLEMENTATION

2.5.1. Microprocessor Design for a Single Array

In designing a microprocessor system, one major concern is the speed of execution of the computation. In the proposed system about 0.1 second is available between the collection of data sets for computations. Some microprocessors, such as the popular Intel 8080 and Motorola 6800, are relatively slow, with clock cycles of 1 microsecond. Also,one instruction may require more than one clock cycle to execute. This application requires much data manipulation for vectors of length 256, and these popular MOS processors are too slow for the proposed system. For example, if an instruction must be applied to all 256 data words of the vector, and that instruction requires 10 microseconds to execute, then the one operation would require 2.56 milliseconds to complete. This, of course, does not consider all the overhead involved in order to get ready to execute the instruction, such as bringing the data from memory into the processor.

Some microprocessors are available with clock cycle times of 100 ns. They are bipolar TTL and each chip has fewer transistors than the MOS processors described above. Thus, they are functionally less complex, being able to process only 2 or 4 bits of information per chip as compared to 8 bits for the 8080 and the 6800. Also, these bipolar chips are "microprogrammed". That is, they have no instructions defined for the processor. External circuitry must define the instructions and supply the control signals to the processor. It is desirable to have more than 2 or 4 bits in a computer and, fortunately, these microprogrammable processors can be combined to provide longer word lengths. The Texas Instrumens SN54/74S481 is a 4 bit processor, and two chips can be combined to make one 8 bit processor. These "bit-slice" processors require more circuitry to control them, and

cuit
UA pro-
programmed by
might be needed
grammer write the code
lgorithm can be written
cycle time of 100 ns, and it is
om 2 to 9.2 times faster than the
od preliminary choice for the IRCCD Intru-
n the following pages, a program is designed and
ds determined. It is shown that the processor
meet the time constraints.
chart of Fig. 5-1 shows the general scheme for computing an
Flow charts in Figs. 5-2 through 5-5 elaborate on each
ision.
the scheme.
gram must first be initialized, as in Fig. 5-2. Certain con-
needed for the main routine to operate. Also, a beginning
eeded. Figure 5-2 suggests that N data sets and their
er to make this computation. An alternative method is
for m(i') and the cummulative sums used to compute
e ready, NOW is set to point to the address of
gram begins.

more effort to design a workable system.

For the present application it is desirable to have a processor with the speed of the bipolar devices without spending the time to design all the instructions. Such an alternative is available in the Signetics 300KT8080SK, an 8080A emulator. This processor fits on one printed circuit board and is provided with all the same instructions as an Intel 8080A processor. In addition, 12 instructions are allowed to be microprogrammed by the system designer. For instance, a square root function might be needed for a certain calcultion. Rather than make the programmer write the code for the algorithm, an instruction to perform the algorithm can be written into the processor. The emulator has a cycle time of 100 ns, and it is claimed that the speed of operation is from 2 to 9.2 times faster than the 8080A that it emulates.

This 8080A emulator is a good preliminary choice for the IRCCD Intrusion Detection System. In the following pages, a program is designed and the memory and time needs determined. It is shown that the processor described above can meet the time constraints.

The flow chart of Fig. 5-1 shows the general scheme for computing an alarm decision. Flow charts in Figs. 5-2 through 5-5 elaborate on each piece of the scheme.

The program must first be initialized, as in Fig. 5-2. Certain constraints are needed for the main routine to operate. Also, a beginning value of $m(\ell')$ is needed. Figure 5-2 suggests that N data sets and their sums be taken in order to make this computation. An alternative method is to provide initial values for $m(\ell')$ and the cummulative sums used to compute it. Once the initial data are ready, NOW is set to point to the address of the newest data, and the main program begins.

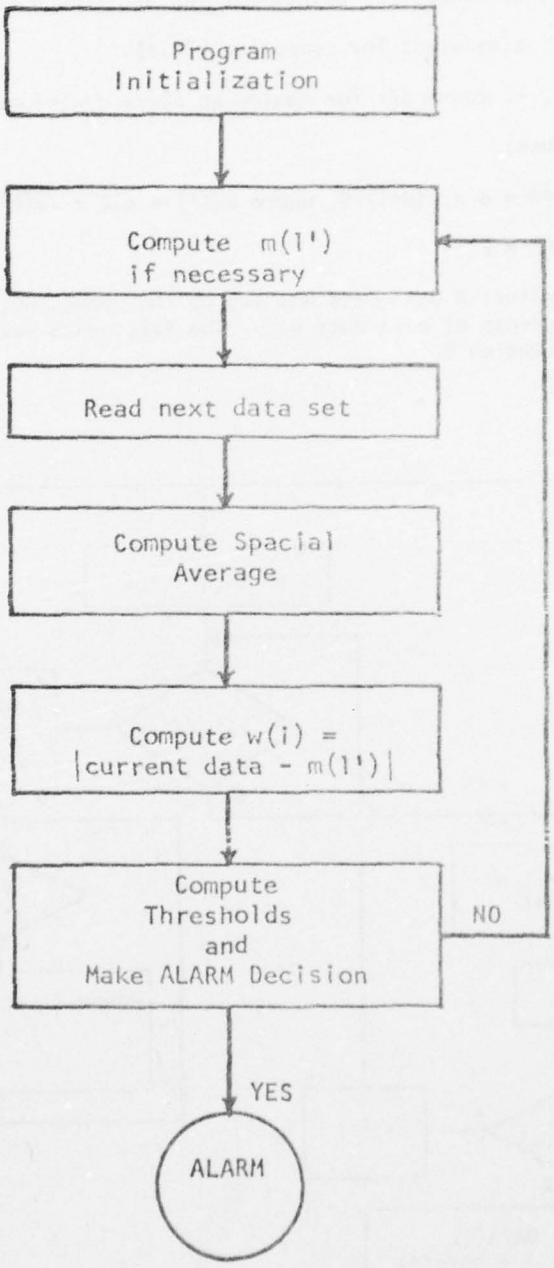

Figure 5-1. General flowchart for computation of IR detection system.

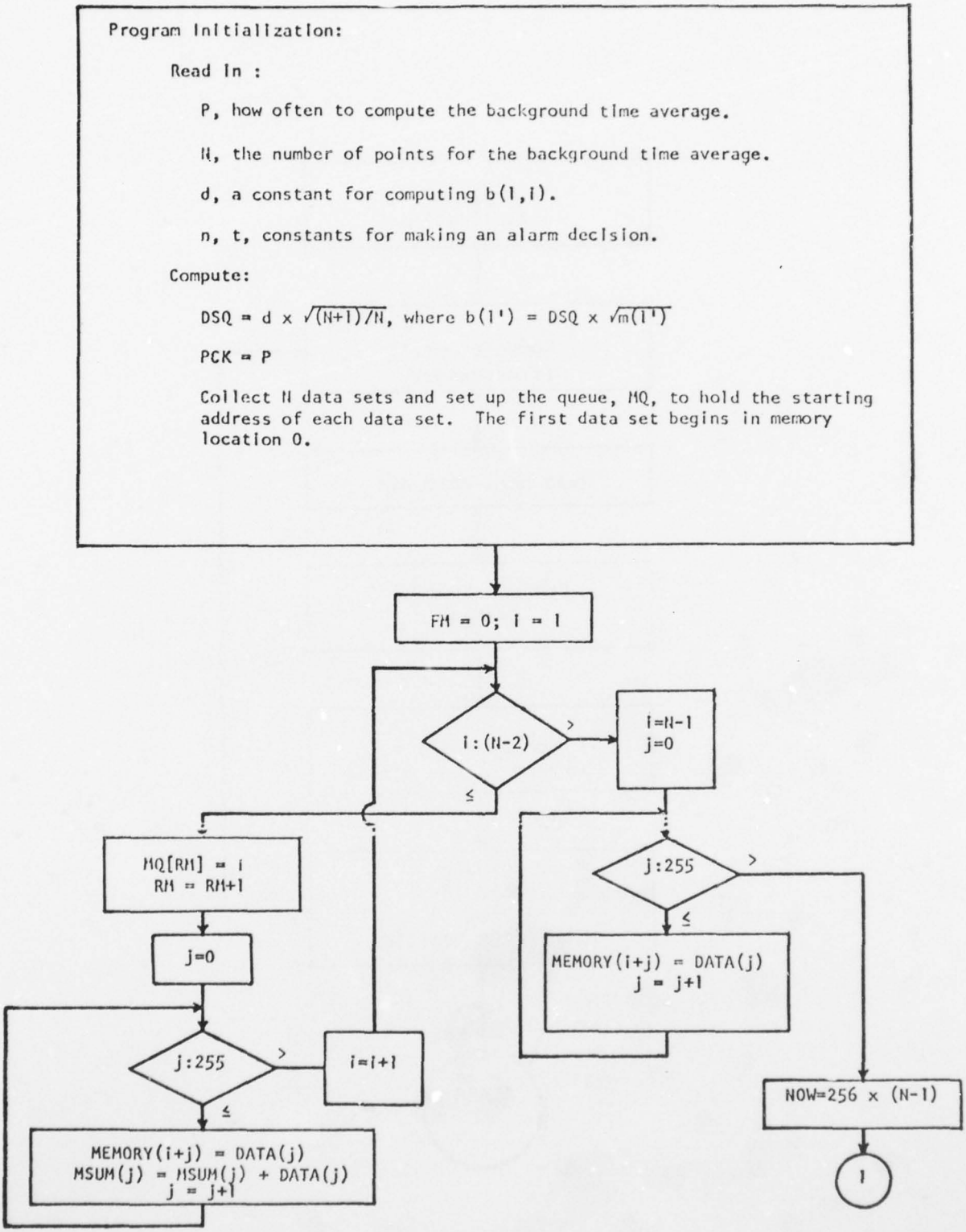

Figure 5-2. Program initialization flowchart.

Figure 5-3 shows the steps for computing m(ℓ'). First, check to see if m(ℓ') should be computed now by checking if PCK = P. If it is, continue with the calculation. Otherwise, load new data, and continue the program. The background time average is defined as

$$m(\ell') = (1/N) \sum_{n=1}^{N} x[P(\ell'-n)] \qquad (5\text{-}1)$$

If m(ℓ') were computed directly for each sensor i, then each time that it was computed (N-1) additions would be required. Clearly, for large N, this requires an unacceptable amount of time.

An alternative is to store cummulative sums for m(ℓ'), where

$$MSUM(i) = \sum_{n=2}^{N} x[P(\ell'-m,i)] \qquad (5\text{-}2)$$

If x(ℓ',i) is an eight bit number, then MSUM will be at most a 16 bit numer if N = 16. For each new data set, m(ℓ') can be computed by adding the new data and subtracting the oldest data from the cummulative sum. So,

$$MSUM(i) = MSUM(i) + \text{new data}$$

$$M(\ell') = (1/N)\ MSUM(i)$$

$$MSUM(i) = MSUM(i) - \text{oldest data}.$$

To find the oldest data, a list ordered by age is kept of the addresses of all the data used in computing m(ℓ'). As new data arrives, the starting address of the data will be added to the end of the queue, and the oldest data address will be deleted from the front of the queue. An explanation of queues and their uses is found in "The Art of Computer Programming", vol. 1, by D. E. Knuth, Addison-Wesley, 1973, pages 240-242.

AD-A063 327 PURDUE UNIV LAFAYETTE IND SCHOOL OF ELECTRICAL ENGI--ETC F/G 17/5
IRCCD INTRUSION DETECTION.(U)
OCT 78 G R COOPER, C D MCGILLEM F30602-75-C-0082
UNCLASSIFIED RADC-TR-77-435 NL

2 OF 2
AD
A063327

END
DATE
FILMED
3-79
DDC

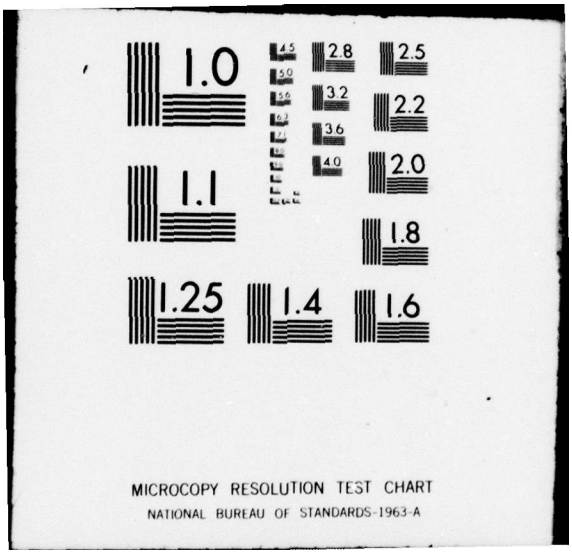
1.0
1.1
1.25
1.4
1.6
1.8
2.0
2.2
2.5
2.8
3.2
3.6
4.0
4.5
5.0
5.6
MICROCOPY RESOLUTION TEST CHART
NATIONAL BUREAU OF STANDARDS-1963-A

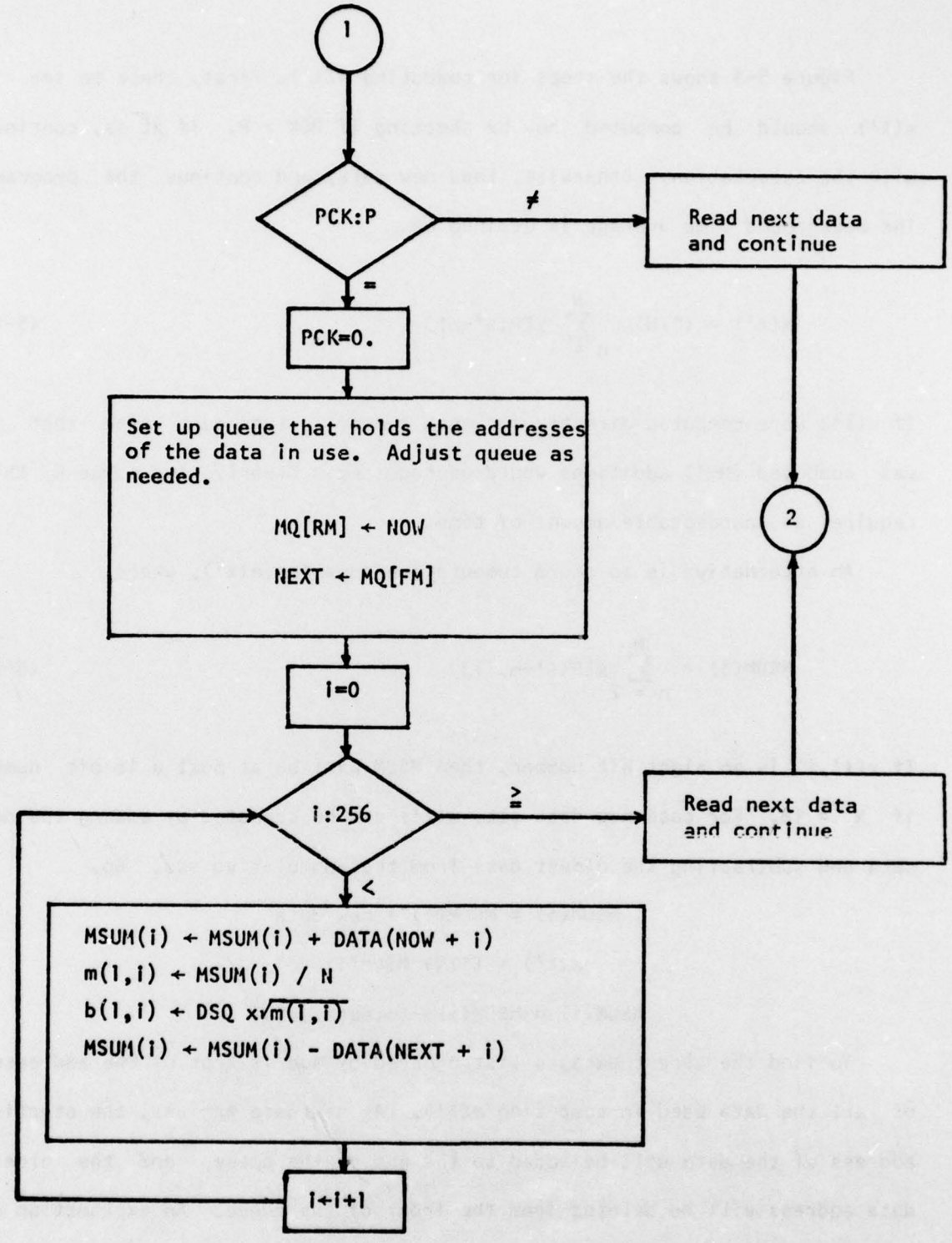

Figure 5-3. Flowchart for computation of $m(\ell')$, the background time average.

The method above requires a small amount more memory space than the method that computes the entire sum each time new data arrives. However, it requires significantly less time to compute.

To compute $\sqrt{m(\ell')}$ the fastest method is table look-up. If $m(\ell')$ is 8 bits long, then all values of $\sqrt{m(\ell')}$ are stored in a table in 256 memory locations. If the table begins at location A, then $\sqrt{m(\ell')}$ is located at location A + $m(\ell')$.

Next, a new data set is loaded and its spatial average computed, as in Fig. 5-4. It is recommended that some sort of direct memory access be available for the incoming data to be loaded into memory. A program controlled data input would not be fast enough to load one datum each 4 microseconds. D should be a power of 2, for then division may be accomplished by a series of right shifts, one for each factor of 2. If the spatial average is too high, t_s is shortened; if it is too low, t_s is lengthened.

Finally, the threshold and alarm computations are made, as in Fig. 5-5. First, $w(\ell)$ is computed for all 256 sensors. The alarm computations can be computed in two steps. First, $v(\ell)$, a vector of length 254, is computed, where each $v(\ell,i)$ is a 3 bit word and reflects a comparison of $b(\ell,i)$ with $w(\ell,i)$, $w(\ell,i+1)$, and $w(\ell,i+2)$. Second, $v(\ell)$ is scanned n/3 words at a time to see if t or more l's are present in the group. But, computing $v(\ell)$ is unnecessary and is bypassed. Fig. 5-5 shows a computation for n = 12 and t = 8. For each set of comparisons between $b(\ell,i)$ and the three consecutive channels of $w(\ell)$, a count of the number of l's is kept. When n/3=4 counts have been made, the sum of the 4 counts is checked to see if it is greater than 8. If it is, an alarm decision is made. If the count is less than 8, the search for an alarm decision is resumed by eliminating the oldest count, c(0), and computing the next count, c(3).

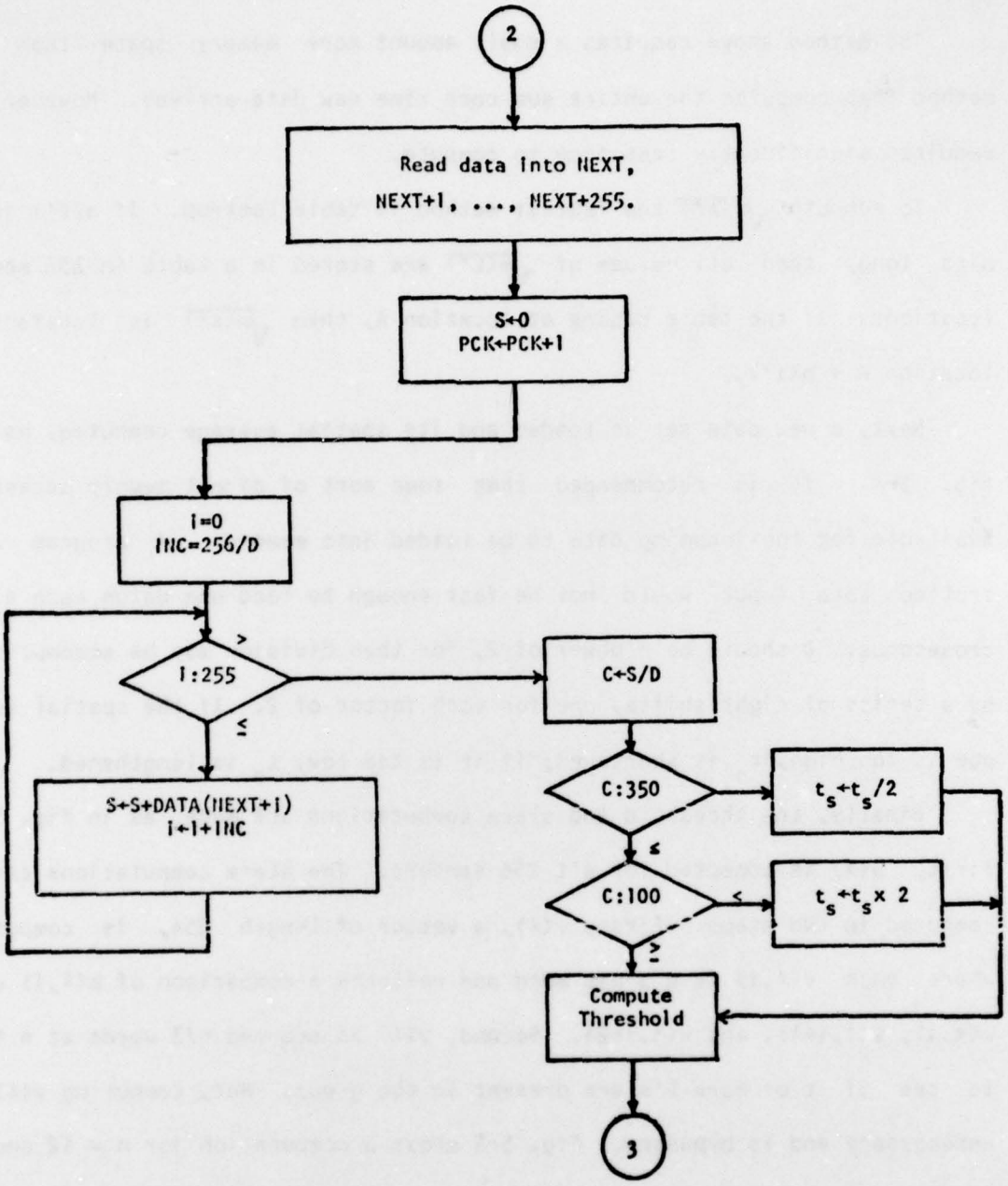

Figure 5-4. Flowchart for background spatial average and loading data.

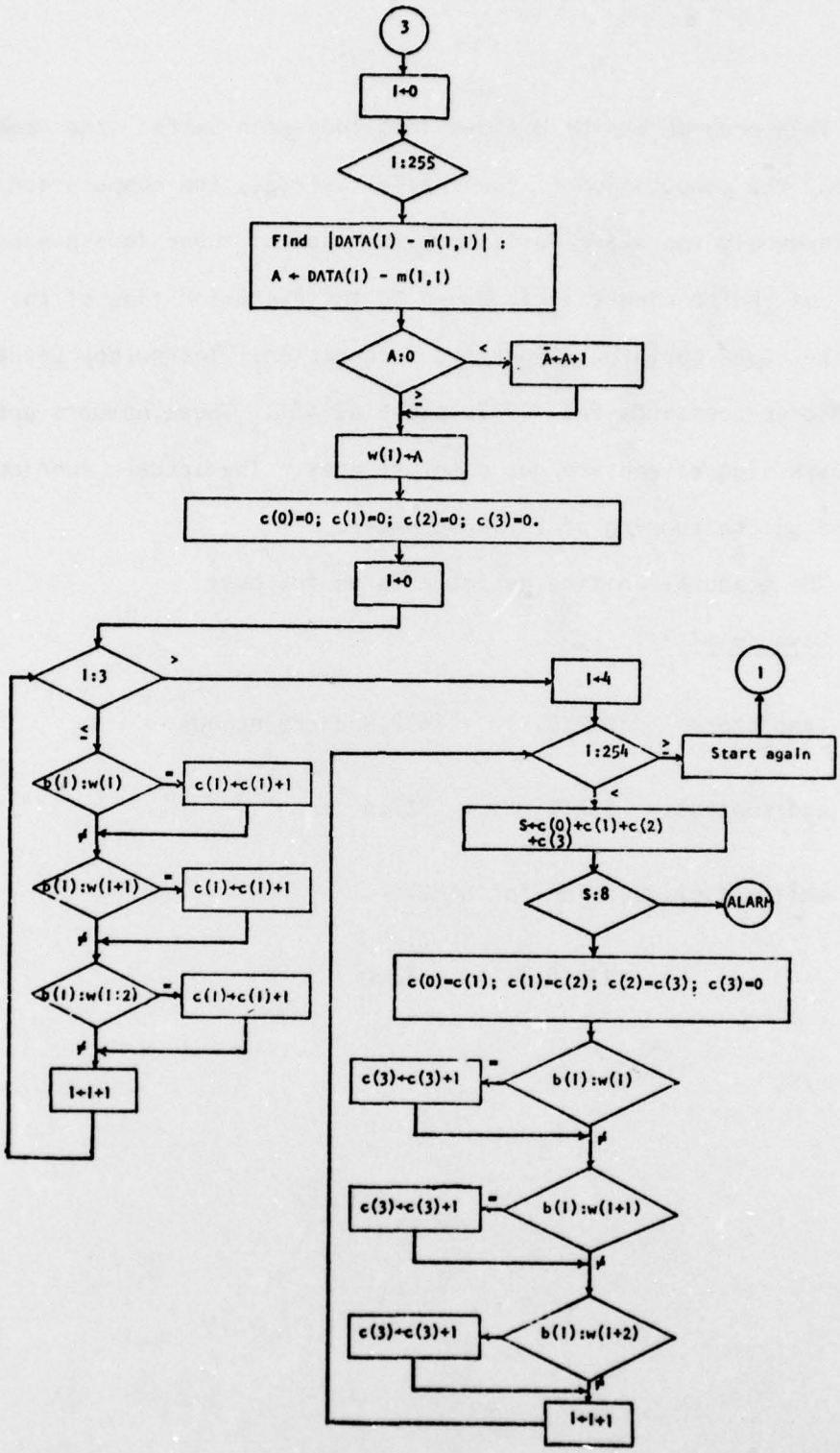

Figure 5-5. Flowchart for computing threshold and ALARM decisions. The program above is written for n=12 and t=8.

This program can be divided into four main parts: the computation of $m(\ell')$, the computation of the spatial average, the computation of $w(\ell)$, and the threshold and alarm decision. For each of these four pieces, an estimate of the running time is based on the execution time of the instructions for the 8080A emulator (Signetics Corporation, "Technology Leadership Bipolar Microprocessor", Feb. 1977, pages 42-43). These numbers are intended as ballpark figures and are not absolute ones. The actual running time will depend on the cunning of the programmer.

The computation time estimate is as follows:

Compute $m(\ell')$:

load/store 1592(0.9) = 1432.8 microseconds

add/subtract 512(1.05) = 537.6

shifts (for division for N=32)

1280(0.6) = 668.0

Compute $\sqrt{m(\underline{\ell}')}$:

double precision load			
	256(1.8)	=	460.8
add	256(.6)	=	153.6
double precision load			
	256(1.8)	=	460.8
multiply	256(3.9)	=	998.4

4712.0 microseconds

Compute Spatial Average:

load	18(0.9)	=	16.2
add	17(0.6)	=	10.2
shift	5(0.6)	=	3.0
compare	2(0.6)	=	1.2
jump	2(0.9)	=	1.8
output t	1(1.2)	=	1.2

33.6 microseconds

Compute $w(\ell,i)$:

load	256(0.9)	=	230.4
subtract	256(1.05)	=	268.8
compare	256(0.6)	=	153.0
jump	256(0.9)	=	230.4
complement	256(0.3)	=	76.8
increment	256(.45)	=	115.2
store	256(0.9)	=	230.4

1305.0 microseconds

Compute Threshold and Alarm:

compare	1266(0.6)	=	759.6
jump	1266(0.9)	=	1139.4
add	754(0.6)	=	452.4
load	1016(0.9)	=	914.4

3265.8 microseconds

Total Computation Time:

$m(\ell'), \sqrt{m(\ell')}$	4.712 milliseconds
Spatial average	.033
$w(\ell,i)$	1.305
Threshold, alarm	3.266
Total	9.316 ms

The Random Access Memory (RAM) needed for data storage may be estimated as follows:

N data sets:

for N = 32:	256 x 8 bits = 8 K words
$m(\ell)$:	256 x 8 bits = 1/4 K words
MSUM:	256 x 16 bits = 1/2 K words
$w(\ell)$:	256 x 8 bits = 1/4 K words
$b(\ell)$:	256 x 8 bits = 1/4 K words
	9 1/4 K words

These are the five largest users of storage. Let us estimate that 12 K, 8 bit words of RAM be used. This estimate is based partially on the fact that often RAM may be bought in multiples of 4K words.

2.5.2. Estimated Cost for a Single Array

The system cost and power need may be estimated as follows:

	Estimated Price	Estimated Power
8080A emulator:		
Signetics 300KT8080K	$ 300	4 amps
4K ROM for program storage		
4 82S184's	160	1 amp
12K RAM for data storage		
96 S4015-3's	600	10 amps
	$1060	15 amps at 5 volts

In the future, new products may make these choices of ROM and RAM obsolete. If the system is built, these choices should be reevaluated.

A typical power supply choice might be DATEL's MPS-5/18, a 5 volte, 18 amp supply with a cost of about $100.

Packaging costs must be added to this parts estimate. These should be determined by the environmental needs when the system is built.

2.5.3. Time-Sharing for Multiple Arrays

It may be possible to use one processor to control more than one sensor array. However, the number of arrays that may be controlled will be limited more by the amount of memory needed than by the time available for computations. The 8080A emulator described above may directly access up to 64K

words of memory. If each array requires 10K words for data storage, then at most 64/10 = 6 arrays may be serviced by one processor due to the direct memory accessing limitations of the processor. If our ballpark figure for the computation time of our program is reasonable, then 6 arrays could be serviced in the given 0.1 seconds.

On the basis of the cost and power estimates given above, the cost for 6 arrays would be on the order of $4460 (not including power supplies and packaging) and the power requirements would be 61 amperes at 5 volts. Thus, the cost per array will be on the order of $750.

3.1. CONCLUSIONS

Based on the analysis presented in this report, and upon the computations that have been performed, there are a number of conclusions that appear to be justified. Most of these have been stated in earlier sections of this report, but they are restated here in a more concise form as a matter of collecting them together in a single place.

1) There is strong analytical and computational evidence that the IRCCD array can be successfully used for intrusion detection.

2) By employing a decision rule that utilizes the outcomes of multiple observation (in both space and time) the detection characteristic can be made sufficiently steep to minimize false alarms due to small targets while maximizing the probability of detection for targets of interest.

3) False alarms due to system noise appear to be negligibly small when the computed thresholds are used.

4) The most serious problem appears to be false alarms due to sun glint and cloud motion.

5) It appears quite possible to implement the electronics required for performing the decision function with a single microprocessor and some associated memory. The cost of this elections, at present prices, is probably under $1200, not including packaging.

6) It also appears possible to use a single microprocessor, with additional memory, to perform the decision function for as many as six IRCCD arrays. The cost of the electronics, per array, is probably under $900, not including packaging.

3.2. RECOMMENDATIONS

The principal recommendation is that the next step in the development of a working system be taken. This recommendation is based on the analytical and computational results that have been obtained in this study. It is believed that these results are sufficiently favorable to indicate a high probability that a successful system can be developed, with the system proposed in this report serving as a reasonable point of departure in this development. The next logical step is to construct a breadboard model of system and test it under as realistic conditions as possible.

If a decision is made to develop the proposed system through the breadboard stage, there are several analytical and computational tasks that need to accompany the more detailed system design. The following recommended tasks are approximately in the order in which they should be done, although of course some of them can be carried out in parallel.

1) Review the available microprocessors and memories with respect to the system requirements, select the components needed and order.

2) Obtain more accurate information regarding the IRCCD's available at that time and re-evaluate the system analysis with respect to selecting firm values of stare time, background averaging time, threshold levels, and observation multiplicity.

3) Write the programs necessary to accomplish the desired computations, after checking the flowcharts to establish that they are correct and complete.

4) Prepare a test program designed to establish the performance of the system relative to the design objective.

5) Construct, de-bug and test.

APPENDIX A

OPTIMUM DETECTION SYSTEM

The analysis presented here, in abbreviated form, follows the general method outlined in [2, Chap. 1. It differs from that analysis only in that the noise level here is a function of signal amplitude rather than being constant.

It is assumed that M observations from each of K detector cells are available. Thse observations form the elements of a vector.

$$\underline{r} = (r_1, r_2, \ldots, r_n) \quad , \quad n = MK \tag{A-1}$$

Target detection is based on a likelihood ratio test defined by

$$\ell(\underline{r}) = \frac{p(\underline{r}|H_1)}{p(\underline{r}|H_o)} \underset{H_o}{\overset{H_1}{\gtrless}} \lambda \tag{A-2}$$

where H_o is a hypothesis that no target is present in any of the MK observations, while H_1 is the hypothesis that a target is present in all observations. The decision threshold, λ, is determined by the desired probability of false alarm and evaluated by the MK-fold integral

$$P_F = \int_{\ell(\underline{r}) > \lambda} p(\underline{r}|H_o)\, d\underline{r} \tag{A-3}$$

The probability of detection yielded by this threshold is

$$P_D = \int_{\ell(\underline{r}) > \lambda} p(\underline{r}|H_1)\, d\underline{r} \tag{A-4}$$

The vector $\underline{r}$ is assumed to be multivariate Gaussian on the basis of the Gaussian approximation to the Poisson distribution for the output of each

cell. Thus, the conditional density function $p(\underline{r}|H_o)$ is

$$p(\underline{r}|H_o) = (2\pi)^{-n/2}|\underline{A}_o|^{-1/2} \exp\left[-1/2(\underline{r}-\underline{m}_o)\underline{A}_o^{-1}(\underline{r}-\underline{m}_o)^T\right] \qquad \text{(A-5)}$$

where

$$\underline{m}_o = (m_{o1}, m_{o2}, \cdots, m_{on})$$

$$m_{oi} = E[r_i|H_o]$$

$$\underline{A}_o = \begin{bmatrix} a_{o11} & a_{012} & \cdot & a_{o1n} \\ \cdot & \cdot & \cdot & \cdot \\ a_{on1} & \cdot & \cdot & a_{onn} \end{bmatrix}$$

$$a_{oij} = a_{oji} = E\{[(r_i-m_{oi})|H_o][r_j-m_{oj})|H_o]\}$$

and the superscript T denotes a transpose. It is assumed here that (r_i-m_{oi}) and (r_j-m_{oj}) are uncorrelated for $i \neq j$ since they represent outputs from different cells or at different times. Thus,

$$a_{oij} = 0, \quad i \neq j$$

$$= \sigma_{oi}^2 \quad , \quad i = j$$

In a similar way the conditional densit, function $p(\underline{r}|H_1)$ is

$$p(\underline{r}|H_1) = (2\pi)^{-n/2}\ |\underline{A}_1|^{-1/2} \exp\left[-1/2(\underline{r}-\underline{m}_1)\underline{A}_1^{-1}(\underline{r}-\underline{m}_1)^T\right] \qquad \text{(A-6)}$$

where

$$\underline{m}_1 = (m_{11}, m_{12}, \cdots, m_{1n})$$

$$m_{1i} = E[r_i | H_1]$$

$$\underline{A}_1 = \begin{bmatrix} a_{111} & a_{112} & \cdot & a_{11n} \\ \cdot & \cdot & \cdot & \cdot \\ a_{1n1} & \cdot & \cdot & a_{1nn} \end{bmatrix}$$

$$a_{1ij} = a_{1ji} = E\{[(r_i - m_{1i}) | H_1][(r_j - m_{1j}) + H_1]\}$$

and, as before,

$$a_{1ij} = 0, \quad i \neq j \qquad \text{(A-7)}$$

$$= \sigma_{1i}^2 \quad , \quad i = j$$

Using (A-5) and (A-6), the likelihood ratio becomes

$$\ell(\underline{r}) = \frac{p(\underline{r}|H_1)}{p(\underline{r}|H_o)} = \sqrt{\frac{|A_o|}{|\underline{A}_1|}} \exp\{-1/2[(\underline{r}-\underline{m}_1)\underline{A}_1^{-1}(\underline{r}-\underline{m}_1)^T \qquad \text{(A-8)}$$

$$- (\underline{r}-m_o)\,\underline{A}_o^{-1}(\underline{r}-\underline{m}_o)^T]\}$$

It is more convenient to consider the natural logarithm of (A-8) and write it as

$$\ell n[\ell(\underline{r})] - \ell n\sqrt{\frac{|A_o|}{|\underline{A}_1|}} = 1/2[(\underline{r}-\underline{m}_o)\,\underline{A}_o^{-1}(\underline{r}-\underline{m}_o)^T - (\underline{r}-\underline{m}_1)\,\underline{A}_1^{-1}\,(\underline{r}-\underline{m}_1)^T] \qquad \text{(A-9)}$$

Hence, a sufficient statistic can be defined as

$$L(\underline{r}) = 2\left[\ell n[\ell(\underline{r})] - \ell n\sqrt{\frac{|\underline{A}_o|}{|\underline{A}_1|}}\right] \tag{A-10}$$

from which the likelihood ratio test becomes

$$L(\underline{r}) = (\underline{r}-\underline{m}_o)\ \underline{A}_o^{-1}\ (r-\underline{m}_o)^T - (\underline{r}-\underline{m}_1)\ \underline{A}_1^{-1}\ (\underline{r}-\underline{m}_1)^T \underset{H_o}{\overset{H_1}{\gtrless}} \eta \tag{A-11}$$

and

$$P_F = \int_{L(\underline{r})>\eta} p(\underline{r}|H_o)d\underline{r} \tag{A-12}$$

and

$$P_D = \int_{L(\underline{r})>\eta} p(\underline{r}|H_1)d\underline{r} \tag{A-13}$$

Because the covariance matrices $\underline{A}o$ and $\underline{A}_1$ are different under the two hypotheses, it is not possible to reduce the decision boundary defined by (A-11) to a plane in n-dimensional space. Thus, further analytical evaluation of (A-12) and (A-13) is not possible and their evaluation by computer is extremely cumbersome when n is greater than 2. However, in order to compare the theoretical optimum results with those obtained by the proposed system, it is desirable to carry out such an evaluation for at least the simplest case.

The simplest case corresponds to M=K=n=1. In this case

$$\underline{r} = r$$

$$\underline{m}_o = m_o$$

$$\underline{m}_1 = m_1$$

$$\underline{A}_o = \sigma_o^2 \quad , \quad \underline{A}_o^{-1} = 1/\sigma_o^2$$

$$\underline{A}_1 = \sigma_1^2 \quad , \quad \underline{A}_1^{-1} = 1/\sigma_1^2$$

Thus,

$$L(r) = (r-m_o)\left(\frac{1}{\sigma_o^2}\right)(r-m_o) - (r-m_1)\left(\frac{1}{\sigma_1^2}\right)(r-m_1) \qquad \text{(A-14)}$$

$$= \frac{(r-m_o)^2}{\sigma_o^2} - \frac{(r-m_1)^2}{\sigma_1^2}$$

$$= r^2\left[\frac{1}{\sigma_o^2} - \frac{1}{\sigma_1^2}\right] + r\left[\frac{2m_1}{\sigma_1^2} - \frac{2m_o}{\sigma_o^2}\right] + \left[\frac{m_o^2}{\sigma_o^2} - \frac{m_1^2}{\sigma_1^2}\right]$$

In the present case, the variances are proportional to the mean values because of the properties of the underlying Poisson distribution. For this situation, the coefficient of r in (A-14) vanishes and the likelihood ratio test becomes

$$r^2 \underset{H_o}{\overset{H_1}{\gtrless}} \frac{m_o m_1}{m_1 - m_o}[\eta - (m_o - m_1)] = \eta' \quad , \quad m_o < m_1 \qquad \text{(A-15)}$$

or

$$r^2 \underset{H_1}{\overset{H_0}{\gtrless}} \frac{m_o m_1}{m_1 - m_o}[\eta - (m_o - m_1)] = \eta' \quad , \quad m_o > m_1 \tag{A-16}$$

In either case

$$P_F = \int_{r^2 > \eta'} (\sqrt{2\pi}\sigma_o)^{-1} \exp[-[r-m_o^2]/2\sigma_o^2]dr \tag{A-17}$$

$$P_D = \int_{r^2 > \eta'} (\sqrt{2\pi}\sigma_1)^{-1} \exp[-[r-m_1]^2/2\sigma_1^2]dr \tag{A-18}$$

Hence, η' is determined by selecting a desired value of P_F, and from this, P_D can be calculated.

4. REFERENCES

[1] Papoulis, A., "Probability, Random Variables, and Stochastic Processes", McGraw-Hill Book Company, 1965.

[2] Van Trees, H. L., "Detection, Estimation, and Modulation Theory, Part I", John Wiley and Sons, 1968.

[3] Shepard, F. D., A. C. Yang, S. A. Roosild, J. H. Bloom, B. R. Capone, C. E. Ludington, R. W. Taylor, "Silicon Schottky Barrier Monolithic IRTV Planes", to be published, Advanced Electronics and Electron Physics.

[4] Kohn, E. S., "Infrared Imaging with Monolithic, CCD-Addressed Schottky-Barrier Detector Arrays: Theoretical and Experimental Results", Conference Proceedings, San Diego, 1975.

[5] Wolfe, W. L. (Ed.), "Handbook of Military Infrared Technology", Office of Naval Research, Department of the Navy, Washington, D.C., 1965.

[6] Hudson, R. D., "Infrared System Engineering" Wiley Interscience, 1969.

[7] Silva, L. F. and R. Kumar, "Infrared Radiometry", TR-EE 73-37, School of Electrical Engineering, Purdue University, West Lafayette, Indiana, 1973.

[8] Gubareff, G. G., J. E. Janssen, and R. H. Tarborg, "Thermal Radiation Properties Survey", Honeywell Research Center, Minneapolis, Minnesota, 1960.

[9] ---, "Review of the Thermal Radiation Values for Metals and Other Materials", Report No. GR 2462-R3, Honeywell Research Center, Minneapolis, Minn., 1956.

[10] Vanzetti, R., "Practical Applications of Infrared Techniques", John Wiley and Sons, 1972.

5. PERSONNEL

The following individuals have participated in this project, and their conributions are gratefully acknowledged.

Principal Investigators:

George R. Cooper

Clare D. McGillem

Postdoctoral Fellow:

Catherine E. Houstis

Graduate Research Assistants:

David A. Bloodgood

Terrance J. Hill

Tien-Chu Lee

Antoine Medard

S. Diane Smith

☆U.S. GOVERNMENT PRINTING OFFICE: 1978-614-023/31